AD

USAAVLABS TECHNICAL REPORT 67-9A

IN-FLIGHT MEASUREMENT OF ROTOR BLADE AIRLOADS, BENDING MOMENTS, AND MOTIONS, TOGETHER WITH ROTOR SHAFT LOADS AND FUSELAGE VIBRATION, ON A TANDEM ROTOR HELICOPTER

VOLUME I

INSTRUMENTATION AND IN-FLIGHT RECORDING SYSTEM

By

Roy Golub
William McLachlan

May 1967

U. S. ARMY AVIATION MATERIEL LABORATORIES
FORT EUSTIS, VIRGINIA

CONTRACT DA 44-177-AMC-124(T)
VERTOL DIVISION
THE BOEING COMPANY
MORTON, PENNSYLVANIA

Disclaimers

When Government drawings, specifications, or other data are used for any purpose other than in connection with a definitely related Government procurement operation, in the United States Government thereby incurs no responsibility nor any obligation whatsoever; and the fact that the Government may have formulated, furnished, or in any way supplied the said drawings, specifications, or other data is not to be regarded by implication or otherwise as in any manner licensing the holder or any other person or corporation, or conveying any rights or permission, to manufacture, use, or sell any patented invention that may in any way be related thereto.

Trade names cited in this report do not constitute an official endorsement or approval of the use of such commercial hardware or software.

Disposition Instructions

Destroy this report when no longer needed. Do not return it to originator.

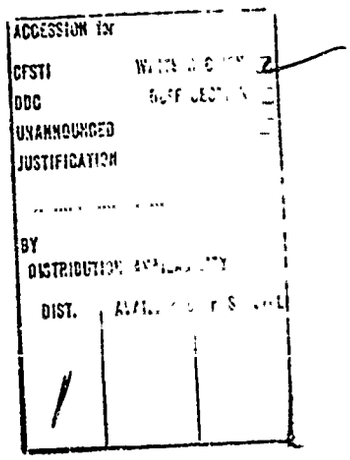

DEPARTMENT OF THE ARMY
U. S. ARMY AVIATION MATERIEL LABORATORIES
FORT EUSTIS, VIRGINIA 23604

This report has been reviewed by the U. S. Army Aviation Materiel Laboratories and is considered to be technically sound.

The work was performed under Contract DA 44-177-AMC-124(T) for the purpose of measuring the dynamic air pressures on the blades of a tandem rotor helicopter, the resulting blade and shaft stresses, and fuselage vibrations during flight.

The report is published for the dissemination and application of information and the stimulation of ideas.

Task 1P125901A14604
Contract DA 44-177-AMC-124(T)
USAAVLABS Technical Report 67-9A
May 1967

IN-FLIGHT MEASUREMENT OF ROTOR BLADE AIRLOADS, BENDING MOMENTS, AND MOTIONS, TOGETHER WITH ROTOR SHAFT LOADS AND FUSELAGE VIBRATION, ON A TANDEM ROTOR HELICOPTER

VOLUME I

INSTRUMENTATION AND IN-FLIGHT RECORDING SYSTEM

D8-0382-1

by

Roy Golub
and
William McLachlan

Prepared by

VERTOL DIVISION
THE BOEING COMPANY
Morton, Pennsylvania

for

U.S. ARMY AVIATION MATERIEL LABORATORIES
FORT EUSTIS, VIRGINIA

SUMMARY

An extensively instrumented tandem rotor helicopter was developed to measure the rotor blade airloads and the resulting rotor blade motions and bending moments, the rotor shaft loads and moments, and the fuselage vibration. This report details the design, assembly, and testing of the instrumentation system and documents the capability of the system for fulfilling the requirements of the program.

The blade pressure transducers that were used for this program were refined versions of the subminiature, flat-diaphragm, strain-gage transducer that was developed at the Battelle Memorial Institute. A differential-pressure configuration of the basic absolute-pressure transducer was also used. Extensive testing was accomplished to ensure that these transducers would perform with adequate accuracy.

The simultaneous recording of the output from 135 transducers from each of the two rotors represents a major advancement in the field of signal-conditioning and transmission systems. The design of a rotating signal-conditioning package, incorporating individual power supplies, balance and calibrating networks, together with miniature data amplifiers and filters, enabled this simultaneous acquisition of all necessary data. The concept, design, and testing of the rotating signal-conditioning package are described.

To reduce further the recording system requirements, a Vertol-designed and -fabricated electromechanical device alternately switched the transducer signals from the forward and aft rotating signal conditioners into the narrow-band frequency modulation multiplex system. The switching network, actuated by the rotor azimuth signal, permitted the recording of 237 transducer signals on a magnetic tape system of 14-track capacity.

This instrumentation system was developed through an extensive series of component tests, laboratory tests, and flight tests. The program included environmental testing to ensure that vibration and temperature changes would not cause spurious data. The details of this functional testing as utilized to develop the rotor hub signal-conditioning package and the associated recording system are presented. Documentation concerning individual component and system accuracies, with emphasis on the

blade pressure measurements, is included to provide a statistically substantiated accuracy estimate. Flight test data obtained in instrument check flights are included to demonstrate the proper functioning of the system.

FOREWORD

This report describes the development of the instrumentation and in-flight recording system which were used for the measurement of dynamic airloads on a CH-47A helicopter. The project was performed under Contract DA 44-177-AMC-124(T) through the period from June 1964 to July 1966. The reports covering the program consist of five volumes, of which this is Volume I. The remaining volumes are as follows:

Volume II, Calibrations and Instrumented Component Testing
Volume III, Data Processing and Analysis System
Volume IV, Summary and Evaluation of Results
Volume V, Investigation of Blade Stall Conditions

The project was conducted under the technical cognizance of William T. Alexander, Jr., of the Aeromechanics Division of the U.S. Army Aviation Materiel Laboratories (USAAVLABS). The authors of this report are Roy Golub and William McLachlan, Vertol flight test instrumentation engineers. A significant contribution to this phase of the program was made by C. B. Shakespeare, Supervisor of Flight Test Instrumentation Applications and Systems Group. The entire program was executed under the direction of Richard R. Pruyn, Dynamic Airloads Project Engineer for The Boeing Company, Vertol Division.

CONTENTS

CONTENTS

ILLUSTRATIONS

ILLUSTRATIONS

ILLUSTRATIONS

ILLUSTRATIONS

TABLES

TABLES

SYMBOLS

A-D	analog to digital
℄	centerline
cmr	common mode rejection
db	decibels
E_b	bridge voltage
F.S.	full-scale range
g	the acceleration of gravity, 32.2 feet per second per second
IRIG	interrange instrumentation group
mv	millivolts
MVCO	millivolt-controlled oscillator
NBFM	narrow-band frequency modulation
NIXIE tube	a gas-filled, cold-cathode, digital indicator tube having a common anode and containing stacked metallic elements in the form of numerals
psia	pounds per square inch, absolute
psid	pounds per square inch, differential
P-P	peak to peak
Rcal	resistance calibration
R_L	lead resistance
RSS	root sum square method of combining errors by the square root of the sum of the squares of the random individual errors
v	volts

SYMBOLS

vac	volts alternating current
VCO	voltage-controlled oscillator
vdc	volts direct current
Δ	difference
σ	standard deviation
Ω	ohms, resistance
1/rev.	one per revolution

INTRODUCTION

The Dynamic Airloads Program was initiated in June 1964 with the award of a contract to The Boeing Company, Vertol Division, for the in-flight measurement of the forces acting on the rotors, fuselage, and flight controls of a tandem rotor helicopter. A complete instrumentation and in-flight recording system was designed, assembled, and developed to carry out this program. One requirement of the contract was the detailed documentation of the instrumentation design philosophy, system accuracy, installation, and checkout procedures for all equipment used in this program.

The text of this report on the instrumentation system is divided into four major sections: Description of Test Equipment, Experimental Procedures, Experimental Results, and Evaluation of Design Based on Experimental Results. The first part specifies the parameters that were to be recorded and describes the basis for the selection of the instrumentation components and subsystems. Detailed descriptions of the selection, assembly, and installation of all components, with their integration into the complete system, are provided.

The second major section, Experimental Procedures, is a comprehensive presentation of the intensive component-qualification and system-testing procedures that were performed to verify the integrity of the system. Major emphasis is placed on the pressure transducers, signal-conditioning amplifiers, and accelerometers, since there was little previous experience with the operation of these specialized components. Detailed information is presented on the laboratory tests of these components and of the systems that were assembled from the components. After the satisfactory completion of laboratory testing, the system was installed in the helicopter and further testing was performed which prepared the system for in-flight recording.

The third section, Experimental Results, presents a brief description of the test results for the components and systems that were used in the Dynamic Airloads Program. Results are provided for all testing, regardless of the successful or unsuccessful conclusion of any particular test. For tests which were unsuccessful or produced unsatisfactory results, information is provided on the diagnosis and correction that were made to obtain successful conclusions.

The final section, Evaluation of Design Based on Experimental Results, presents in brief descriptive and tabular form a summary of all testing integrated into an overall system evaluation. The statistical methods that were used to compile this summary are described briefly; the detailed methods are fully documented in an appendix.

The extensive design, analysis, and testing outlined in this report resulted in a unique, fully qualified instrumentation system capable of acquiring the necessary information for the Dynamic Airloads Program. The report presents a logical sequence of design, fabrication, installation, and testing of the instrumentation system, unique in many respects, which successfully recorded the data.

DESCRIPTION OF TEST EQUIPMENT

THE INSTRUMENTATION SYSTEM

The instrumentation system was to provide data in a reliable manner within a substantiated maximum value of error and in a form which was usable for automated processing. Sensitivity changes and drift corrections as functions of ambient temperature and interaction load value were to be made during the computer processing. All instruments and systems were selected to meet accuracy targets and were laboratory-evaluated in the temperature and vibration environment to prove their accuracy and integrity. The signals from a large majority of the transducers were considered as dynamic measurements with all frequencies of information from 0 to 60 cycles per second to be accurately determined. All signals were corrected for phase shifts caused by the recording and reproducing systems and by the data filter networks on the aircraft.

ROTOR INSTRUMENTATION

The rotor instrumentation consisted of the blade instrumentation shown in Figure 1, blade root angle (flap, lead/lag, and pitch) transducers, and the rotor shaft and hub instrumentation shown in Figures 2 through 4. Two types of pressure transducers were considered for the blade differential-pressure measurements. One was the NASA variable-reluctance differential sensor which had been used on several previous programs. The other choice was the absolute and differential surface-mounted strain-gage transducer developed by Battelle Memorial Institute and manufactured by Scientific Advances Incorporated. The Scientific Advances transducer was chosen because it was easier to install and replace; and with the use of pairs of absolute sensors on the top and bottom of the blade, it would not be necessary to drill the structural blade spar. The choice was not a clear-cut one because the Scientific Advances transducers required a signal-conditioning system which necessitated a large development effort. Operational amplifiers, located on the rotating system, were needed to preamplify the lower level signals and to reduce the number of sliprings required.

Blade Pressure Measurements

Pressure transducers were used to measure the rotor airload (differential) pressure in a chordwise and spanwise array of

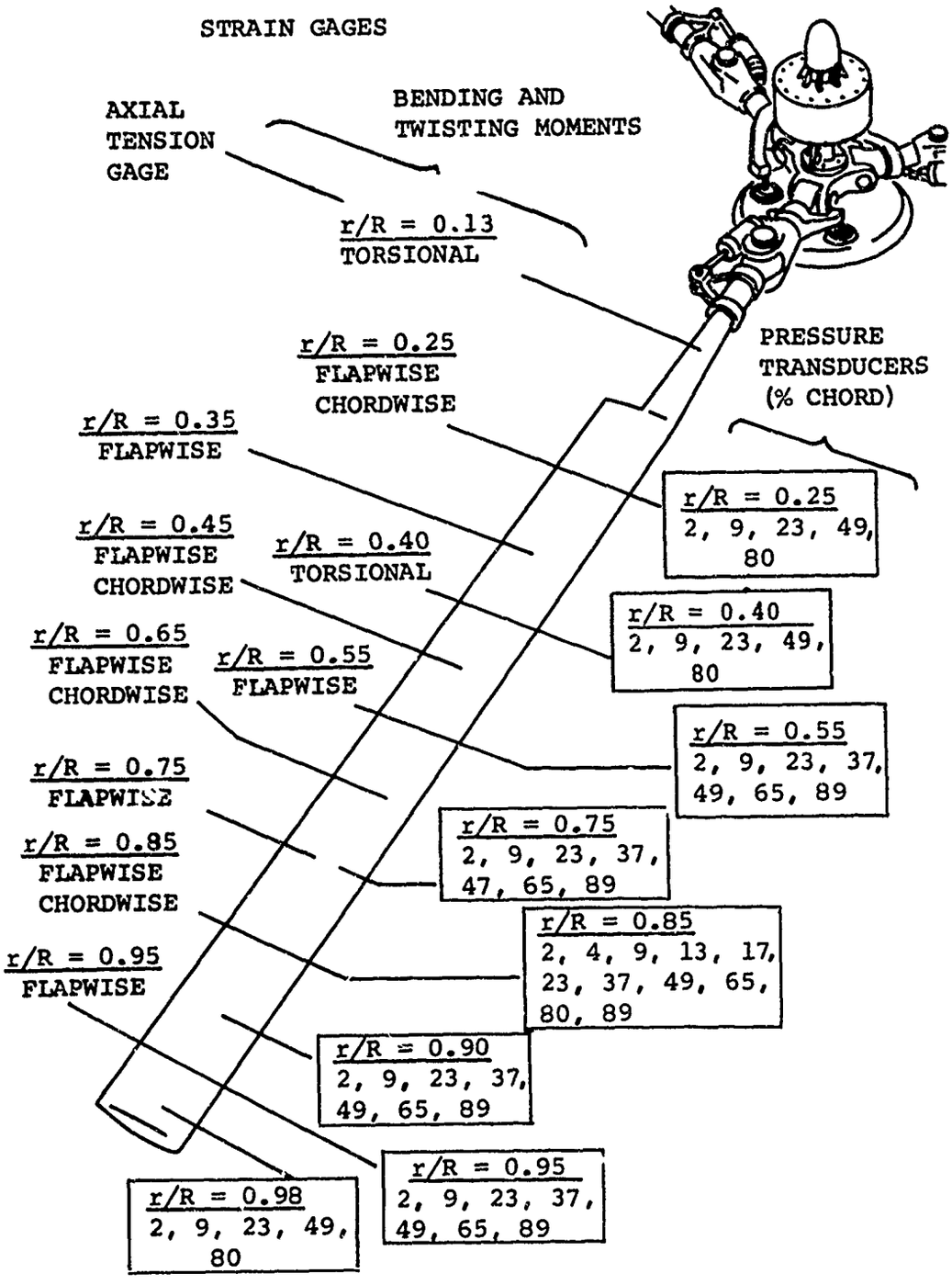

Figure 1. Installation of Rotor Blade Instrumentation.

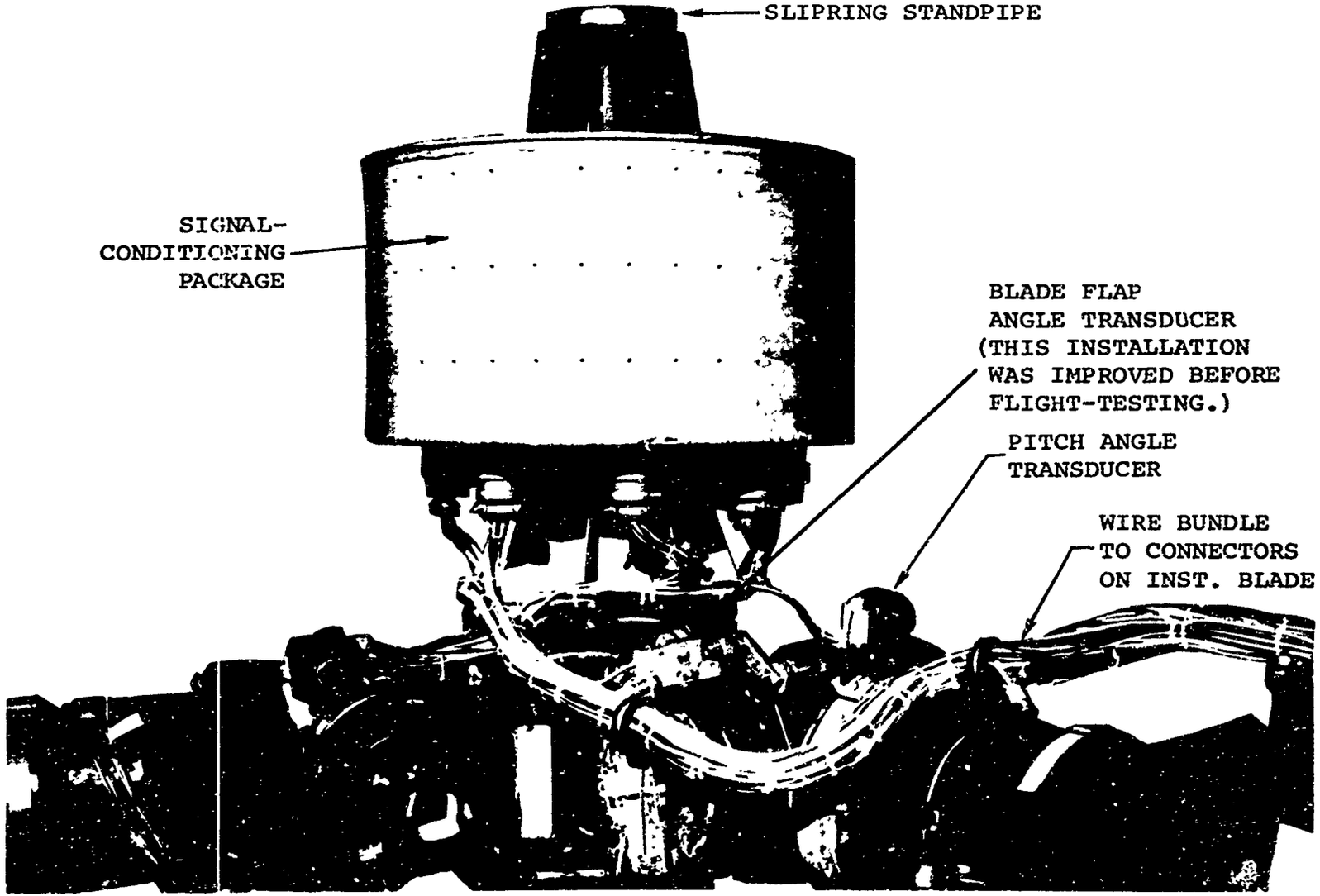

Figure 2. Aft Rotor Signal-Conditioning Package and Instrumentation.

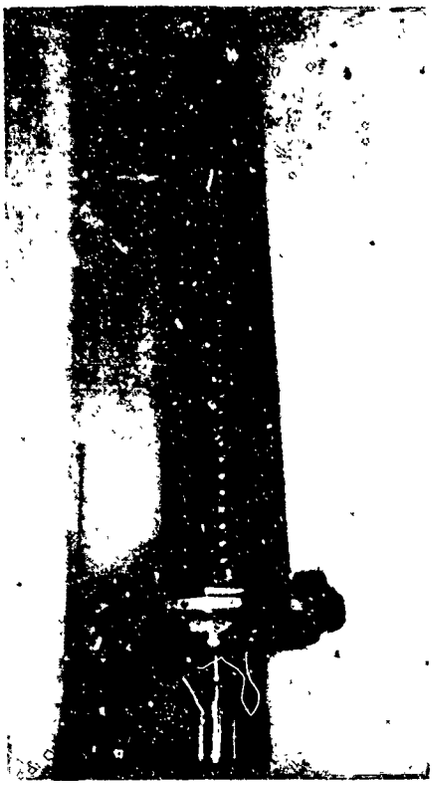

Figure 3. Rotor Head Slipring Assembly.

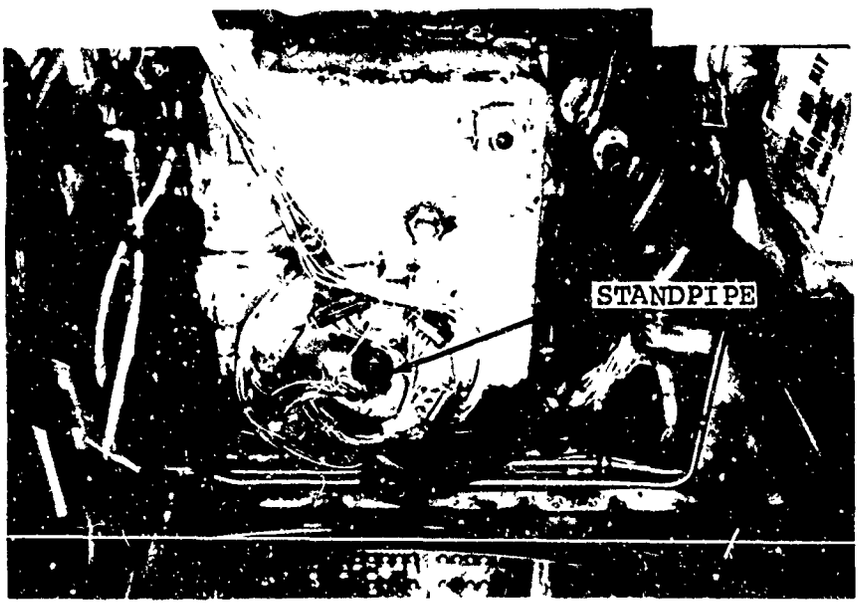

Figure 4. Forward Transmission Sump Showing Standpipe, Wiring, and Disconnect Points.

blade locations as shown in Figure 1. The pressure transducers were installed as shown in Figure 5. The sensors were attached to the blades by bonding the tabs to the blade surface with an elastic adhesive which allowed negligible strain transmittal from the blade. A wide sleeve of epoxy filler was applied around the chord of the blade at the sensor location. The effect was to have a flush diaphragm with little change in the airfoil dimensions. The units installed in this manner were the 5-to-20-psi absolute-pressure transducers and the differential-pressure transducers of three different sensitivities (2, 5, and 10 psi). A plastic tube supported within the blade was used to port each differential-pressure transducer to the bottom blade surface.

Absolute-Pressure Transducers

The absolute-pressure transducers utilized were Model M-7 types manufactured by Scientific Advances Incorporated. These units sense pressure by means of a strain-gaged diaphragm. A 4-arm etched-foil strain-gage bridge is bonded to the inside surface of a flat diaphragm, which is an integral part of a thin evacuated capsule. The cavity is sealed with a 0.003-inch-thick cover. Four small wires are connected to the bridge and brought out through the edge of each transducer for the electrical connections. The transducer is mounted on a 1-inch-long paddle with epoxy resin as shown in Figure 6. A terminal strip is also mounted on the paddle and the transducer leads are soldered, with 500°F solder, to the terminal strip. Specifications for the type M-7 transducer are shown in Table I.

TABLE I
ABSOLUTE-PRESSURE TRANSDUCER SPECIFICATIONS

Range	Linearity and Hysteresis % F.S.	Sensitivity mv/v/psi	Temp. Effect on Sensitivity %/°F	Temp. Effect on Zero % F.S./°F
5-20 psia	± 1.5	0.05	0.16	0.24

Differential-Pressure Transducers

The differential-pressure transducers utilized were also manufactured by Scientific Advances Incorporated. Each of these units was a Model SPT-7 and was essentially the same as the type M-7 absolute-pressure transducer with the exception that

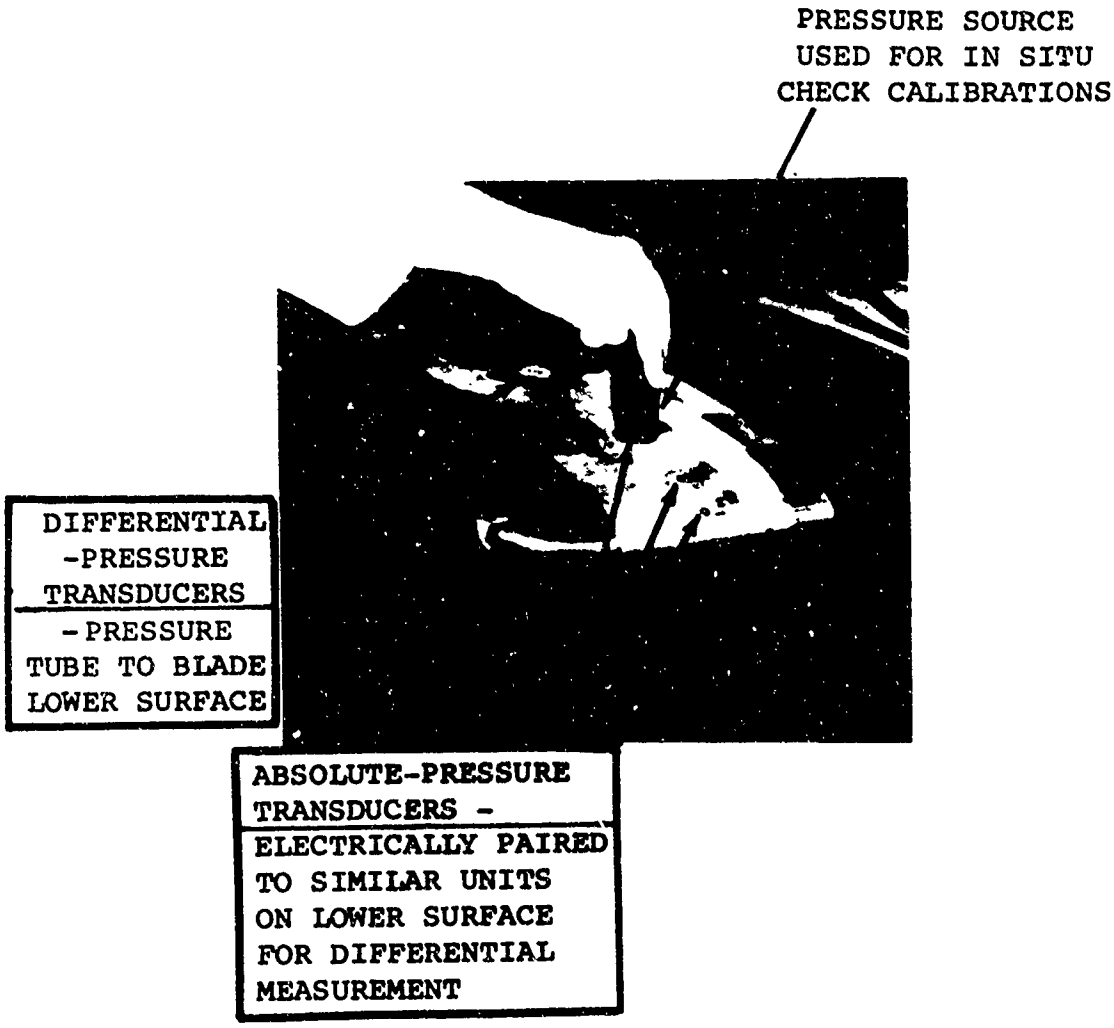

Figure 5. Installation of Pressure Transducers on Rotor Blade Tip.

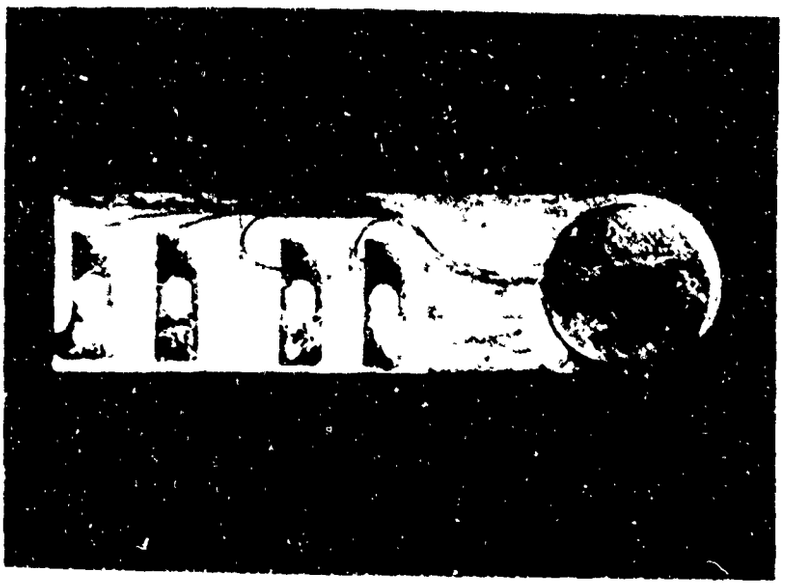

Figure 6. Absolute-Pressure Transducer.

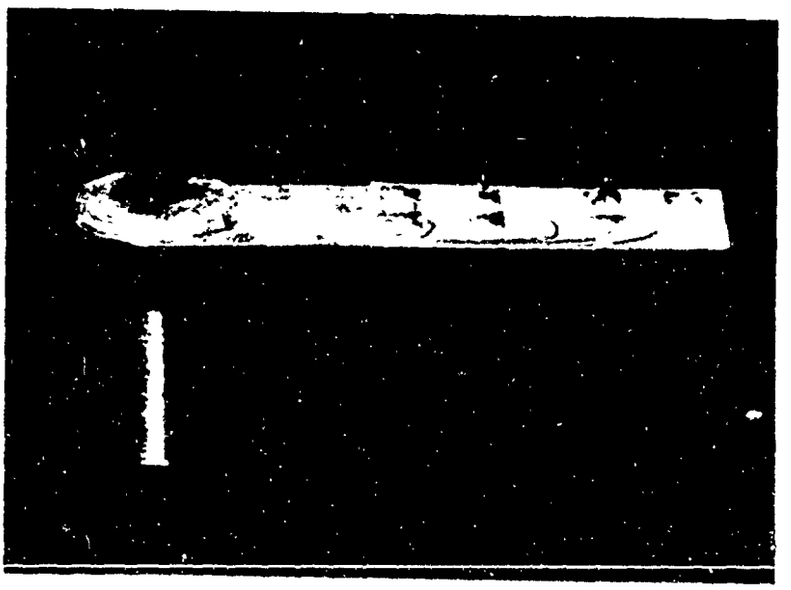

Figure 7. Differential-Pressure Transducer.

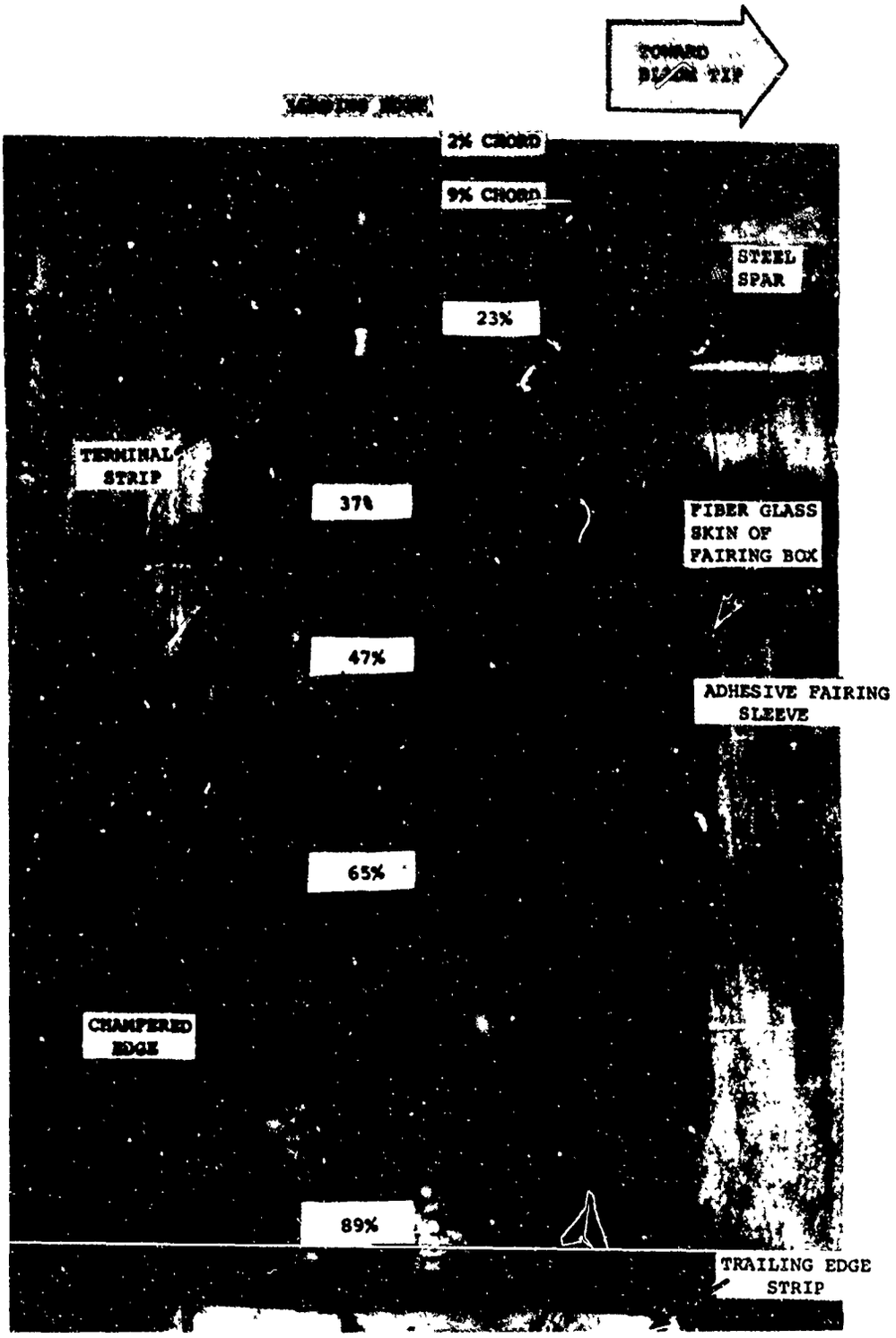

Figure 8. Typical Rotor Blade Pressure Transducer Installation.

the capsules were not sealed and evacuated but had a pressure port drilled in the back of the case. A length of tubing was attached to the transducer to extend the port to the bottom surface of the blade as shown in Figure 7. Differential transducers of three different ranges were used: ±10 psid, ±5 psid, and ±2 psid. The sensitivity in mv/v/psi for an input of 3 volts and the temperature effects on sensitivity and on zero are shown in Table II.

TABLE II
DIFFERENTIAL-PRESSURE TRANSDUCER SPECIFICATIONS

Range	Sensitivity mv/v/psi	Temp. Effect on Sensitivity %/°F	Temp. Effect on Zero % F.S./°F
±10 psid	0.05	0.16	0.24
± 5 psid	0.06	0.16	0.24
± 2 psid	0.07	0.16	0.26

Blade Pressure Transducer Locations

The pressure transducers were installed on the blades in accordance with Boeing-Vertol installation drawing number 114FT5666 in the locations listed in Table III. Typical installations are shown in Figure 8.

TABLE III
PRESSURE TRANSDUCER INSTALLATION ON FORWARD AND AFT ROTOR BLADES

Data Code			Blade Span in Inches from ℄ Rotor Hub	Blade Chord in Inches from Leading Edge
Fwd. Blade	Aft. Blade	Item		
4177	4231	Absolute-pressure pair	89.41	0.46
4178	4232	Absolute-pressure pair	89.41	2.09
4179	4233	Absolute-pressure pair	89.41	5.29
4180	4234	Differential-pressure	89.41	11.25
4181	4235	Differential-pressure	89.41	18.30

TABLE III - Continued

Data Code Fwd. Blade	Data Code Aft Blade	Item	Blade Span in Inches from ℄ Rotor Hub	Blade Chord in Inches from Leading Edge
4182	4236	Absolute-pressure pair	140.62	0.46
4183	4237	Absolute-pressure pair	140.62	2.09
4184	4238	Absolute-pressure pair	140.62	5.29
4185	4239	Differential-pressure	140.62	11.25
4186	4240	Differential-pressure	140.62	18.30
4187	4241	Absolute-pressure pair	194.68	0.46
4188	4242	Absolute-pressure pair	194.68	2.09
4189	4243	Absolute-pressure pair	194.68	5.29
4190	4244	Differential-pressure	194.68	8.50
4191	4245	Differential-pressure	194.68	11.25
4192	4246	Differential-pressure	194.68	15.10
4193	4247	Differential-pressure	194.68	20.40
4194	4248	Absolute-pressure pair	267.25	0.46
4195	4249	Absolute-pressure pair	267.25	2.09
4196	4250	Absolute-pressure pair	267.25	5.29
4197	4251	Differential-pressure	267.25	8.50
4198	4252	Differential-pressure	267.25	11.25
4199	4253	Differential-pressure	267.25	15.10
4200	4254	Differential-pressure	267.25	20.40
4201	4255	Absolute-pressure pair	299.92	0.46
4202	4256	Absolute-pressure pair	299.92	0.92
4203	4257	Absolute-pressure pair	299.92	2.09
4204	4258	Absolute-pressure pair	299.92	2.99
4205	4259	Absolute-pressure pair	299.92	3.91
4206	4260	Absolute-pressure pair	299.92	5.29
4207	4261	Differential-pressure	299.92	8.50
4208	4262	Differential-pressure	299.92	11.25
4209	4263	Differential-pressure	299.92	15.10
4210	4264	Differential-pressure	299.92	18.30
4211	4265	Differential-pressure	299.92	20.40
4212	4266	Absolute-pressure pair	318.02	0.46
4213	4267	Absolute-pressure pair	318.02	2.09
4214	4268	Absolute-pressure pair	318.02	5.29
4215	4269	Differential-pressure	318.02	8.50
4216	4270	Differential-pressure	318.02	11.25

TABLE III - Continued

Data Code Fwd. Blade	Data Code Aft Blade	Item	Blade Span in Inches from ℄ Rotor Hub	Blade Chord in Inches from Leading Edge
4217	4271	Differential-pressure	318.02	15.10
4218	4272	Differential-pressure	318.02	20.40
4219	4273	Absolute-pressure pair	339.07	0.46
4220	4274	Absolute-pressure pair	339.07	2.09
4221	4275	Absolute-pressure pair	339.07	5.29
4222	4276	Differential-pressure	339.07	8.50
4223	4277	Differential-pressure	339.07	11.25
4224	4278	Differential-pressure	339.07	15.10
4225	4279	Differential-pressure	339.07	20.40
4226	4280	Absolute-pressure pair	347.64	0.46
4227	4281	Absolute-pressure pair	347.64	2.09
4228	4282	Absolute-pressure pair	347.64	5.29
4229	4283	Differential-pressure	347.64	11.25
4230	4284	Differential-pressure	347.64	18.30

Blade Bending, Twisting, and Tension Gages

Strain gages were installed on the rotor blades in the locations shown in Figure 1. Fifteen type C6-141-350 strain gages (manufactured by The Budd Company) were installed on one forward and one aft rotor blade, with bridge configurations arranged to measure flapwise and chordwise bending and torsional and axial loads. The gages were installed in accordance with Boeing-Vertol drawing number 114FT5666 in the locations listed in Table IV.

TABLE IV
STRAIN-GAGE INSTALLATION ON FORWARD AND AFT ROTOR BLADES

Data Code Fwd. Blade	Data Code Aft Blade	Item	Blade Span in Inches from ℄ Rotor Hub	Blade Chord in Inches from Leading Edge
5261	5276	Radial tension	46.16	Pitch axis
5262	5277	Flap bending	89.41	4.49
5265	5280	Flap bending	124.00	4.49

TABLE IV - Continued

Data Code Fwd. Blade	Data Code Aft Blade	Item	Blade Span in Inches from ℄ Rotor Hub	Blade Chord in Inches from Leading Edge
5267	5282	Flap bending	159.44	4.49
5269	5284	Flap bending	194.68	4.49
5270	5285	Flap bending	230.95	4.49
5272	5287	Flap bending	267.25	4.49
5273	5288	Flap bending	299.92	4.49
5275	5290	Flap bending	339.07	4.49
5263	5278	Chord bending	89.41	5.20
5268	5283	Chord bending	159.44	5.20
5271	5286	Chord bending	230.95	5.20
5274	5289	Chord bending	299.92	5.20
5264	5279	Torsion	47.83	4.49
5266	5281	Torsion	140.62	4.49

Blade Root Motions

Rotary potentiometers were used for indicating blade root angular positions in the flap, lead/lag, and pitch axes. The installations on the forward and aft rotors were identical, using Type 2094 rotary potentiometers manufactured by the Markite Products Corporation. The instrumentation installations for the forward blade root motions are shown in Figures 9, 10, and 11. Table V shows the blade root motion potentiometer data codes and parameters.

TABLE V
BLADE ROOT MOTION POTENTIOMETER INSTALLATION

Data Code Forward	Data Code Aft	Item
2024	2025	Blade pitch angle
2026	2027	Blade flap angle
2028	2029	Blade lead/lag angle

Hub Motion Accelerometers

To provide information for the vectorial solution of hub motion, three Type 4-203, ±5g-range accelerometers (manufactured by Consolidated Electrodynamics Corporation) were installed on each rotor hub, equally spaced at 0-degree, 120-degree, and 240-degree positions. The forward hub installation

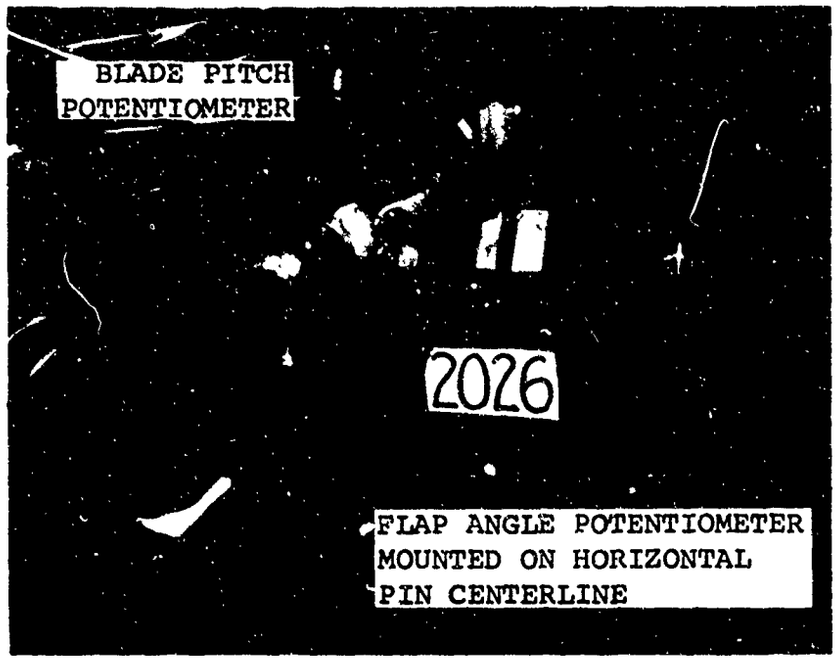

Figure 9. Rotor Blade Flap Angle Potentiometer Installation.

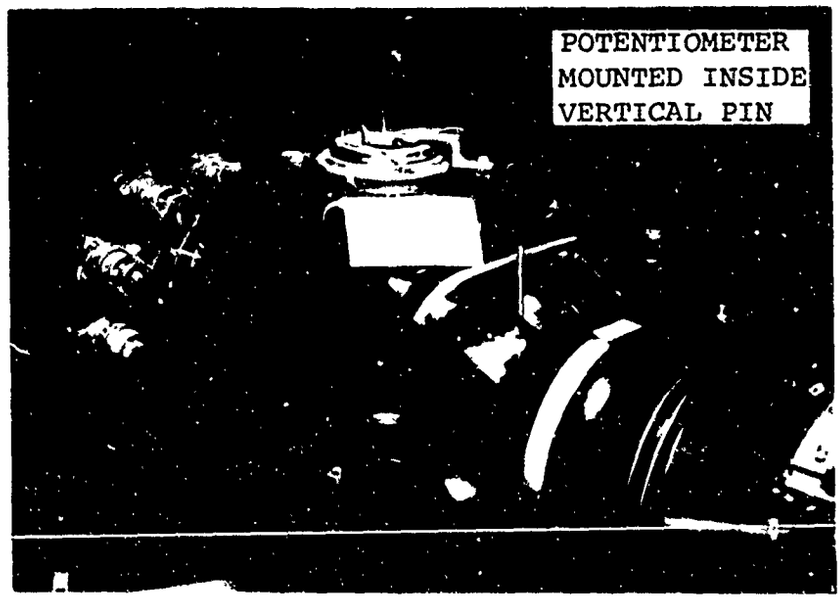

Figure 10. Rotor Blade Lead/Lag Angle Potentiometer Installation.

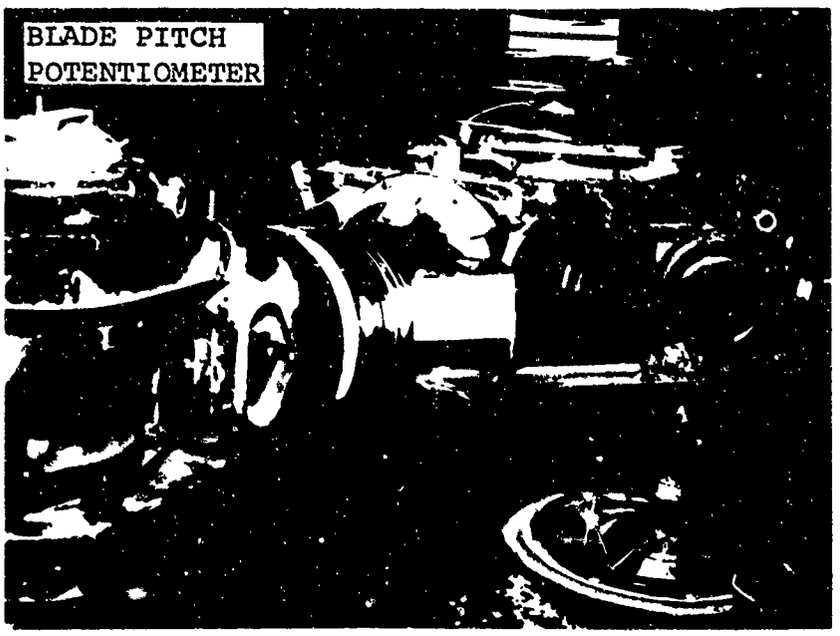

Figure 11. Rotor Blade Pitch Angle Potentiometer Installation.

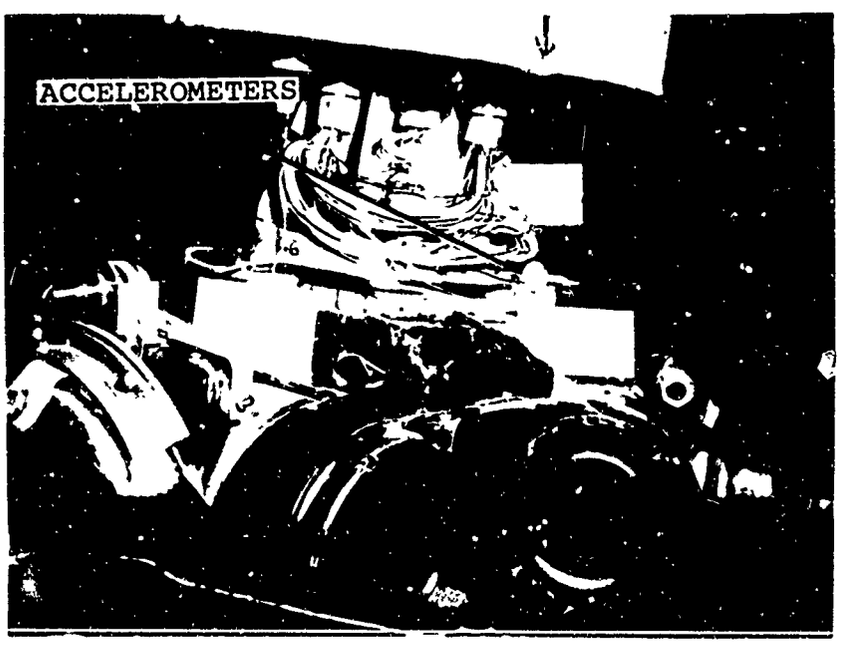

Figure 12. Rotor Hub Accelerometer Installation.

is shown in Figure 12; the aft hub installation is identical. Table VI provides the accelerometer data codes and parameters.

TABLE VI
HUB MOTION ACCELEROMETERS INSTALLATION

Data Code	Item
1044	Forward hub 0° position - yellow arm
1046	Forward hub 120° position - green arm
1048	Forward hub 240° position - red arm
1045	Aft hub 0° position - yellow arm
1047	Aft hub 120° position - green arm
1049	Aft hub 240° position - red arm

Rotor Shaft Load and Moment Gages

Seven strain-gage bridges were installed in accordance with Boeing-Vertol drawings numbers 114FT5667 and 114FT5668 on the forward and aft rotor shafts respectively. Epoxy-backed foil strain gages, Type C6-141-350, manufactured by The Budd Company, were used for the bridge configurations to measure shaft shear, bending, and torque loads. P-type semiconductor gages, Type SPB2-07-35-C6, manufactured by Baldwin-Lima-Hamilton, were used for the lift load measurements because of the very small dynamic strain produced along the shaft lift axis. The installation of the strain gages on both rotor shafts is shown in Figure 13. Table VII shows the rotor strain-gage data codes and parameters.

TABLE VII
ROTOR SHAFT LOAD AND MOMENT GAGES INSTALLATION

Data Code		
Forward Shaft	Aft Shaft	Item
5247	5254	Shear 0-180° azimuth
5248	5255	Shear 90-270° azimuth
5249	5256	Bending 0-180° azimuth
5250	5257	Bending 90-270° azimuth
5251	5258	Torque
5253	5259	Lift-steady
5252	5260	Lift-alternating

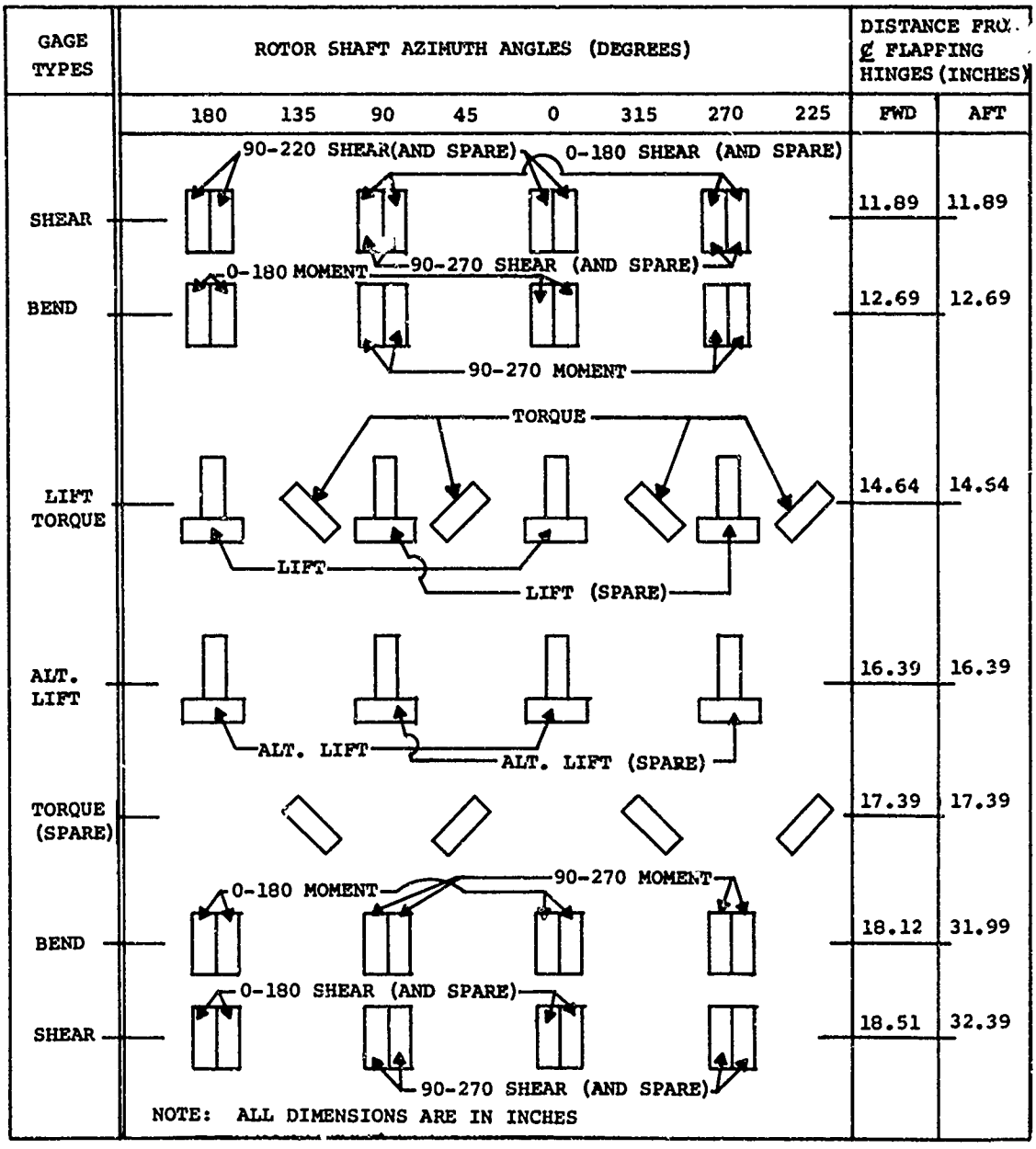

Figure 13. Rotor Shaft Load and Moment Gages Installation.

One-Per-Revolution Pulse - Forward Rotor Head

The rotor rpm (1/rev.) pulse was produced by an Electro-Products Laboratory Incorporated magnetic pickup, part number 3040. The pickup was attached to the stationary swashplate ring, and a striker plate was attached to the rotating swashplate. A pulse is created during each rotor revolution when the striker plate passes over the magnetic pickup. Figure 14 shows the installation, and Figure 15 shows the azimuthal position of the instrumented blades at the instant the 1/rev. pulse occurs. The pulse counter output was identified by data code 3027.

Signal Conditioning (Rotating-Source Data)

The decision to use amplifiers in the rotating conditioner was based on three considerations. First, some of the differential transducers at the trailing edge of the rotor blade were expected to have low outputs in the range of 300 microvolts, and it was felt that a preamplifier in the rotating system was necessary to keep a proper signal-to-noise ratio. Second, the available slipring assemblies had insufficient capacity for the conventional 4-wire strain-gage system, so a means of converting a differential signal to a single-ended signal was desired where a common signal return could be shared. Third, the amplifier afforded a good means of performing the algebraic addition of absolute-pressure measurements to obtain differential signals in advance of the sliprings. One of the circuit modules used for performing these functions is shown in Figure 16.

Additional slipring economy was required and was accomplished by the incorporation of ac-to-dc isolated power converters in the rotating system for pressure transducer excitation. These power circuits comprised a small transformer to provide isolation, a full-wave rectifier, a 5-volt regulator diode, and a filter capacitor. Regulation was ensured by having a regulated power input, a regulator diode with a low temperature coefficient, and a constant load. For the 54 pressure measurements on the instrumented blade, 59 sliprings were needed. One ring was required for each amplifier output, plus one ring for a common signal return and two rings for prime ac power to the strain-gage power converters. Two additional rings were needed for supplying power to the operational amplifiers. To enhance reliability, the power supply employed several rings redundantly.

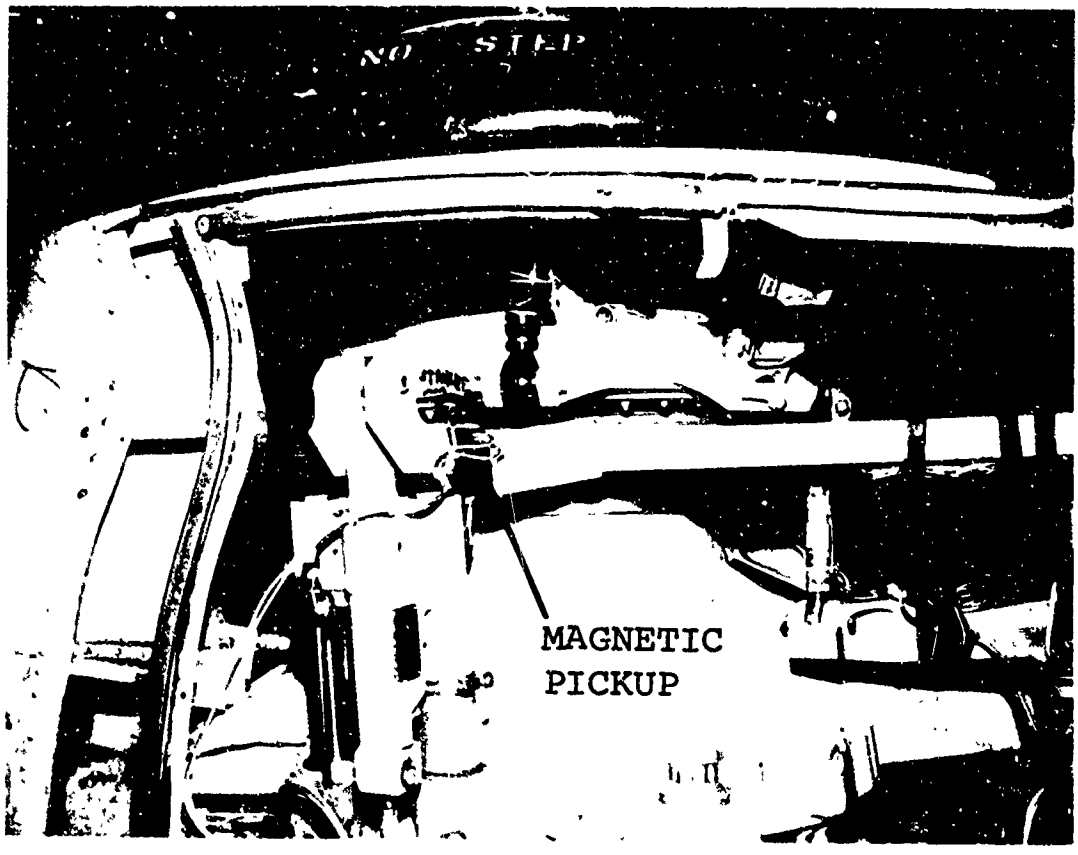

Figure 14. One-Per-Revolution Pulse Counter Installation.

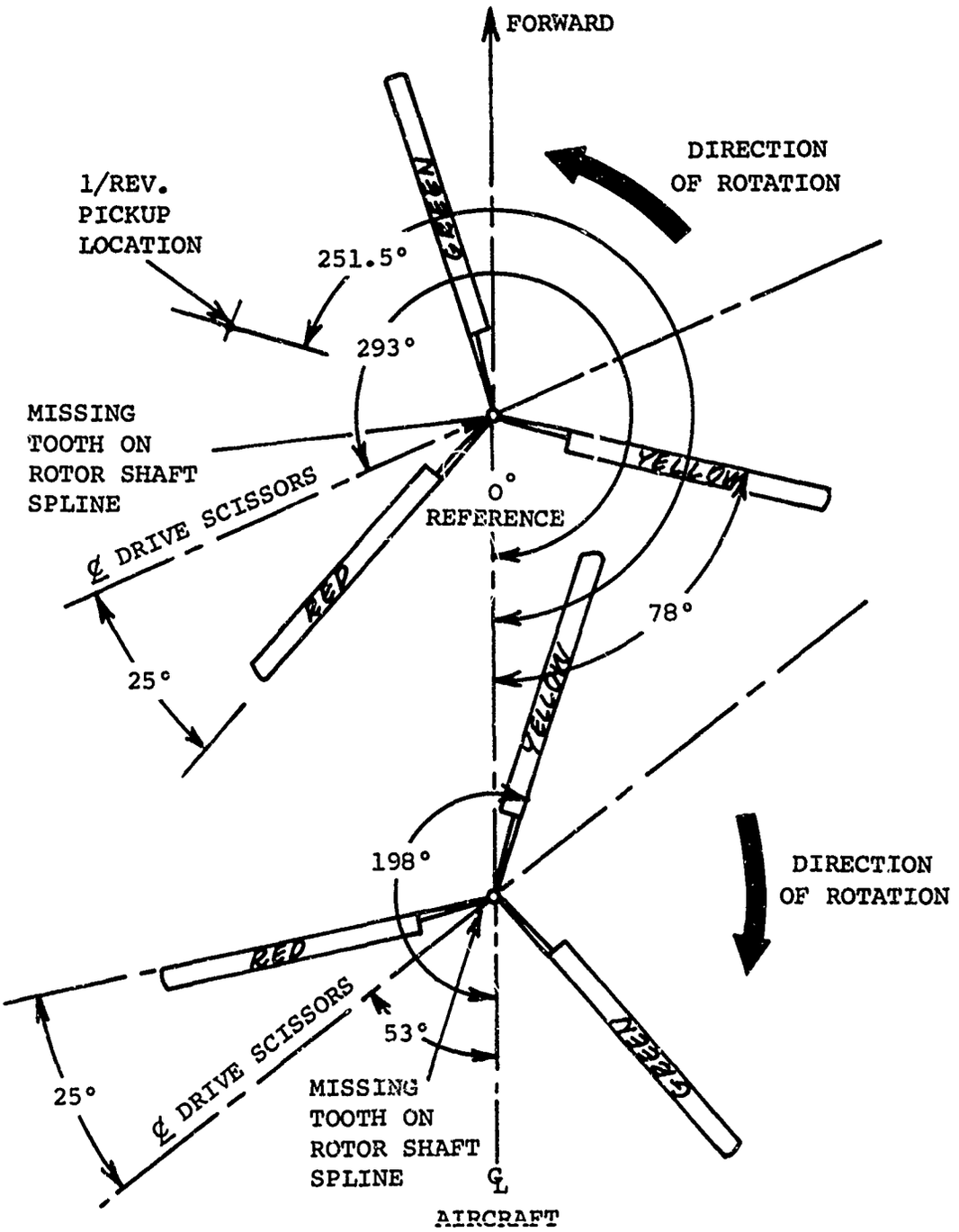

Figure 15. Position of Rotor Blades at Instant of One-Per-Revolution Pulse.

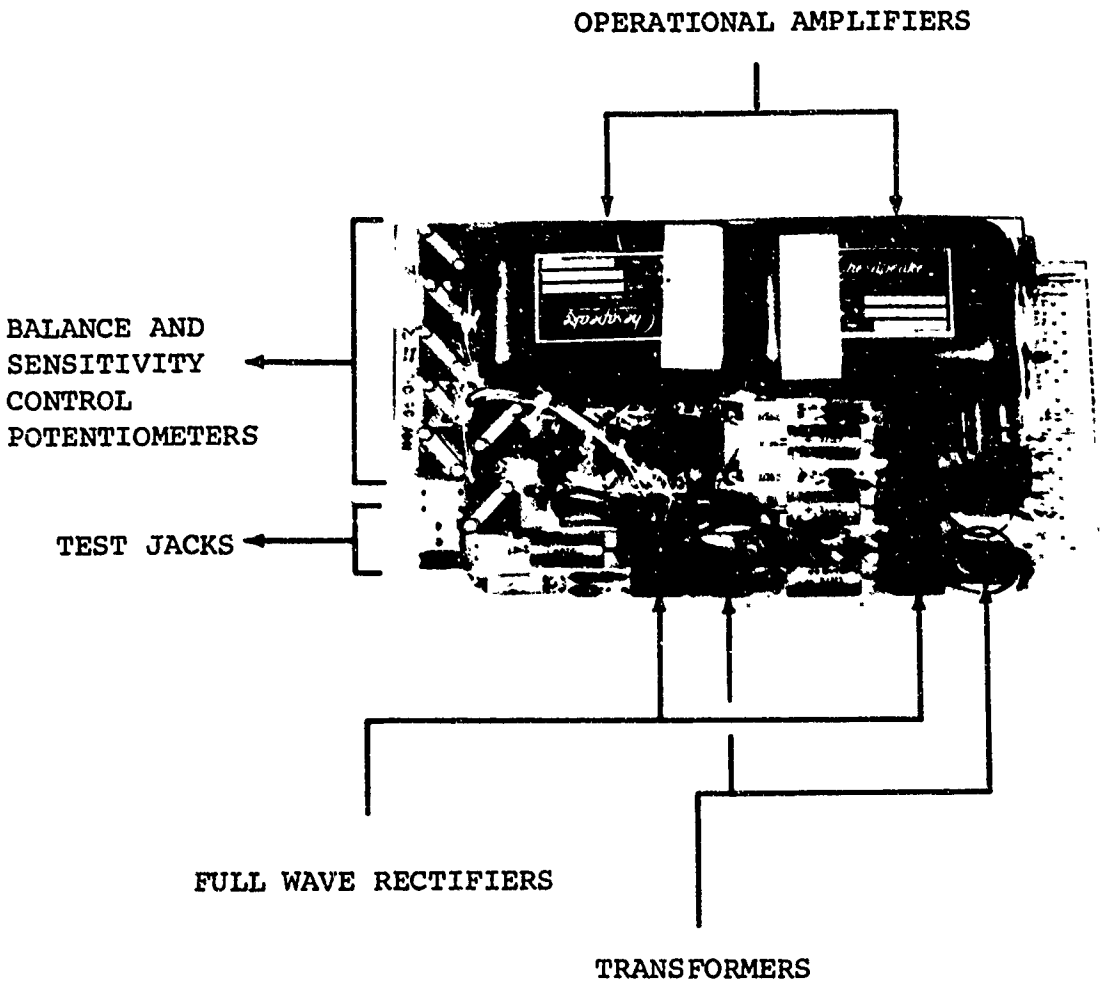

Figure 16. Signal-Conditioning Amplifier.

For the circuits where a pair of absolute transducers was used for differential measurements, a means of standardizing the sensitivity of one transducer to the other was necessary. This was accomplished by a series potentiometer in the excitation circuit of the more sensitive transducer. As will be explained later, the transducers were individually selected for each rotor blade location. The more sensitive ones were placed on the top of the blade. The shunt standardization resistors for the top and bottom transducers were then adjusted to the same equivalent pressure. The values of the shunt standardizing resistors were predetermined in laboratory calibrations of the transducers. The sensitivity normalization procedure was as follows:

1. Each bottom transducer was individually zero-balanced by first removing the excitation from the top transducer and then balancing the bottom unit to a null output. Power was then applied to both transducers, and the top transducer was balanced to achieve a net null.

2. For sensitivity standardization, a shunt resistor was applied to one leg of the transducer of the pair which had the least sensitivity. A shunt of equal equivalent pressure was then applied to the other transducer. The series sensitivity control was adjusted until the net output of the pair was zero.

The balance procedure for the differential transducers was conventional, and no sensitivity controls were necessary.

Since the transformers on the rotating power supplies were small and not designed for high isolation, and because the operational amplifiers had only fair common mode rejection, the danger of undesirable common mode signals was present. To diminish this danger, several precautions were taken. First, a high-impedance loop to aircraft ground was provided to keep the common mode currents as small as possible. The limiting factor in keeping the loop impedance high was the stray coupling due to the mechanical proximity of the wiring to the aircraft structure. The potential midpoints of the transducer circuits were connected to the output common to provide a balance path for common mode currents. With these precautions, the output of the amplifier still had an average peak-to-peak output of 15 millivolts from the common mode signal, in addition to 4 millivolts peak-to-peak random noise

generated internally by the amplifier. Because the information spectrum necessary for the airload study was only 0 to 60 cycles per second, a low-pass filter was employed to diminish the undesired common mode signal and noise to less than 0.5 millivolt peak-to-peak. The filter was followed by a T-pad attenuator for signal-level control and a constant-impedance match to the filter. The millivolt-controlled oscillator (MVCO) followed the filter.

As mentioned previously, data from the forward and aft instrumented rotor blades were time-shared by the recording system as an economy measure. Data from one rotor were recorded for two rotor cycles, followed by the other rotor for two rotor cycles. The first rotor cycle was provided to allow the switching transients to decay and to provide for relay cycle time. Data were reduced from the second rotor cycle. The signal-switching task was accomplished by a group of six-pole double-throw relays which switched the signal leads and the shield. Both rotors had identical transducer configurations and were switched on a one-for-one basis. This switching was done at the amplifier output (downstream of the slipring) so that the filters, T-pad attenuators, and the MVCO's were also time-shared.

The in-flight sensitivity and zero-reference standardization corrections were also provided by the signal-conditioning units. Short-circuit and reference-millivolt signals were substituted for the data signals at the MVCO inputs to provide standardizing signals. An operational amplifier zero-drift reference signal was also provided by removing the transducer excitation.

The circuits discussed in the preceding paragraphs were housed in the rotor hub signal-conditioning package assemblies, Boeing-Vertol Part Number 114FT5672, which were installed on each rotor head. The package accommodated 36 printed-circuit-type modules for conditioning and amplifying, where necessary, the signal outputs from the blade, rotor shaft, and rotor head transducers. A cover, which was removable to allow for circuit adjustments, was installed for flight. A typical installation is shown in Figure 2.

The rotor slipring assemblies, Boeing-Vertol Part Numbers 114FT3000-32 and 114FT3000-33, were installed on the forward and aft rotor heads to handle the signal outputs from the rotor instrumentation. See Figure 3. Each slipring consisted

of a mandrel which incorporated 120 sliprings, a housing assembly to accept 8 brush holders, a special adapter to connect the slipring assembly mechanically to the rotor shaft, and an external cover tube, which in this case was a housing assembly which provided the main support for the rotor head signal-conditioning package. To enable the wire packs from each rotor slipring to be routed into the cabin area and recording table, a standpipe was installed inside each rotor shaft. The standpipe passed through a special transmission oil sump, where it was secured with a large locknut. Disconnect points for the slipring wiring were located at the base of the oil sump adjacent to the standpipe opening, as shown in Figure 4.

AIRFRAME INSTRUMENTATION

The airframe instrumentation consisted of flight control load transducers and motion potentiometers, fuselage and transmission vibration accelerometers, and aircraft attitude instrumentation. This type of instrumentation is generally considered to be routine for helicopter flight testing, except for the large number of transducers required. Since sequencing of the rotor signals provided ample recording capacity, the number of transducers caused no problems. The general details of the system are as follows:

1. Potentiometers - Potentiometers were used for control actuator and attitude vanes position measurements.

2. Accelerometers - Accelerometers were used to measure the aircraft response to the dynamic airloads. The type used was the force-balance type which affords a large accurate dynamic range and a high-level (10-volt-per-g) output.

3. Pressure transducers - Pressure transducers were used to provide an airspeed and altitude recording.

4. Attitude and rate gyros - Attitude and rate gyros were also included.

Control Loads

Forward and aft rotor control loads were recorded by use of epoxy-backed foil strain gages, Types C6-141-350, C12-141-350,

and C6-141-R2B, manufactured by The Budd Company. The control loads instrumentation is shown in Figures 17 through 20; Table VIII shows the control loads instrumentation data codes and parameters.

TABLE VIII
CONTROL LOADS INSTRUMENTATION

Data Code Forward	Aft	Item
5207	5208	Pivoting actuator tension
8207	8208	Swiveling actuator tension
8153	5153	Long. cyc. trim actr. (fixed link tension)
5295	5296	Pitch link tension - yellow blade

Control Motions

Upper and lower flight control motions were measured by Type 2094 rotary potentiometers (manufactured by Markite Products Corporation) and by Models 108 and 109 linear potentiometers (manufactured by Bourns Laboratories Incorporated). Several of the installations are shown in Figures 21 and 22. Tables IX and X show the control motions data codes and parameters.

TABLE IX
UPPER CONTROL MOTIONS INSTRUMENTATION

Data Code Forward	Aft	Item
2019	2021	Pivoting actuator motion
2018	2022	Swiveling actuator motion
2020	2023	Longitudinal cyclic trim actuator motion

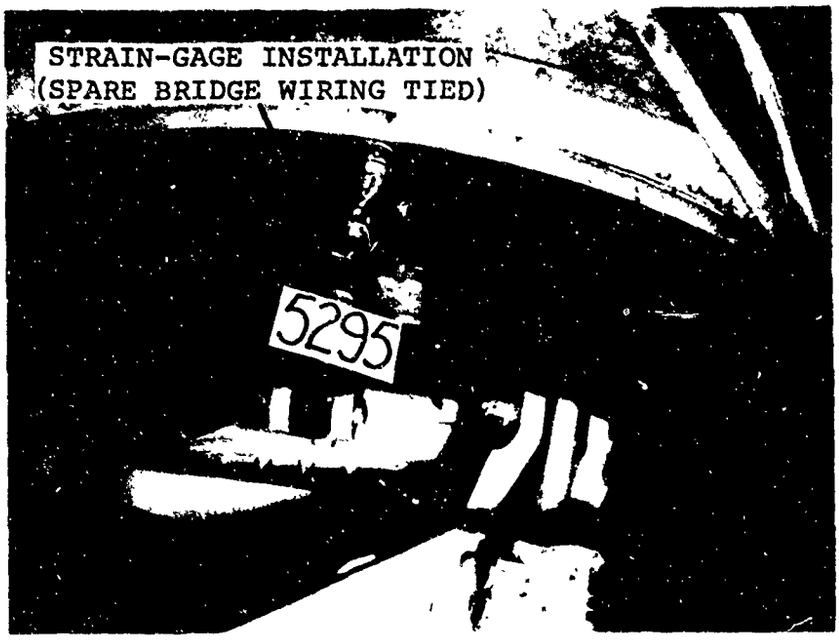

Figure 17. Pitch Link Load Strain-Gage Installation.

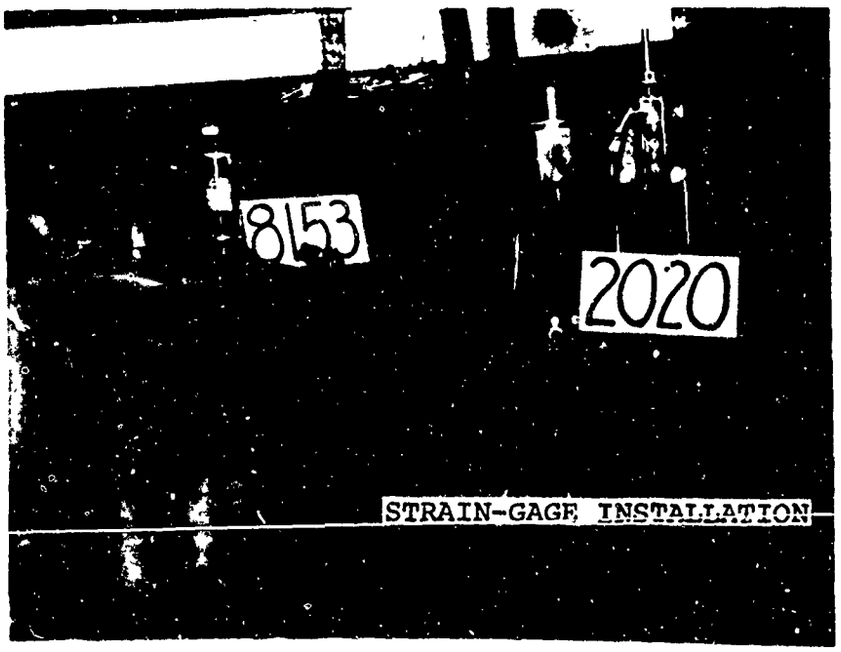

Figure 18. Longitudinal Cyclic Trim Actuator Load (Fixed-Link Tension) Strain-Gage Installation.

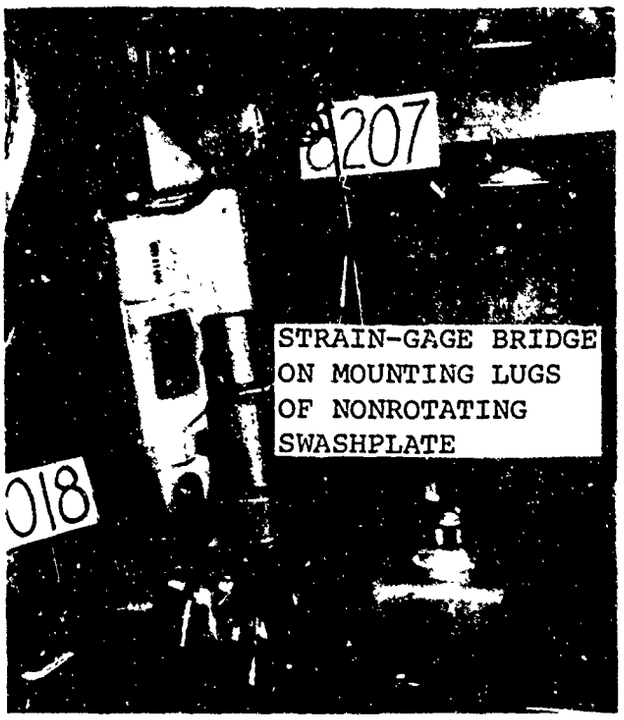

Figure 19. Swiveling Actuator Load Strain-Gage Installation.

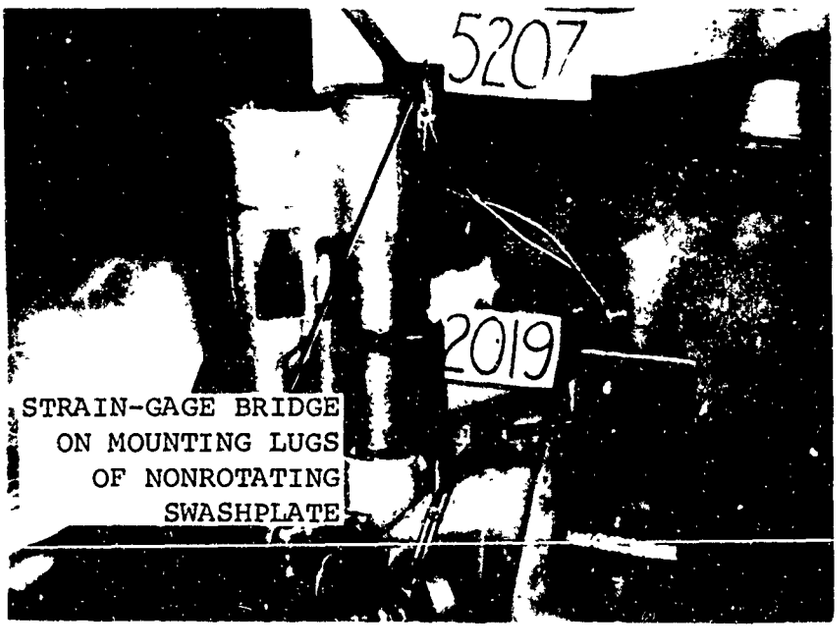

Figure 20. Pivoting Actuator Load Strain-Gage Installation.

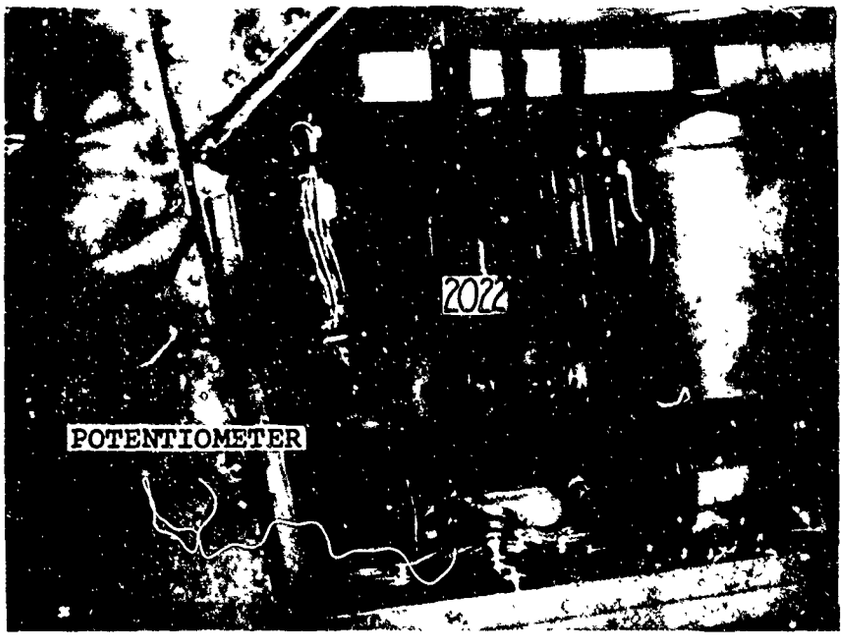

Figure 21. Swiveling Actuator Motion Potentiometer Installation.

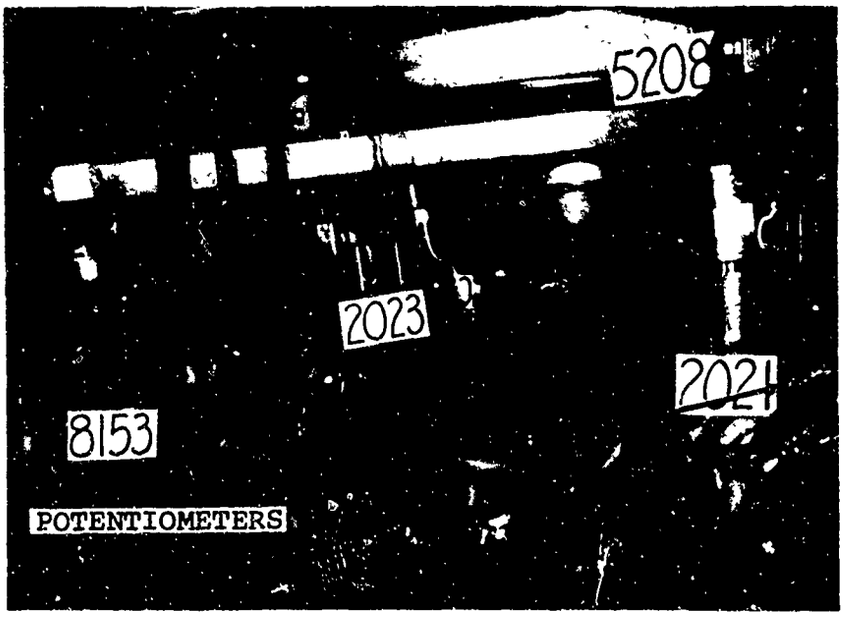

Figure 22. Pivoting Actuator and Longitudinal Cyclic Trim Actuator Motion Potentiometers Installations.

TABLE X
LOWER CONTROL MOTIONS INSTRUMENTATION

Data Code	Item
2001	Collective stick position
2002	Longitudinal control stick position
2003	Lateral control stick position
2004	Directional pedal position
2016	DCP speed trim actuator
2017	DCP stick trim position

Fuselage Vibration

Linear force-balance accelerometers (transducers) were used to measure the aircraft response to the dynamic airloads. These transducers, Model 4310A manufactured by Systron-Donner Corporation, have a large accurate dynamic range and a high-level (10-volt-per-g) output. The transducers were installed throughout the helicopter as listed in Table XI and as shown in Figure 23. A typical transducer installation is shown in Figure 24.

TABLE XI
FUSELAGE VIBRATION TRANSDUCER INSTALLATION

Data Code	Item	Location			
		Station	Waterline	Buttline	Direction
7101	Cockpit floor	52.0	- 17.0	37.75R	Vertical
7105	Pilot's panel	50.0	+ 3.0	30.50R	Vertical
7106	Cockpit floor	70.6	- 17.0	32.00R	Vertical
7115	Cockpit floor	95.0	- 17.0	0.0	Vertical
7116	Cockpit floor	95.0	- 17.0	0.0	Lateral
7117	Cockpit floor	95.0	- 17.0	0.0	Long.
7129	Cabin floor	160.0	- 30.0	44.0L	Vertical
7131	Cabin floor	160.0	- 30.0	44.0R	Vertical
7134	Cabin floor	240.0	- 30.0	44.0L	Vertical
7135	Cabin floor	240.0	- 30.0	44.0L	Lateral
7136	Cabin floor	240.0	- 30.0	44.0R	Vertical
7138	Frame crown	240.0	+ 50.12	0.0	Lateral
7139	Cabin floor	320.0	- 30.0	44.0L	Vertical
7141	Cabin floor	320.0	- 30.0	44.0R	Vertical
7145	Cabin floor	400.0	- 30.0	44.0L	Vertical

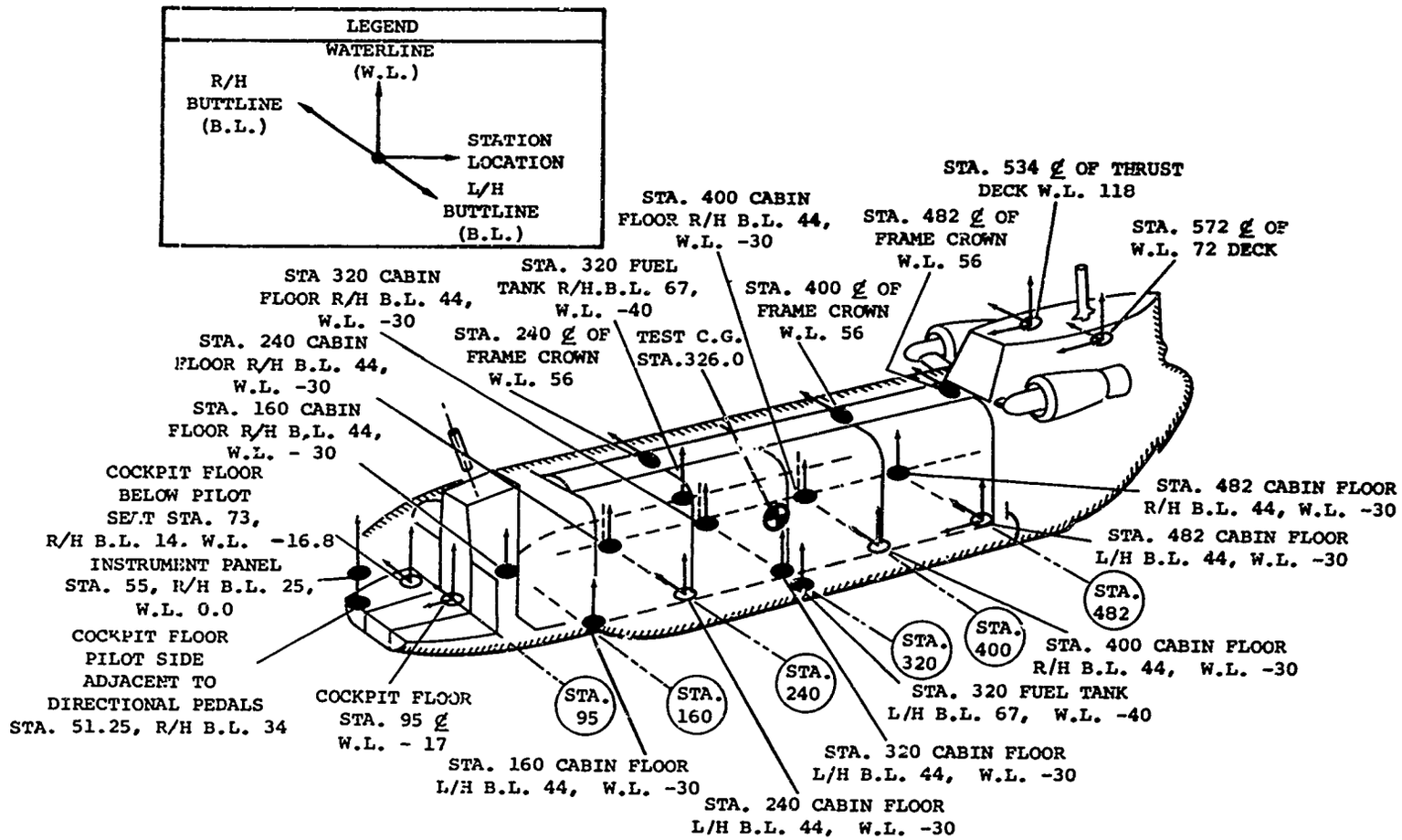

Figure 23. Location and Orientation of Fuselage Response Accelerometers.

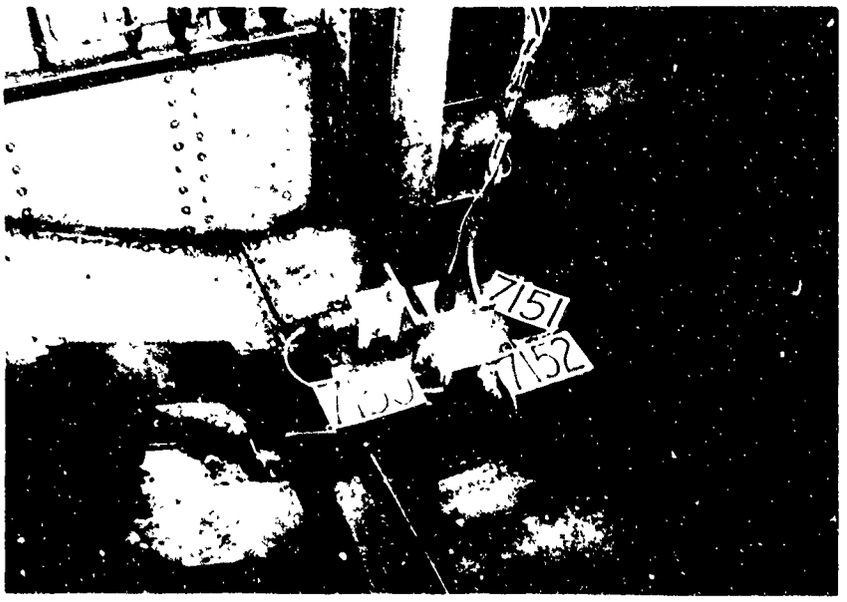

Figure 24. Typical Fuselage Accelerometer Installation.

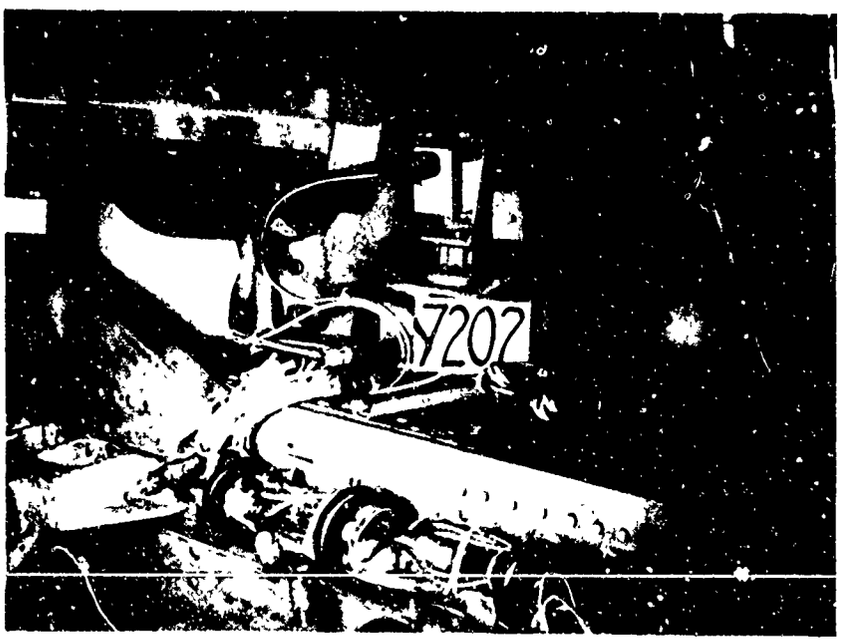

Figure 25. Typical Transmission Accelerometer Installation.

TABLE XI - Continued

Data Code	Item	Location Station	Waterline	Buttline	Direction
7146	Cabin floor	400.0	- 30.0	44.0L	Lateral
7147	Cabin floor	400.0	- 30.0	44.0R	Vertical
7149	Frame crown	400.0	+ 50.12	0.0	Lateral
7150	Cabin floor	482.0	- 30.0	44.0L	Vertical
7151	Cabin floor	482.0	- 30.0	44.0L	Lateral
7152	Cabin floor	482.0	- 30.0	44.0L	Long.
7153	Cabin floor	482.0	- 30.0	44.0R	Vertical
7156	Frame crown	482.0	+ 47.25	0.0	Lateral
7163	Aft deck	534.0	+118.0	0.0	Vertical
7164	Aft deck	534.0	+118.0	0.0	Lateral
7165	Aft deck	534.0	+118.0	0.0	Long.
7166	Aft pylon	572.0	+ 72.0	8.0R	Vertical
7167	Aft pylon	572.0	+ 72.0	8.0R	Lateral
7168	Aft pylon	572.0	+ 72.0	8.0R	Long.
7206	Left fuel tank	320.0	- 40.8	67.0L	Vertical
7207	Right fuel tank	320.0	- 40.8	67.0R	Vertical

Transmission Vibration

The motions of the forward and aft rotors relative to their mounting points were measured by mounting linear force-balance accelerometers (transducers) at the transmission and aft rotor thrust-bearing mounting points. These transducers were the same types that were used to measure fuselage vibration, Model 4310A manufactured by Systron-Donner Corporation. The transducers were installed as listed in Table XII, with a typical installation shown in Figure 25.

TABLE XII
TRANSMISSION VIBRATION TRANSDUCER INSTALLATION

Data Code	Item	Forward Transmission Station	Waterline	Buttline	Direction
7197	Fwd. foot - thrust motion	76.0	66.0	0.0	Vertical
7198	Fwd. foot - thrust motion	76.0	66.0	0.0	Lateral

TABLE XII - Continued

Data Code	Item	Station	Waterline	Buttline	Direction
7199	Fwd. foot - thrust motion	76.0	66.0	0.0	Long.
7200	R.H. foot - thrust motion	91.0	69.0	18.0R	Vertical
7202	Aft foot - thrust motion	111.0	72.0	0.0	Vertical
	Aft Transmission				
7174	Aft thrust bearing	550.6	119.28	11.00R	Vertical
7175	Aft thrust bearing	550.6	119.28	11.00R	Lateral
7212	Aft thrust bearing	550.6	119.28	11.00R	Long.
7213	Aft foot r.h.	569.6	72.00	11.00R	Lateral
7214	Aft foot r.h.	569.6	72.00	11.00R	Long.

Aircraft Attitude

A pitot-static swivel-type head and dual vane assembly, Boeing-Vertol Part Number RD2FT5626-3, was used to measure airspeed, altitude, sideslip, and attack angles (see Figure 26). The assembly was mounted on the end of a nose boom which extended 11 feet from the nose of the aircraft. The pitot-static lines from the swivel head were routed through the tubular-section boom to the airspeed- and altitude-measuring equipment. This equipment, mounted in the nose of the helicopter, consisted of an airspeed-measuring transducer with a range of 0 to 350 knots and an accuracy of ±0.5 psid, Model Number PT283, manufactured by Statham Instruments Incorporated; and an altitude-measuring transducer with a range of 0 to 15 psia, Model Number 4-312, manufactured by Consolidated Electrodynamics Corporation. These units are shown in Figure 27.

Model TSP-1KΩ potentiometers (manufactured by Beckman), directly driven by the movement of each vane of the dual vane assembly, were used to obtain angle-of-sideslip and angle-of-attack measurements.

Pitch, roll, and yaw attitudes were recorded by two gyros, Type K3, Part Number JG7044A35, manufactured by Minneapolis-

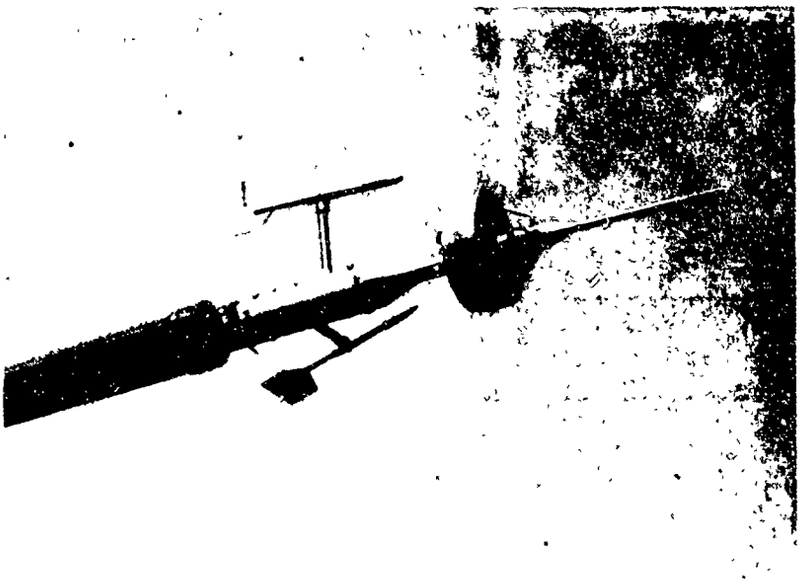

Figure 26. Nose Boom Instrumentation Installation.

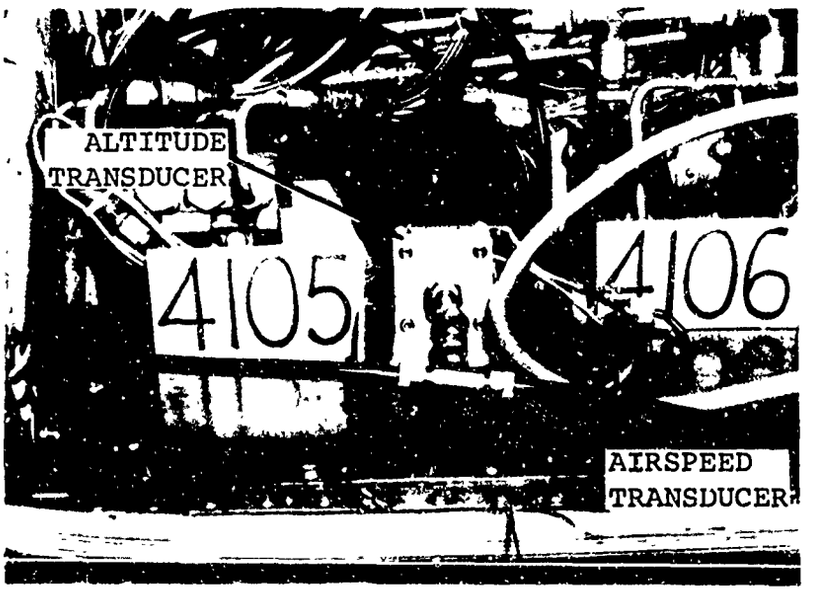

Figure 27. Airspeed and Altitude Transducer Installation.

Honeywell. One gyro was utilized to measure pitch and roll and one to measure yaw. Both units were located on the aft instrumentation table (see Figure 28) and were capable of measuring a maximum of ±45 degrees of pitch, roll, and yaw. Table XIII shows the attitude instrumentation data codes and parameters.

TABLE XIII
AIRCRAFT ATTITUDE INSTRUMENTATION

Data Code	Item
4105	Airspeed (boom system)
4106	Altitude (boom system)
2035	Sideslip angle (boom system)
2034	Attack angle (boom system)
3052	Pitch attitude
3053	Roll attitude
3017	Yaw attitude

Signal Conditioning (Nonrotating-Source Data)

Conventional signal-conditioning methods were used as an interface between the end instruments with the recording system. As is the usual case, each strain-gage circuit had a balance control, an excitation-voltage control, and a means of applying a shunt resistance standardization. The strain-gage signals were low but of sufficient level to drive the MVCO's. Control of the excitation voltage and a reference signal were provided by the signal conditioner for the potentiometers. The force-balance accelerometers had a potentiometer voltage divider at the output in order to provide a level control. The conditioned potentiometer and accelerometer signals were high level. The signal-conditioning system also included an in-flight standardization unit which provided several functions. Similar to the rotor standardization units in sequence, it disconnected the driving signals to all low-level and high-level subcarrier oscillators and substituted a short circuit and a voltage reference signal. The recorded information from this sequence was used to correct the data for oscillator zero and sensitivity changes.

SIGNAL MULTIPLEXING AND SEQUENCING

The requirements for the in-flight recording of approximately

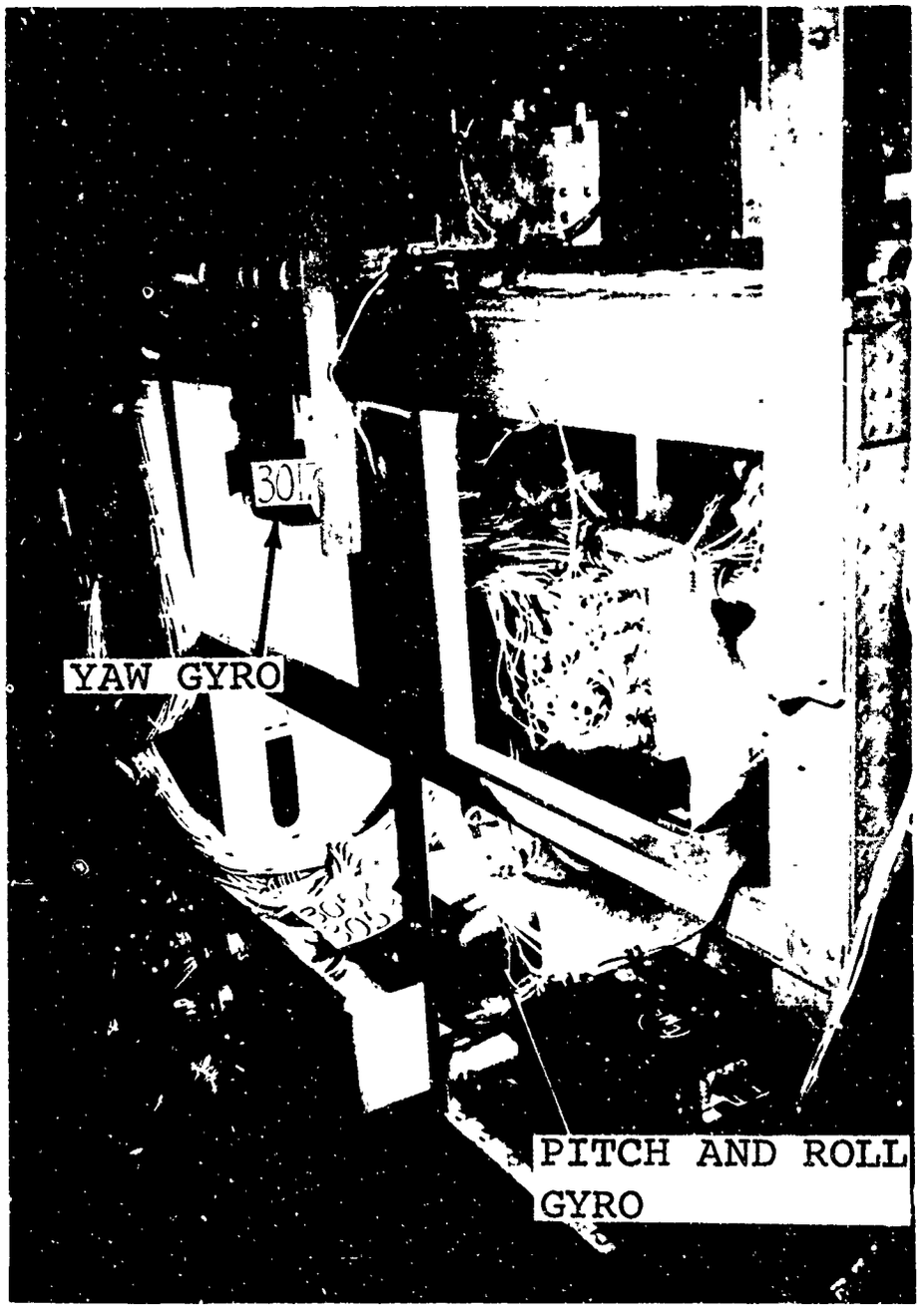

Figure 28. Attitude Gyro Installation.

237 data channels on one 14-track magnetic tape recorder made multiplexing necessary. The standard interrange instrumentation group (IRIG) narrow-band frequency modulation (NBFM) method was used. Low-level signals (0 to 20 millivolts) were conditioned to the NBFM signal using millivolt-controlled oscillators (MVCO); similarly, high-level signals (0 to 5 volts) were conditioned using voltage-controlled oscillators (VCO). These units were custom-built to a Boeing specification but did not differ appreciably from standard instruments.

The inputs to the recording system VCO's were obtained from signal-conditioning and standardizing units. As shown in Figure 29, separate systems for each of the two rotors and for the airframe instrumentation were provided with correlating voice recordings from the pilot. In-flight time reference was based on rotor cycles and azimuth. For convenience, time was prerecorded on a separate track as a common input for identifying the digitizing process runs in the ground station.

Sequencing

The number of parameters to be recorded exceeded the capacity of the single magnetic tape system despite the use of frequency multiplexing on narrow-band frequency modulation (NBFM). Therefore, it was decided to sequence (time-share) the rotor data. The sequencing was triggered by a one-per-revolution pulse fed through a trigger circuit designed specifically to cycle once for two pulses in every two cycles. The sequenced and nonsequenced parameters are shown in Table XIV.

INSTRUMENTATION CONTROL

The following controls were provided for operation of the instrumentation system during data flights.

Recording

The CARGO HOOK RELEASE on the pilot's control stick was diverted from its normal function for use as a recording START switch for the instrumentation system. A parallel START switch was also provided, adjacent to the troop commander's seat, for use by the flight test operations engineer, to relieve the pilot of this function during certain flight maneuvers. Figure 30 shows the location of the pilot's recording START switch.

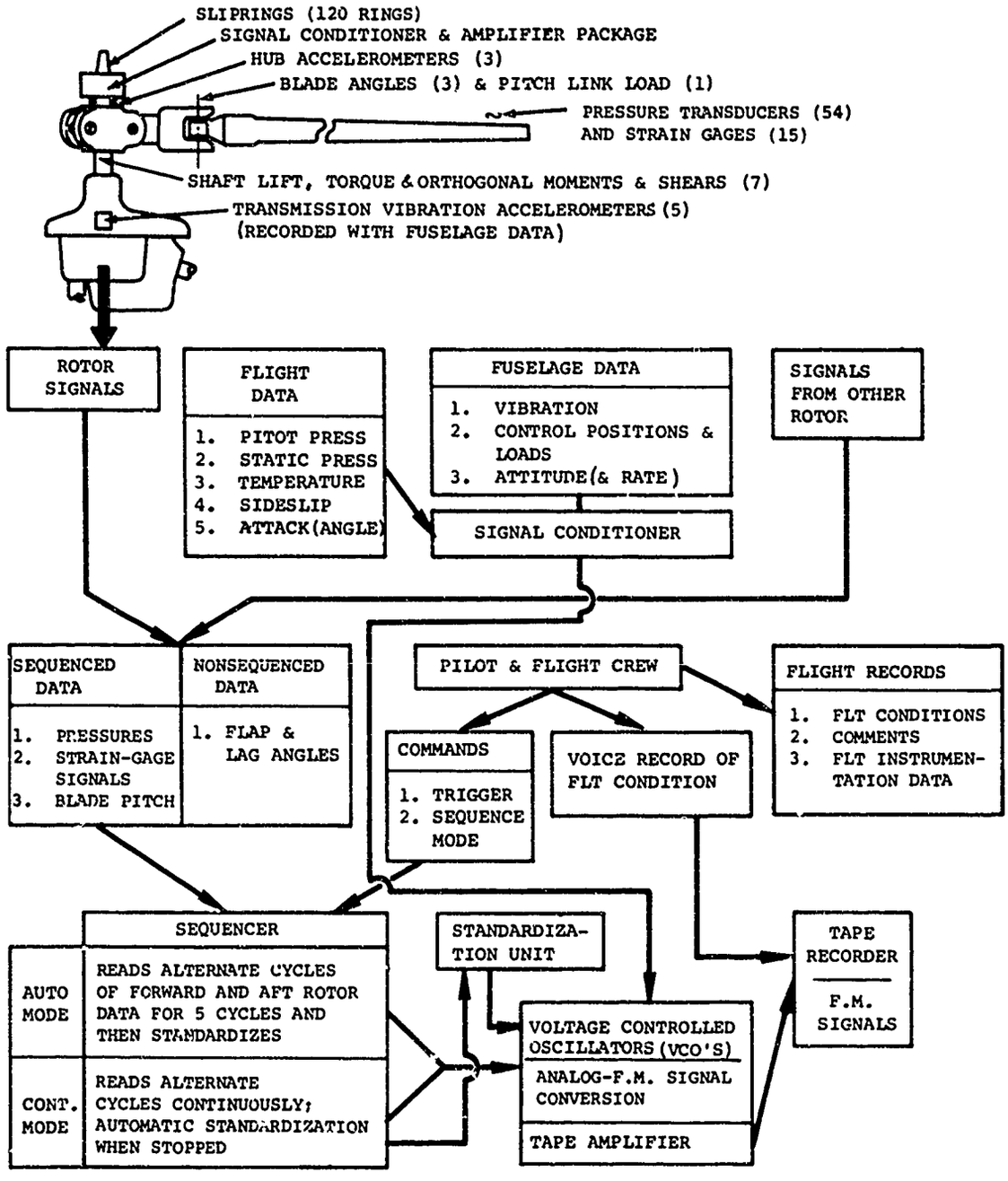

Figure 29. Dynamic Airloads Program Instrumentation System.

TABLE XIV
SEQUENCED AND NONSEQUENCED RECORDING PARAMETERS

Sequenced Parameters

Sequence 1 Data Codes
Forward Blade Pressures

4177	4195	4213
4178	4196	4214
4179	4197	4215
4180	4198	4216
4181	4199	4217
4182	4200	4218
4183	4201	4219
4184	4202	4220
4185	4203	4221
4186	4204	4222
4187	4205	4223
4188	4206	4224
4189	4207	4225
4190	4208	4226
4191	4209	4227
4192	4210	4228
4193	4211	4229
4194	4212	4230

Forward Blade Loads

5261	5266	5271
5262	5267	5272
5263	5268	5273
5264	5269	5274
5265	5270	5275

Forward Rotor Shaft Loads

5247	5250	5453
5248	5251	
5249	5252	

Forward Pitch Link Load

5295

Sequence 2 Data Codes
Aft Blade Pressures

4231	4249	4267
4232	4250	4268
4233	4251	4269
4234	4252	4270
4235	4253	4271
4236	4254	4272
4237	4255	4273
4238	4256	4274
4239	4257	4275
4240	4258	4276
4241	4259	4277
4242	4260	4278
4243	4261	4279
4244	4262	4280
4245	4263	4281
4246	4264	4283
4247	4265	4283
4248	4266	4284

Aft Blade Loads

5276	5281	5286
5277	5282	5287
5278	5283	5288
5279	5284	5289
5280	5285	5290

Aft Rotor Shaft Loads

5254	5257	5260
5255	5258	
5256	5259	

Aft Pitch Link Load

5296

TABLE XIV - Continued

Sequence 1 Data Codes Forward Upper Control Loads			Sequence 2 Data Codes Aft Upper Control Loads		
5207	8207	8153	5208	8208	8154
Forward Blade Motions			**Aft Blade Motions**		
2024			2025		
Forward Upper Control Motions			**Aft Upper Control Motions**		
2018	2019	2020	2021	2022	2023
Sequence 1 Data Codes Forward Hub Rotating Accelerometers			**Sequence 2 Data Codes Aft Hub Rotating Accelerometers**		
1044	1045	1046	1047	1048	1049

**Nonsequenced Parameters
Data Codes**

Fuselage and Transmission Vibration Measurements

7101	7105	7106	7115	7116	7117	7129
7131	7134	7135	7136	7138	7139	7141
7145	7146	7147	7149	7150	7151	7152
7153	7156	7163	7164	7165	7166	7167
7168	7174	7175	7197	7198	7199	7200
7202	7206	7207	7212	7213	7214	

Altitude and Flight Conditions			Forward and Aft Blade Motions	
4105	4106	2034	2026	2027
2035	3052	3053	2028	2029
3017	6017			

One-Per-Revolution Pulse	Lower Control Motions		
3027	2001	2002	2003
	2004	2016	2017

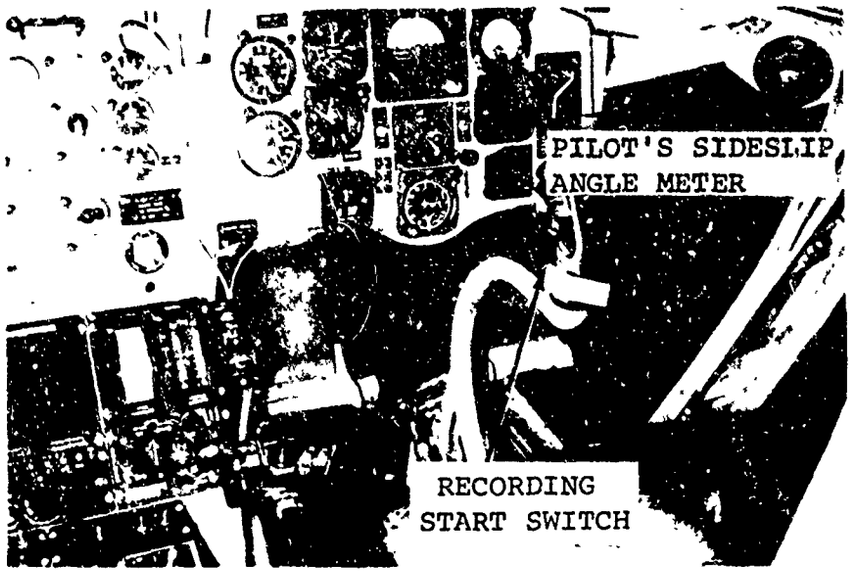

Figure 30. Pilot's Controls and Instruments.

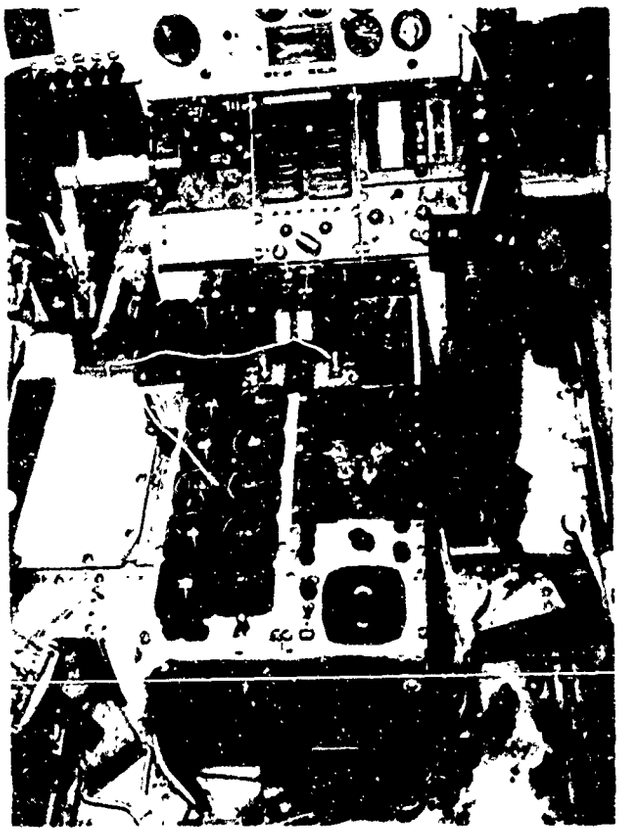

Figure 31. Pilot's Instrumentation Control Panel.

Pilot's Instrumentation Control Panel

A pilot's instrumentation control panel was located on the console and provided the following controls and indications:

1. Instrumentation MASTER POWER switch with indicator light for power ON position
2. Pitch and roll attitude gyro CAGED indicator light
3. Yaw attitude gyro CAGED indicator light
4. Magnetic tape FOOTAGE REMAINING indicator light
5. MODE OF SEQUENCE selector switch
6. SEQUENCE 1 indicator light
7. SEQUENCE 2 indicator light
8. Run counter indicator

The MODE OF SEQUENCE selector switch had four positions which actuated the following functions:

Sequence 1 - (switch in position 1) - provided for recording forward rotor head parameters only

Sequence 2 - (switch in position 2) - provided for recording aft rotor head parameters only

Sequence AUTO - (switch in position A1) - provided for automatic sequencing of the forward and aft rotor heads. Two rotor cycles were sampled on each head alternately five times

Sequence AUTO -CONTINUOUS - (switch in position AC) - provided for automatic sequencing of the forward and aft rotor heads continuously for as long as the switch was left in this position

The installation of the pilot's instrumentation panel is shown in Figure 31.

RECORDER, POWER, AND SUPPORT EQUIPMENT

Two instrumentation tables, one located forward and one aft of the rescue hatch in the helicopter cabin, were used to accommodate the recording system and associated equipment. The

tables contained equipment as follows:

Forward Instrumentation Table

1 Magnetic tape recorder and associated electronics (Ampex AR 200)
8 Racks of low-level voltage-controlled oscillators (VCO's)
8 Mixer amplifiers for VCO's
1 Reference oscillator
1 300-cps filter and signal attenuator box
1 Standardization box
2 Balance panel racks
14 Signal-conditioning modules (for non-rotor head parameters)
8 Regulated dc power supplies
1 Patch panel
1 One-per-revolution sequencing trigger circuit
1 Intervalometer
1 Power supply (Hathaway)
1 Record coder
1 Microphone
2 Sequencer boxes, each capable of sequencing 48 parameters
2 Amplifier racks
12 Amplifiers

Aft Instrumentation Table

1 Pitch and roll attitude gyro
1 Yaw attitude gyro
5 Racks of high-level voltage-controlled oscillators (VCO's)
1 Balance panel rack
15 Signal-conditioning modules (for non-rotor head parameters)
1 Pitch rate gyro
1 Roll rate gyro
1 Yaw rate gyro
1 Patch panel
1 Regulated dc power supply
2 Amplifier racks
12 Amplifiers

Installations of the instrumentation tables are shown in Figures 32 through 35.

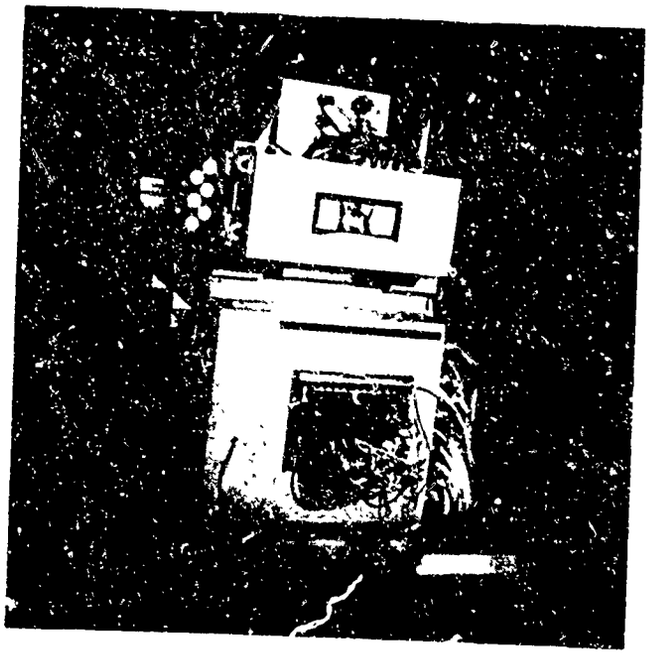

Figure 32. Forward Instrumentation Table Showing Patch Panel and Tape Recorder.

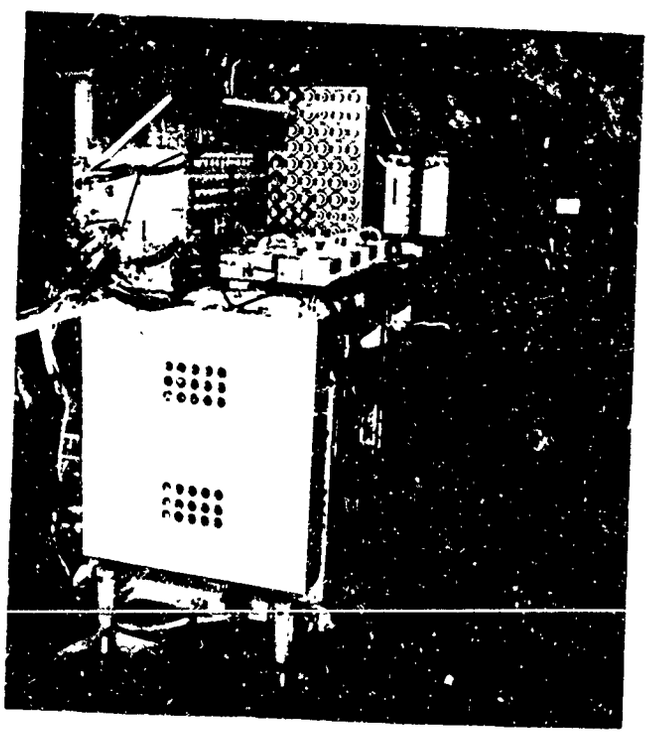

Figure 33. Forward Instrumentation Table - View Looking Forward.

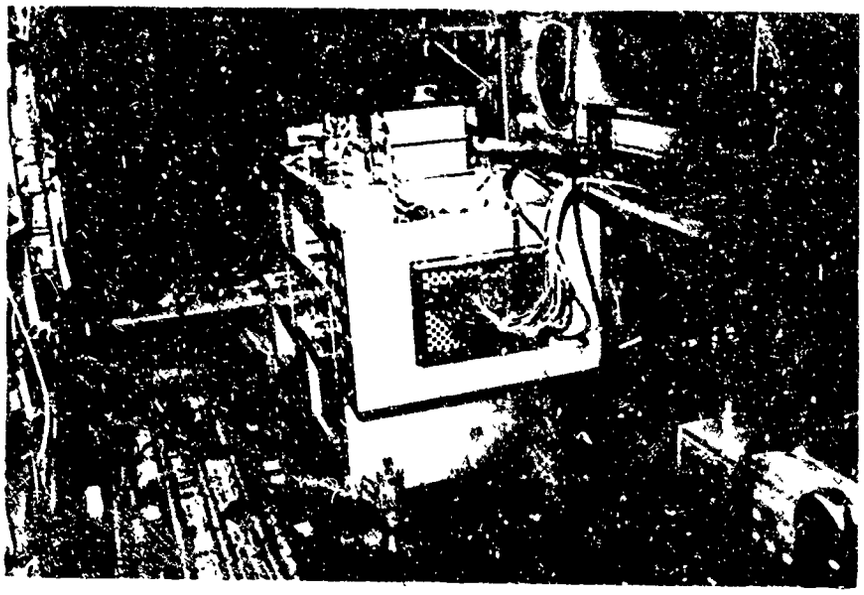

Figure 34. Aft Instrumentation Table Showing Patch Panel.

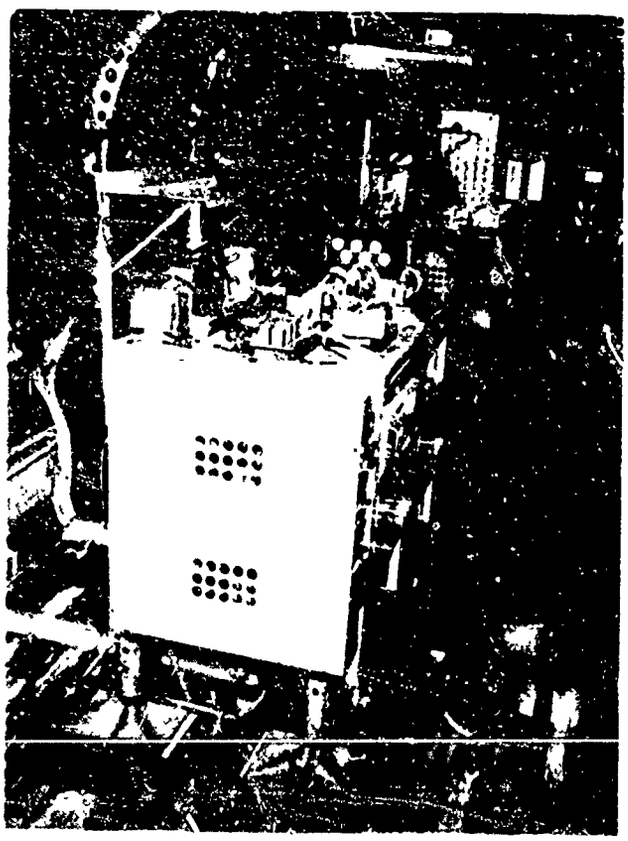

Figure 35. Aft Instrumentation Table - View Looking Forward.

Signal Wiring

Disconnect panels were installed in the forward and aft cabin areas to provide disconnects for collecting and distributing all transducer circuits to the appropriate instrumentation table, balance panel, or patch panel where they were patched to a specific tape track through VCO's. The forward main and auxiliary disconnect panels are shown in Figure 36; the aft panels are identical.

Power

Power for the instrumentation system was obtained from the aircraft power distribution boxes; 28 volts dc and 115 volts ac at 400 cps were fed to the main instrumentation power distribution box in the cabin area.

Coordination

Record identification and coordination were effected by using the Boeing-Vertol encoder which provided run identification, total time of run, and provision time reference. The code was presented by use of an 8-bit decimal format. This decimal signal was recorded on the magnetic tape and was also numerically displayed on NIXIE tubes on the copilot's instrument panel. The NIXIE indicator is shown in Figure 37.

DISCRIMINATING AND DIGITIZING

Following a flight, the recorded data were reproduced to analog form in the flight test telemetry and data processing center (ground station). The narrow-band frequency modulation (NBFM) data were discriminated by commercial pulse-averaging discriminators. Discriminators for interrange instrumentation group (IRIG) bands 9 through 16 had 60-cycle-per-second low-pass constant-amplitude filters in the output. Discriminators for the lower bands were equipped with low-pass filters of frequencies consistent with the IRIG schedule (modulation index greater than 5). Three sets of 12 discriminators were available to enable three multiplexed composite signals to be simultaneously discriminated into a total of 36 analog signals. At the same time, functions such as time and the one-per-revolution rotor azimuth reference pulse were reproduced from their separate FM tape recording tracks. These signals were fed to the digitizing equipment as illustrated in Figure 38.

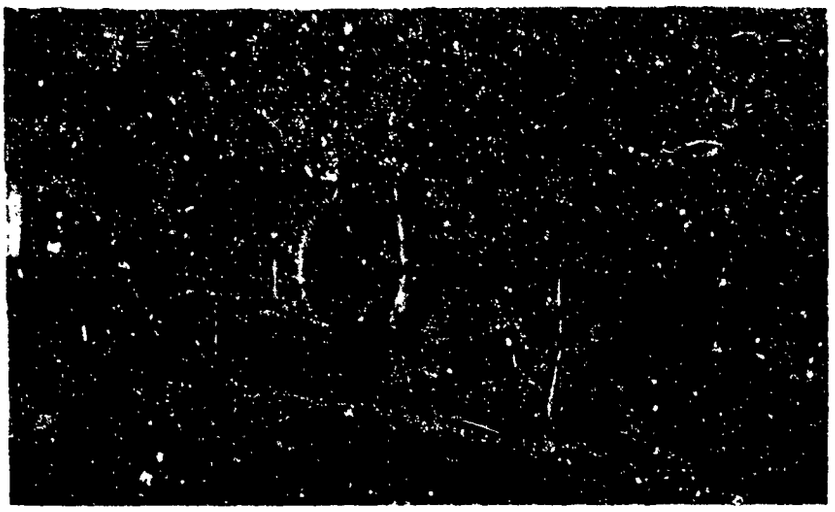

Figure 36. Main and Auxiliary Disconnect Panels.

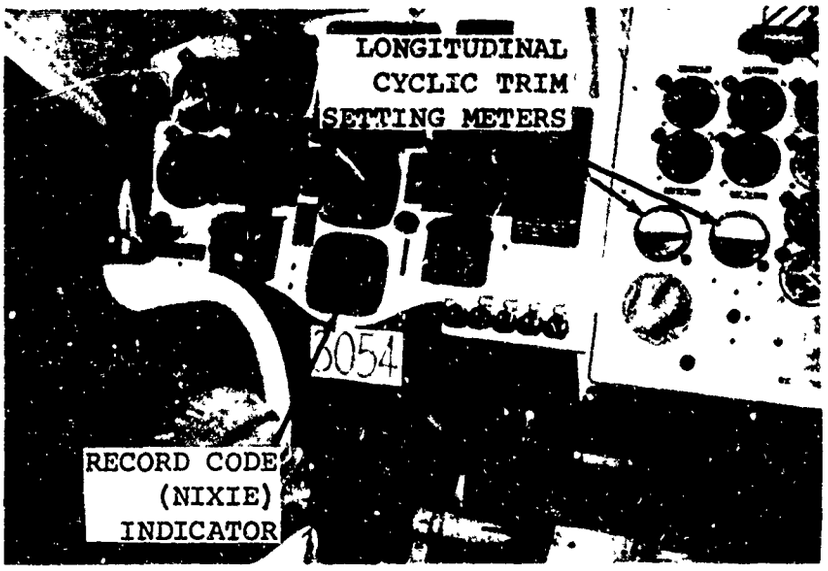

Figure 37. Copilot's Controls and Instruments.

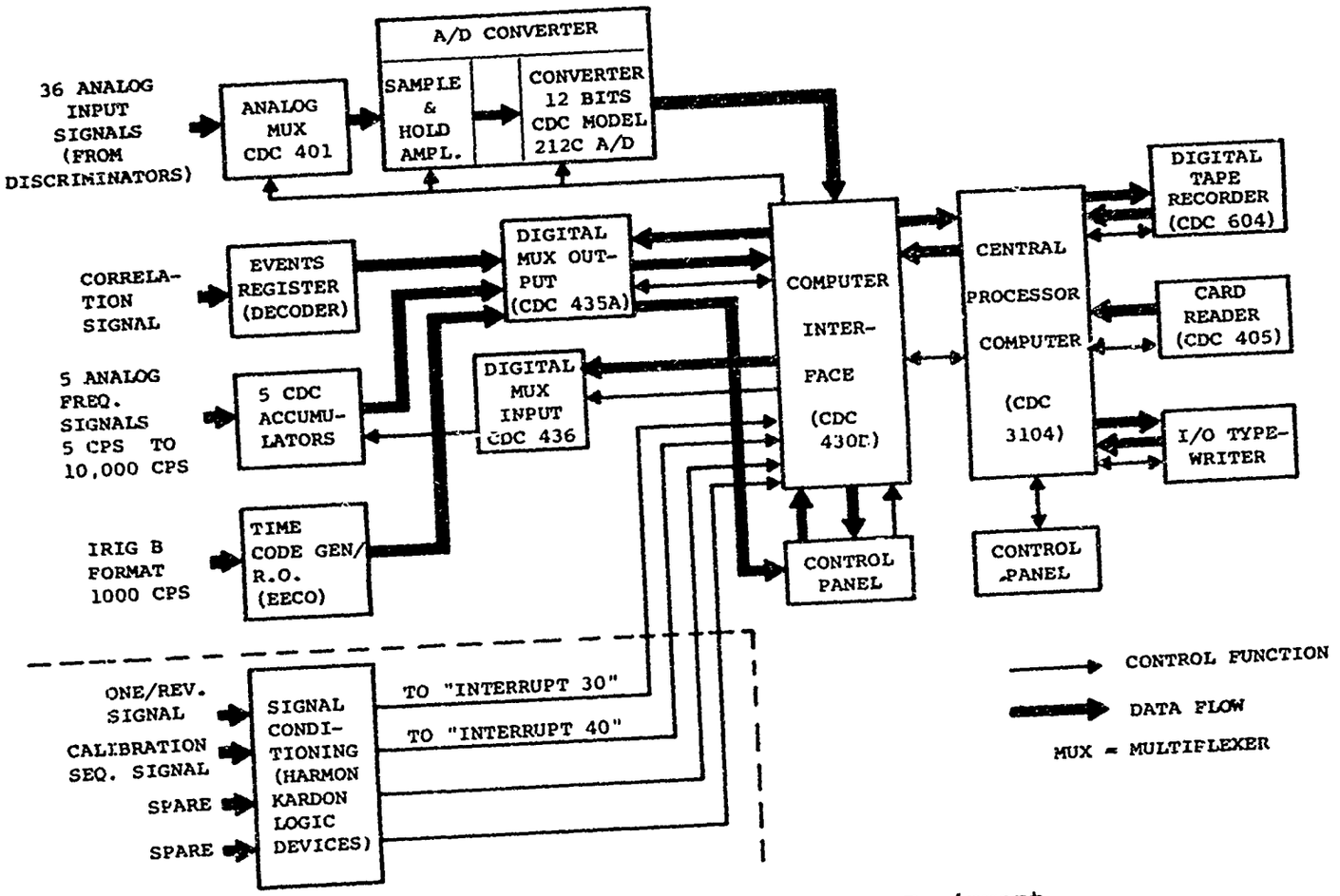

Figure 38. Ground Station Digitizing Equipment.

The analog data were converted to 11-bit digital words and recorded again on magnetic tape in a special format. This tape then became the data which were processed in the manner described in Volume III of this report. The digitizing process was accomplished by a 40-channel high-level multiplexer gated to an 11-bit analog-to-digital converter. The analog signals were connected to the multiplex inputs through patch panels, and the addressing of the multiplexer was controlled by the computer in a sequence defined in the computer program. The sampling rate was also controlled by the computer; it was established to be such that each of the 36 analog channels was sampled at a rate at least 5 times greater than the highest frequency expected to be of interest in the reproduced signal.

Accuracy of Digitized Data

The approach taken in attaining high-accuracy data was to determine each error cause, to eliminate errors if possible, and if not, to provide a means of correcting for the more significant errors. For example, the blade differential-pressure transducers were calibrated to determine their nonlinearity and hysteresis, and the coefficients of zero shift and sensitivity change with temperature. Linearity characteristics and temperature coefficients were compiled for each of the differential transducers and were used during the computer processing to make corrections for nonlinearity and temperature effects.

For differential-pressure measurements where pairs of absolute transducers were used, nonlinearity or temperature sensitivity corrections could not be made. To make these corrections, it would be necessary to know the instantaneous operating points for each absolute transducer, because nonlinearity is a function having a different value at each point of the transducer range and because sensitivity to temperature is also a function of the absolute pressure. The zero shift with temperature was corrected in the paired-absolute configuration by selecting pairs with close matching of the temperature sensitivity coefficients and by obtaining a temperature calibration of the system in a ground run of the instrumentation after installation on the aircraft.

Another source of error which was compensated was lead wire resistance. A 4-wire system connected the blade pressure transducers to the rotating signal conditioners. The lead

wire resistance was measured for each transducer, and the shunt Rcal equivalent was corrected by the factor 4 R_L/R_B, where R_L is the resistance per lead and R_B is the bridge resistance (120 ohms). An in situ pressure calibration was taken for each transducer to verify the Rcal equivalent.

To minimize inaccuracies from the operational amplifiers, these units were required to meet the following specifications:

Temperature zero drift = 4 microvolts per °C referred to input
Gain stability with temperature = 0.1 percent per °C
Gain stability with supply voltage = 0.5 percent per volt (power supplies used had 0.1 percent combined line and load regulation)

Every amplifier was tested to ensure compliance. The effect of zero drift was secondary because, as mentioned previously, a zero input-signal reference was taken at the time of each data recording and was used during the computing process to correct the data. Zero drift did compromise resolution because the data bandwidth had to be compressed so the combination of the transducer and amplifier zero drift plus the maximum data signal level would not exceed the recording system bandwidth. Approximately 25 percent of the bandwidth had to be sacrificed for drift of the systems measuring the trailing edge differential pressures, but only 5 percent was required for most of the other measurements on the blade. Following each data recording, a short circuit and a voltage reference were substituted to the inputs of the MVCO's and the VCO's. This information was used during the computing process to correct the data for drift of the recording/reproducing system.

Another potential source of error in the dynamic signals was the sensitivity attenuation and the phase shifts caused by the response of the transducers and the recording/reproducing system. To provide for these effects, a nominal variation was established for use in data processing with a tolerance bandwidth for variations within the pairs of absolute-pressure transducers. For example, the accelerometers were required to have a flat amplitude characteristic from 0 to +10 percent between 0 and 40 cycles per second, and they were required to match a composite characteristic within 1 percent at 20 cycles and within 5 percent at 40 cycles per second.

The phase characteristic with frequency similarly had to match

within 5 degrees from a nominal characteristic compiled from the aggregate between 0 and 40 cycles per second. The dynamic characteristics of other parts of the recording systems were also determined. The blade pressure transducers had a calculated natural frequency of about 3000 cycles per second, so that no corrections were required as to the phase shift in the transducer. Each operational amplifier was calibrated and an average phase characteristic was determined. Phase calibrations were also performed on the recording/reproducing system. These phase characteristics determined from calibration were used as corrections in data processing.

The accuracy of the data also depended on the calibrations. Considerable care was taken in calibrating the instrumented components; particular attention was given to interaction load effects as discussed in Volume II of this report. With the addition of the previously mentioned errors and the calibration errors, the maximum inaccuracy was less than 10 percent in all cases and less than 5 percent for all primary data.

EXPERIMENTAL PROCEDURES

The Dynamic Airloads Program presented a technological challenge involving several new concepts in aircraft flight test instrumentation. The requirements of the program were such that the reliability and accuracy of each component to be used in the program had to be determined by comprehensive laboratory testing before the component could be used in the helicopter. Accepted components were then assembled into their respective systems, which were in turn exhaustively tested in the laboratory to determine their various operating parameters. When all components and systems were successfully and satisfactorily laboratory-tested, they were installed in the helicopter where a final operational and compatibility test series was performed. Finally, after the successful completion of all in situ testing, the helicopter, with all instrumentation operational, was ready for data flights.

COMPONENT TESTS

This program utilized subminiature pressure transducers manufactured by Scientific Advances Incorporated, differential amplifiers manufactured by Chesapeake Instrument Corporation, and force-balance accelerometers manufactured by Systron-Donner. These components were all new and unfamiliar to Vertol's instrumentation group; as such, they were evaluated thoroughly before being installed in the aircraft. The procedures and results of the transducer evaluations are described in Volume II of this report. Data utilized in data reduction are summarized in Volume II. Transducer data which were used only in system design are included as applicable later in this volume.

Differential Amplifier Tests

Laboratory testing was performed on 120 differential amplifiers, Model DCD-46, manufactured by the Chesapeake Instrument Corporation. The specifications for this amplifier are shown in Table XV.

TABLE XV
MODEL DCD-46 AMPLIFIER SPECIFICATIONS

Parameter	Requirement
Gain	200 ±10%
Linearity	±0.1% best straight line

TABLE XV - Continued

Parameter	Requirement
Drift	<23mv ambient to -20°C <30mv ambient to +55°C
Gain stability	<2¼% ambient to -20°C <1½% ambient to +55°C
Environmental	<5mv noise peak-to-peak
Output noise	<5mv noise peak-to-peak (wide band)
Frequency response	±1% - dc to 100 cps
Phase response	1% - dc to 100 cps
Dc common mode	>90db dc to 400 cps or >20mv
Ac common mode	>90db dc to 400 cps or >6.1mv
Long-term drift	10mv in 8 hours

The amplifier characteristics that were tested are as follows, in the order performed: gain, output noise, dc common mode rejection, ac common mode rejection, frequency response, phase response, linearity, environmental, temperature drift and gain stability, and long-term drift. The long-term drift test was performed on the first 14 amplifiers. The amplifiers were accepted or rejected according to the specifications provided in Table XV.

Amplifier Test Procedures

The test equipment for the differential amplifiers was set up as shown in Figure 39. A schematic diagram of the test equipment setup is shown in Figure 40. The amplifiers were then installed on test boards, as shown in Figures 41 through 44. The test function switch was placed in the dc differential input position (No. 2), the potentiometer was set for zero volts, and the power was turned on. The amplifiers were allowed 30 minutes to stabilize, and the balance potentiometer for each amplifier was adjusted for zero volts output. The test procedure was then begun.

Amplifier Gain, Noise, Drift, Gain Stability, Environmental, Long-Term Drift, and DC Common Mode Test Procedures

A similar test setup was used to perform all these tests. A

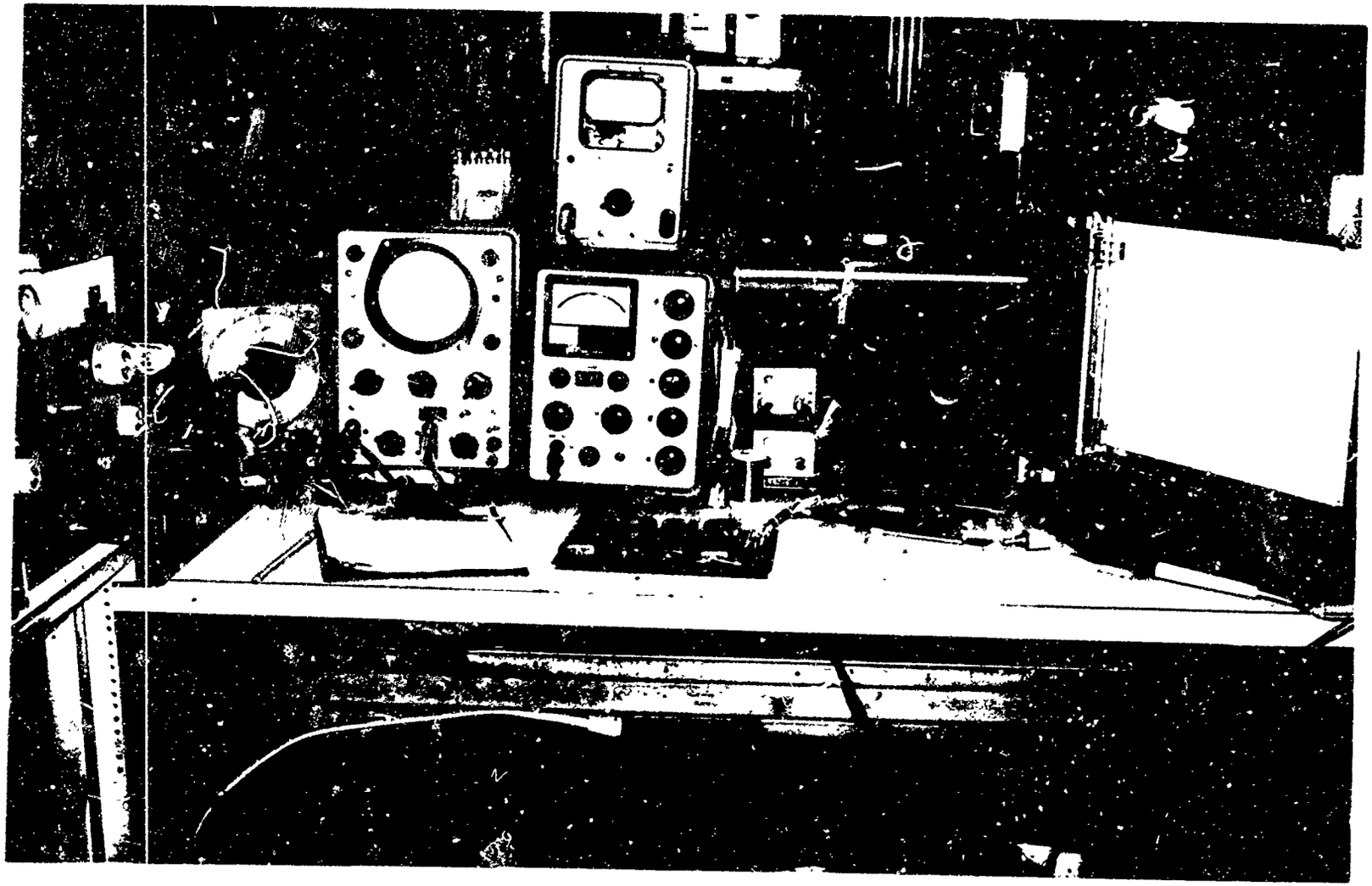

Figure 39. Amplifier Test System Components.

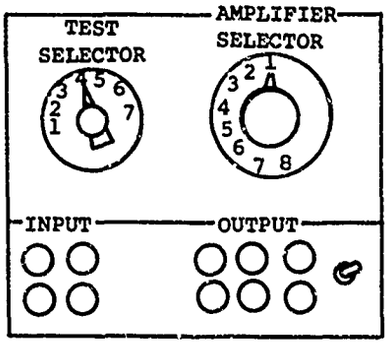

SELECTOR TEST BOX CONTROL PANEL

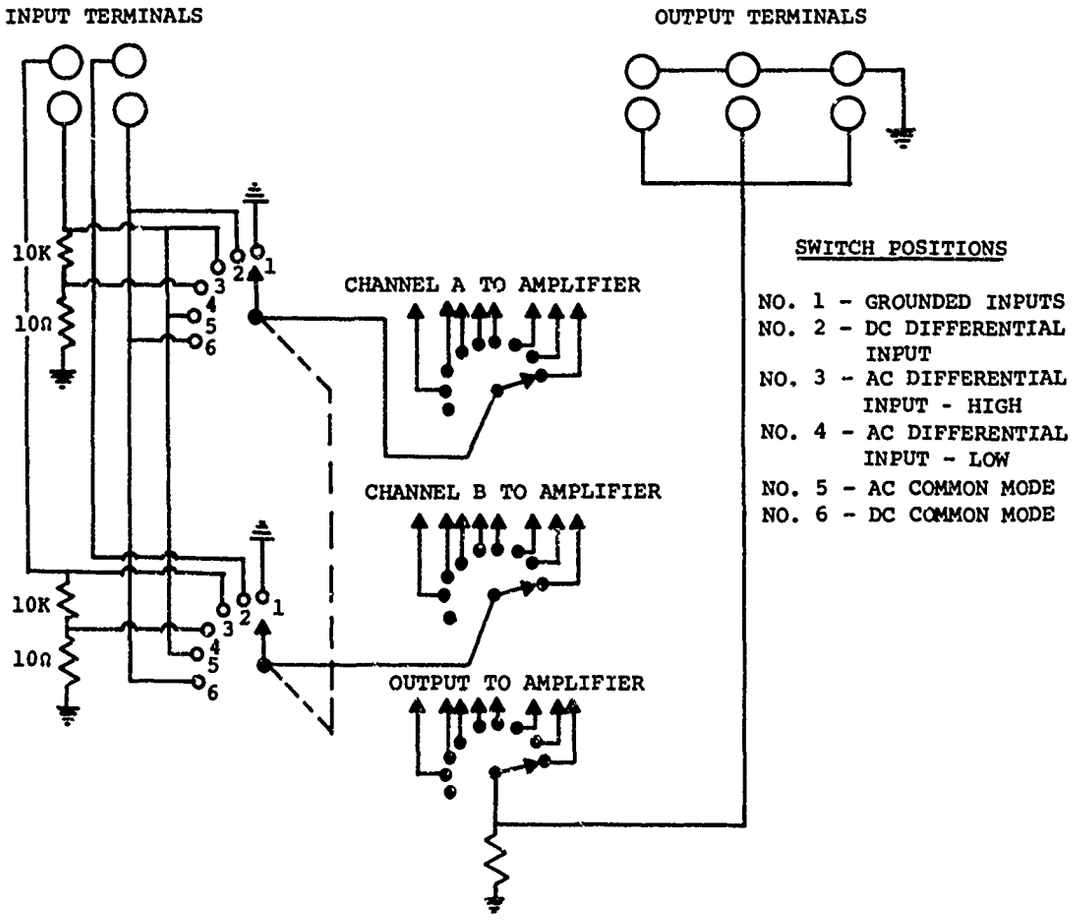

Figure 40. Amplifier Test System Schematic Diagram.

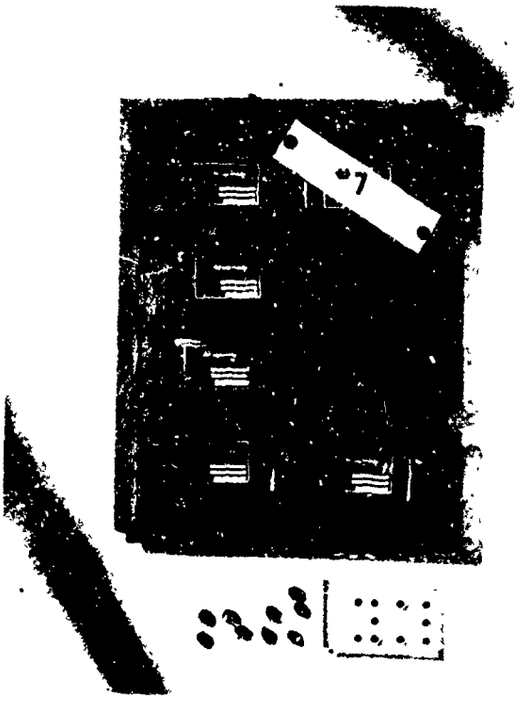

Figure 41. Differential Amplifier Test Board No. 1 - Front View.

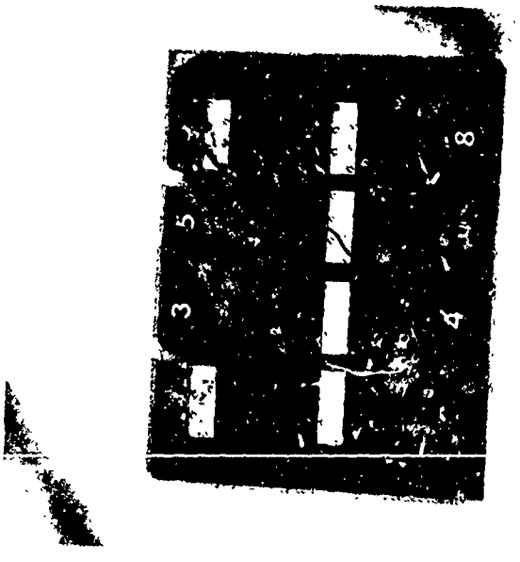

Figure 42. Differential Amplifier Test Board No. 1 - Back View.

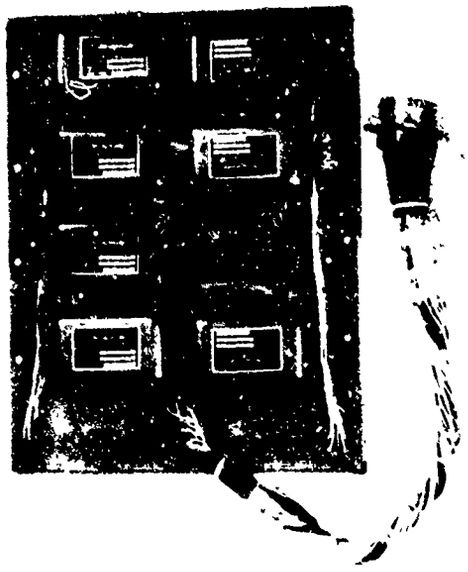

Figure 43. Differential Amplifier Test Board No. 2 - Front View.

Figure 44. Differential Amplifier Test Board No. 2 - Back View.

block diagram of this system is shown in Figure 45.

Amplifier Gain Testing

After the initial warmup period, the potentiometer was set to 1 millivolt and the gain was read directly from the differential ac-dc voltmeter.

Amplifier Noise Testing

The test box function switch was set in the grounded input position (No. 1), and output noise was read from the scope.

Amplifier Temperature Shift and Gain Stability Testing

The amplifiers were placed inside the temperature test chamber at ambient temperature as shown in Figure 46. Readings were taken at ambient, -20°C, and +55°C.

At ambient, the balance was recorded at zero volts input, the output was recorded at 20 millivolts input, and the temperature was recorded.

At -20°C and at +55°C, the output was recorded for zero volts input and 20 millivolts input.

The amplifiers were allowed 20 minutes to stabilize at each temperature.

Amplifier Environmental Testing

The test box function switch was in the dc differential input position (No. 2), and the potentiometer was set to 5 millivolts output. The amplifiers were mounted on the electrodynamic shaker as shown in Figure 47. The output voltage and noise level were observed on the scope under static conditions, 3g at 50 cps, and 10g at 200 cps conditions. The axis of acceleration was perpendicular to the direction of the amplifier pins.

Amplifier Long-Term Drift Testing

This test was performed on the first 14 amplifiers. The selector test box switch was set in position No. 2. The amplifiers were allowed 30 minutes to stabilize and then balanced for zero volts output with zero volts input from the potentiometer. The output was monitored over an 8-hour period,

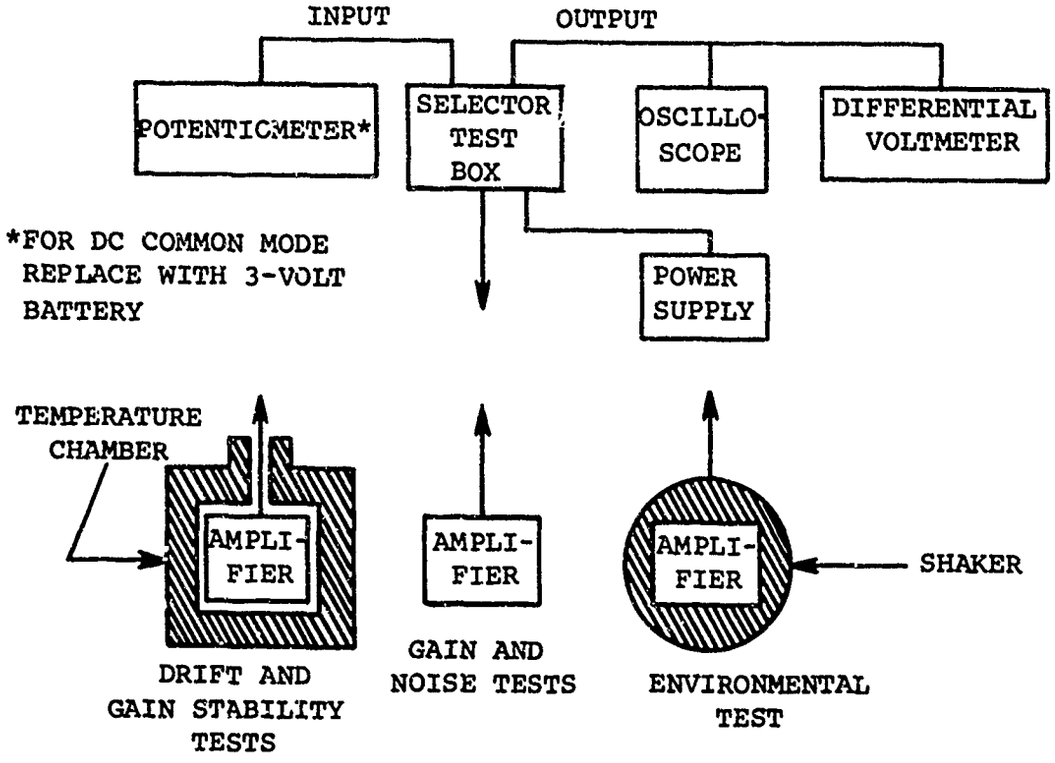

Figure 45. Differential Amplifier Test Setup - Seven Test Procedures.

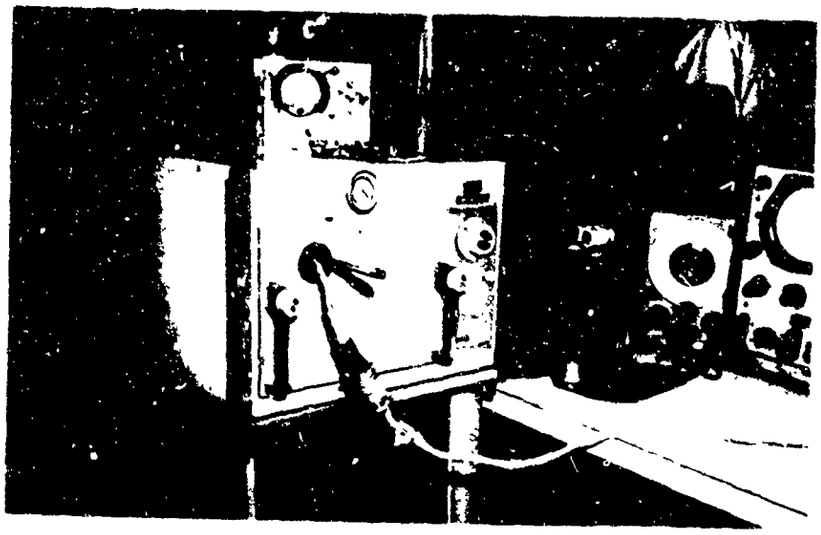

Figure 46. Temperature Test Chamber.

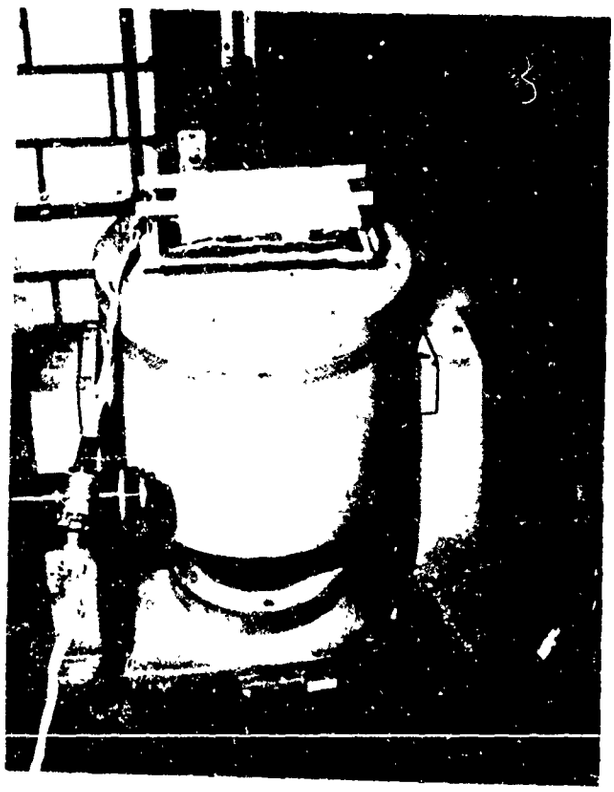

Figure 47. Electrodynamic Shaker.

and hourly drift was recorded.

Amplifier DC Common Mode Testing

The test box function switch was moved to the dc common mode position (No. 6). The potentiometer was replaced by a 3-volt battery, and a jumper lead was placed between the input and output common terminals on the test box. The input and output voltages were noted and recorded.

The 100Ω trim potentiometers, which were in series with the input, were initially set to minimize resistance (3Ω). If an acceptable common mode rejection (cmr) was not obtained, these potentiometers were adjusted to obtain the best cmr.

$$\text{Calculated dc cmr (db)} = 20 \log \frac{\text{input voltage} \times \text{gain}}{\text{output voltage}}$$

$$= 20 \log \frac{\text{input voltage}}{\text{output voltage}} + \text{gain (db)} \quad (1)$$

Amplifier AC Common Mode, Frequency Response, and Phase Response Test Procedures

A similar test setup was used to perform all these tests. A block diagram of this system is shown in Figure 48.

Amplifier AC Common Mode Testing

The test box function switch was moved to the ac common mode position (No. 5). A jumper lead was placed between the signal generator common and the amplifier output common on the test box. The signal generator was adjusted for 1 volt root mean square at 400 cycles, with the voltage being read on the vacuum tube voltmeter.

As in the dc cmr test, the trim pots were initially set to a minimum resistance. The input and output voltages were recorded and the cmr was calculated.

$$\text{Calculated ac cmr (db)} = 20 \log \frac{\text{input voltage} \times \text{gain}}{\text{output voltage}}$$

$$= 20 \log \frac{\text{input voltage}}{\text{output voltage}} + \text{gain (db)} \quad (2)$$

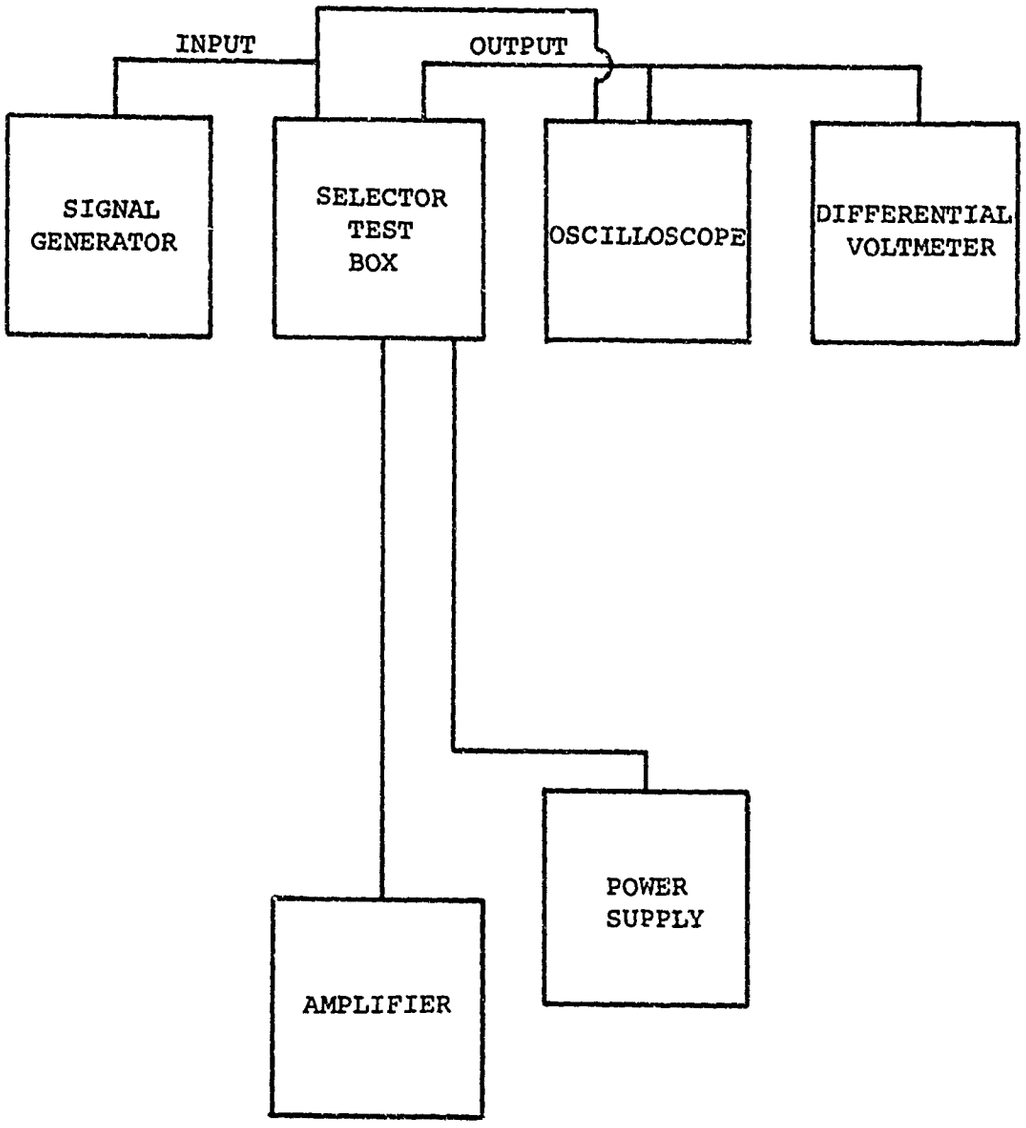

Figure 48. Differential Amplifier Test Setup - Three Test Procedures.

Amplifier Frequency Response Testing

The test box function switch was moved to the ac differential input-low position (No. 4). The jumper used in the ac common mode test was removed. An input of 5 volts root mean square to the test box, or actually 5 millivolts to the amplifiers, was maintained from 10 to 200 cps.

Because the test equipment was not perfectly linear at all frequencies, it was necessary to use the scope to maintain the input of 5 volts root mean square at all frequencies and to correct the output reading of the differential ac-dc voltmeter.

The procedure was as follows:

1. Signal generator voltage maintained at 5 volts root mean square through use of scope

2. Differential ac-dc voltmeter output reading correction necessary at 10 cps and 25 cps only.

   Subtract 0.7 percent at 10 cps
   Subtract 0.2 percent at 25 cps

Amplifier Phase Response Testing

With the same setup being used as for the frequency response test, the input and output waveforms were monitored on a dual beam scope. Through scale calibration the phase shift was read directly and recorded at frequencies of from 10 cps to 200 cps.

Amplifier Linearity Testing

The equipment was set up as shown in the block diagram in Figure 49. The test box function switch was moved to the dc differential input position (No. 2). The input (ordinate) versus output (abscissa) voltages were plotted for each amplifier by keying the sweep supply. Figure 50 shows the linearity plots for a typical group of amplifiers.

The first several batches of amplifiers did not receive this form of linearity check. The first few amplifiers were subjected to varied input voltages (0 to 20 millivolts) while recording their respective output voltages and determining their linearities.

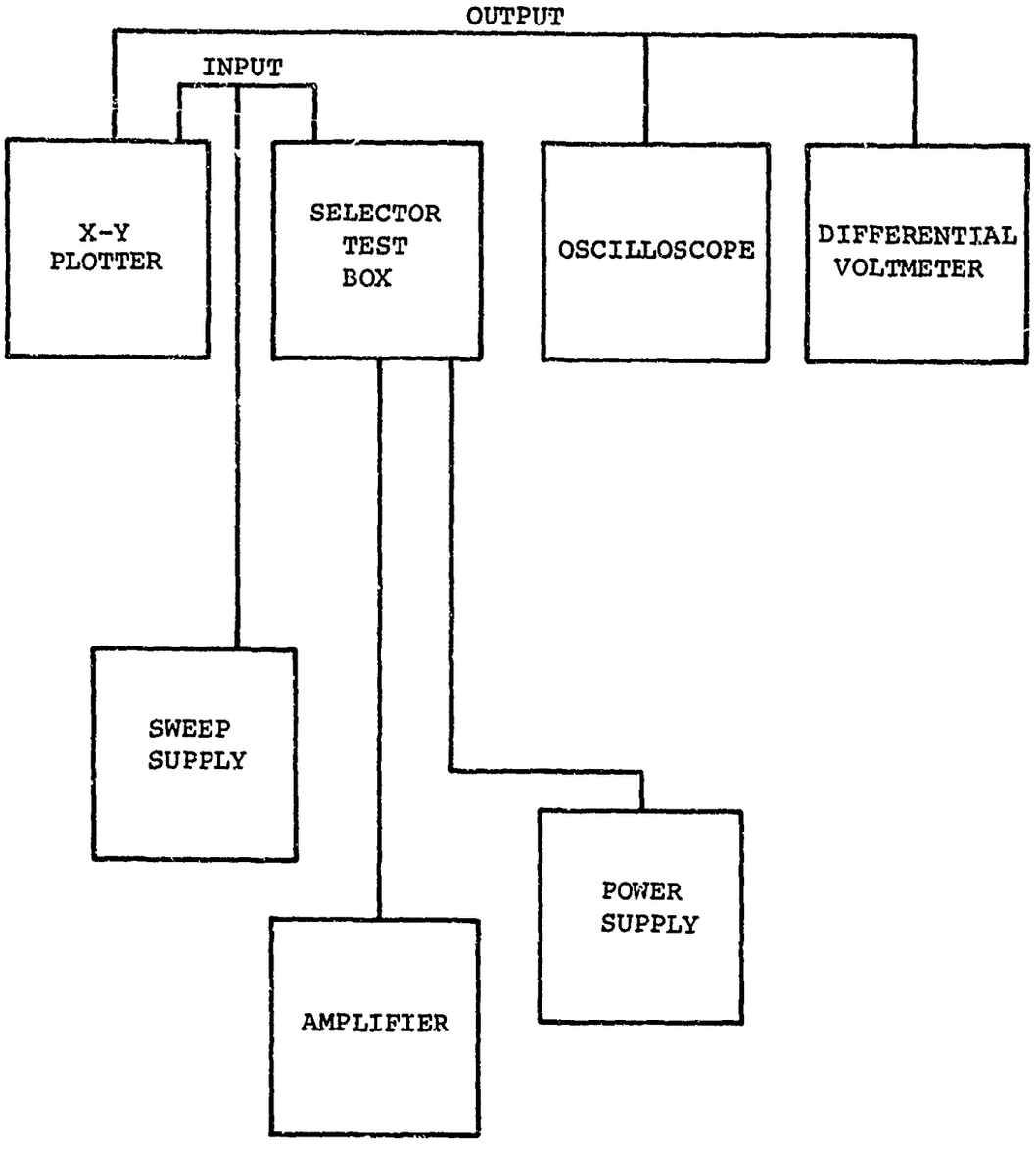

Figure 49. Differential Amplifier Test Setup - Linearity Test Procedure.

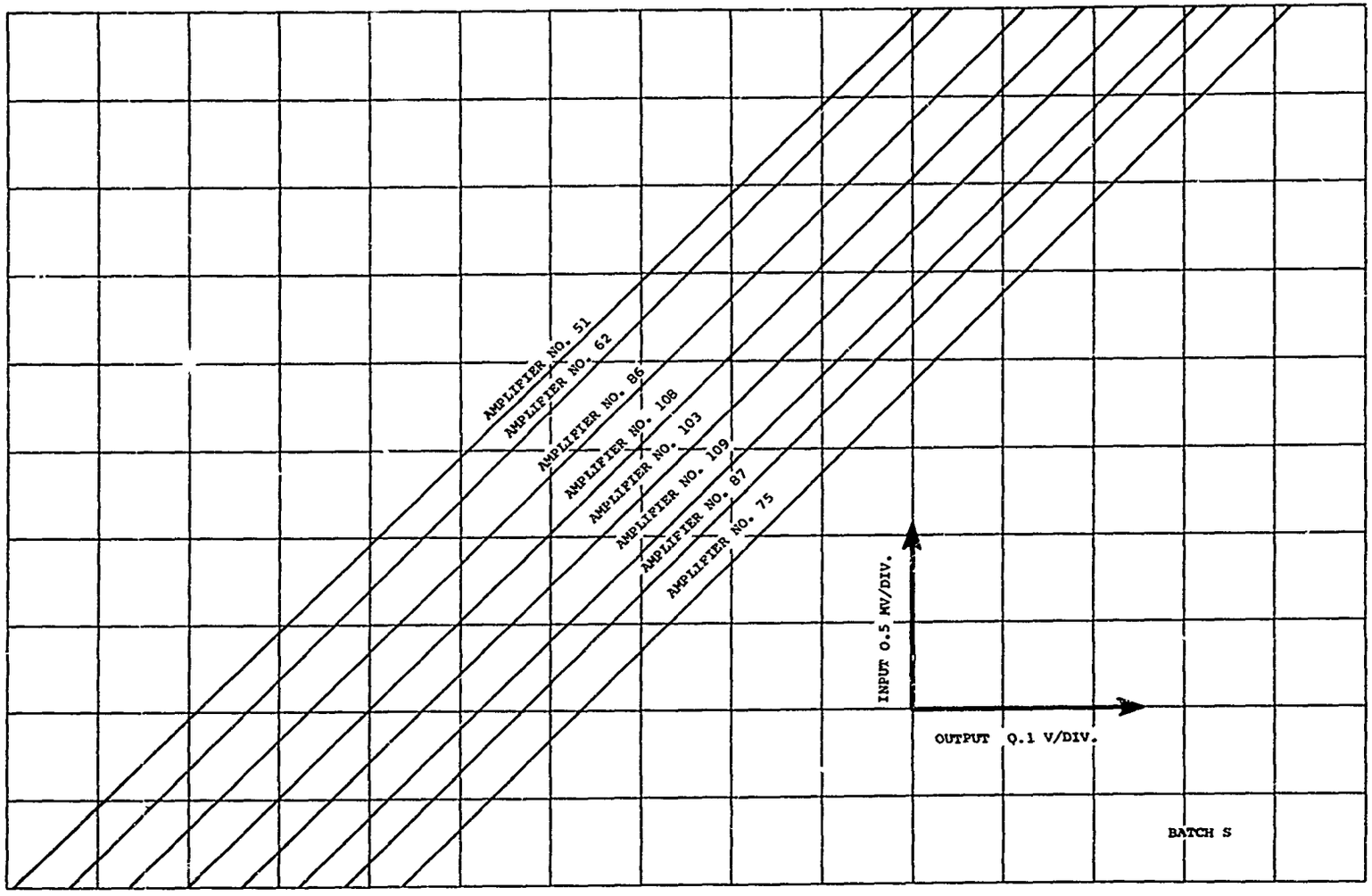

Figure 50. Differential Amplifier Linearity Plots.

Data Processing

The data sheets were initially reviewed as the test information was being recorded. Any amplifier which did not respond as required was checked. If nothing external could be found to be the cause for the amplifier's questionable behavior, it was assumed that the amplifier was at fault, and the test was continued.

Immediately after concluding the testing of each group of 8 amplifiers, the data were carefully checked against the specifications (Table XV) to determine which amplifiers were acceptable. The amplifiers which were not accepted tentatively were retested to obtain two sets of repeatable data. These amplifiers were then tentatively accepted or rejected.

SYSTEM TESTS IN THE LABORATORY

A complete plan of testing was established to substantiate and document system compatibility and the statistical accuracy of individual components and subsystems, which were combined to develop the instrumentation system. System compatibility tests were performed on the voltage-controlled oscillator (VCO) calibrator circuits, on the millivolt-controlled oscillators (MVCO's), and on the high-level voltage-controlled oscillators (VCO's). The rotating signal conditioner, which included the filter and attenuator assembly and the MVCO multiplex system, was subjected to extended compatibility testing. The installation of the pressure transducers on each rotor blade was tested and thoroughly evaluated before the blade was installed on the helicopter. The thorough testing in the laboratory thus assured the proper operation of the instrumentation system when it was installed in the aircraft.

VCO Calibrator Circuit, MVCO, and VCO Testing

The VCO calibrator supplied precise known voltages to the inputs of the MVCO's and VCO's. These voltages served two purposes:

1. They provided convenient means of supplying the necessary voltages to set up the frequency and sensitivity of the individual VCO's.

2. They provided precise known inputs for the VCO's during certain preflight and in-flight calibration

sequences.

This test procedure verified the compatibility of the VCO calibrator with the VCO's and the ability of this equipment to perform the aforementioned functions.

VCO Calibrator Circuit, MVCO, and VCO Test Procedures

A full complement of MVCO's and VCO's was installed on the instrumentation test tables. All MVCO's and VCO's had a valid calibration certification from previous testing. A VCO calibration chassis was installed on the table, and an operational tape deck was connected. A calibrated differential ac-dc voltmeter was used for measuring voltage and a counter was used to monitor VCO output frequency. The calibrator output was monitored and the output level potentiometers were adjusted to indicate the required voltages within ±0.1 percent of reading.

To determine if the calibrator could supply voltage to the full load of the VCO's, the input plugs were removed from all VCO racks except one. All VCO's in that rack were removed except the 40K cps oscillator. The 40K cps VCO was adjusted for frequency and sensitivity to 0.1 percent of design bandwidth. The input plugs and VCO's were then installed in their original positions. The calibrator was then operated and the 40K cps VCO was monitored to check that the calibrator voltages were still within 0.1 percent of design bandwidth.

The frequency and sensitivity of all VCO's were then set to 0.5 percent of design bandwidth. The output voltages of the VCO's and the mixer were then adjusted, and the following data were recorded on tape:

1. First record - manual control

   Lower band edge - 60 seconds
   Center frequency - 60 seconds
   Upper band edge - 60 seconds

2. Second record - manual control

   Lower band edge - 1 second
   Center frequency - 1 second
   Upper band edge - 1 second

3. Third record

   Preflight sequence

4. Fourth record

   In-flight sequence

The record coder signal was recorded on the third and fourth records.

The first record was then played back. The VCO frequency inputs were monitored and manually recorded at the input monitor point of the ground station discriminator. The tape laboratory was requested to set up the discriminators and to adjust the galvanometers with the panoramic calibrator for 4-inch deflection for the design bandwidth on each channel. A test oscillogram of the telemetry calibrator setup and a data stripout oscillogram of records 2, 3, and 4 were obtained from the tape laboratory. This stripout was used to verify the VCO and MVCO calibration points within 1 percent of the tape laboratory input and to verify the proper operation of the sequencer and the sequence coder.

Rotating Signal-Conditioner Testing

The rotating signal-conditioning assembly was designed to supply power, to provide balance and sensitivity adjustment, to provide means for resistance shunt calibration processes, and to provide signal amplification for three types of transducers. This testing verified the ability of the signal-conditioning package to perform these functions within a normal static environment and a simulated operating environment. The test procedure also verified the compatibility of the signal conditioner with all components and subsystems of the system which followed the conditioner.

Rotating Signal-Conditioner Test Procedures

All tests conducted with the rotating signal conditioners were accomplished by using a differential ac-dc voltmeter, an oscilloscope, a band-switching discriminator, and a counter. The rotating signal conditioner was installed on an environmental shake table; the signal-conditioning modules were installed, and dummy bridges were connected to simulate the transducers. All the required wiring was installed between

the signal conditioner and the instrumentation system, and normal power was supplied to all circuits.

Test 1

The signal-conditioning modules were set up according to the following procedure, and the outputs were monitored at the test point with the differential voltmeter. The procedure that was used for a paired-transducer module is as follows:

1. Rotate the 2 Rcal potentiometers full counterclockwise (no resistance).

2. Bridge power off. Adjust amplifier offset to +0.010 volt.

3. Top bridge power on. Adjust top bridge balance potentiometer to +0.010 volt.

4. Both bridge power switches on. Adjust bottom balance potentiometer to +0.010 volt.

5. Top and bottom Rcal relays energized. Adjust bottom sensitivity potentiometer for +0.010 volt.

6. Record the output from each test point at the balance and Rcal positions.

The test procedure that was used for a differential-transducer module is as follows:

1. Rotate Rcal potentiometers full counterclockwise.

2. Bridge power off. Adjust amplifier offset to +0.010 volt.

3. Bridge power on. Adjust bridge balance +0 to +0.010 volt.

4. Record the output from each test point at the balance and Rcal positions.

The test procedure that was used for a strain-gage module is as follows:

1. Adjust balance for +0.005 volt at the test jack.

2. Record the output for each test point at the balance and Rcal positions.

Test 2

The filter-attenuator T-pads were set to the position of no attenuation.

The output from each signal-conditioning channel, as measured from the output of the filter-attenuator outputs on the patch panel for the paired transducer and differential transducer modules and from the patch outputs for the strain-gage modules, was recorded and checked. All channels had to meet the required output of +0.005 volt.

Test 3

All channels were resistance-calibrated. The Rcal outputs as monitored at the patch panel outputs were measured and listed.

The outputs from the paired-transducer and differential-transducer modules, as measured at the patch panel, had to indicate one-half the value of the test point outputs. The outputs from the strain-gage modules had to be the same at the patch panel and the test points.

Test 4

The output at the test point was monitored on the oscilloscope. The output noise level in terms of peak-to-peak averages of the major frequency components was recorded.

Test 5

The output at the patch panel was monitored on the oscilloscope. The output noise level in terms of peak-to-peak averages of the major frequency components was recorded.

Test 6

Four different test tapes were recorded to check the rotating signal-conditioner performance. The four procedures that were used were as follows:

1. Using manual control, record the lower band edge, the center frequency, and the upper band edge on

test tape.

2. Run a 5-second record of all channels of the signal conditioner with the conditioner static.

3. Run a 5-second record of all channels of the signal conditioner with the conditioner shaking at 2g and 12 cps.

4. Rotate the package 90 degrees and take a 5-second record with the conditioner shaking.

Results of the test tape were then summarized.

In Situ Rotor Blade Pressure Transducer Tests

The rotor blades were tested, individually, with all pressure transducers installed (in situ) in order to verify the analytical error analysis and system integrity and to establish the sensitivities which included the effects of the lead wire resistance. All test procedures were performed in the flight test center calibration laboratory.

In Situ Pressure Transducer Test Procedures

The instrumented rotor blades were installed in the calibration laboratory to provide a suitable stable environment. A calibration test box was fabricated to provide power and control for the signal-conditioner circuit card. A pressurization test fixture was designed to enable a known pressure to be applied to individual transducers. The accuracy of the pressure source was documented to ±0.5 percent of the indicated value over all ranges.

A data sheet was prepared listing the following information, which was obtained from the computer tab runs of the static calibrations and blade wiring checkout data:

1. Transducer slope

2. Transducer temperature sensitivity coefficient

3. Rcal equivalent

4. Line resistance - measured during transducer installation

From this information, a calculated calibration resistance was established for the equivalent Rcal pressure for each transducer. The data sheet also listed the theoretical millivolt output from each transducer, assuming a nominal gain of 200 from the signal-conditioning amplifiers. The object of these calculations was to verify the integrity of the transducer as installed on the blade by comparison with laboratory calibration data.

Each transducer was calibrated over its expected operating range; this was considerably less than the full-scale range in a majority of cases. The adjustable Rcal resistor was set to simulate a pressure in the middle of the expected operating range. The Rcal resistance and the millivolt output for the Rcal pressure were read and listed on the data sheet. These figures were then compared to the calculated figures on the following basis:

1. For the absolute-pressure transducers, the combined linearity and hysteresis specification was ±1.5 percent of full scale; full scale was 15 psia. If the Rcal pressure was listed as 6 psi, this specification would indicate that any value within ±3.75 percent of best-straight-line calculated data was within specification. Concurrently, the figure obtained from the in situ calibration represented a more accurate representation of the transducer at that point. Rcal equivalent pressures as low as 2 psi had been established for some of the absolute measurements. At the 2-psi point, ±11.75 percent of calculated best-straight-line figures were allowed. Again, the in situ calibration data provided a better representation of the transducer characteristics at that point.

2. For the differential-pressure transducers, the combined linearity and hysteresis specification was ±2 percent of full scale; full scale represented ±10 psid, ±5 psid, and ±2 psid. The same analysis was applied to the comparison of calculated and measured Rcal millivolt output and Rcal resistances, as was previously explained for the absolute-pressure transducers.

SYSTEM TESTS ON THE HELICOPTER

The instrumentation system was installed on the helicopter after the satisfactory completion of all laboratory testing. Initial testing showed the installation to be entirely satisfactory.

Three instrumentation check flights were conducted, the first of which revealed a problem which the two subsequent flights verified. Investigation disclosed the causes of this problem, and they were quickly resolved. Further flight tests showed the instrumentation system to be completely satisfactory and ready for the initiation of recording flight tests.

Instrumentation System Test Procedures

The instrumentation system that was developed for the Dynamic Airloads Program was installed in the test aircraft, and all circuits were interconnected, checked, and verified for the first test flight. The equipment used to check the system consisted of discriminators for channels 5 through 16 with 59 cps output filters, a 4-inch oscilloscope, and a differential voltmeter. The tests were begun in the hangar, with the helicopter operating on a ground power unit, and were completed with the aircraft flying in hover and in forward flight.

Test 1

The instrumentation system was operated in the helicopter with power provided by a ground power unit. The signal-conditioning modules were set up according to the following procedure. The card outputs were monitored with the differential voltmeter. The test procedure that was used for a paired-transducer module is as follows:

1. Bridge power off. Adjust amplifier offset to +0.010 volt.

2. Top bridge power on. Adjust top bridge balance potentiometer to +0.010 volt.

3. Both bridge power switches on. Adjust bottom potentiometer to +0.010 volt.

4. Record the output from each test point at the balance and Rcal positions.

The test procedure that was used for a differential-transducer module is as follows:

1. Bridge power off. Adjust amplifier offset to +0.010 volt.

2. Bridge power on. Adjust bridge balance to +0.010 volt.

3. Record the output from each test point at the balance and Rcal positions.

The test procedure that was used for a strain-gage module is as follows:

1. Adjust balance for +0.005 volt at test jack.

2. Record the output from each test point at the balance and Rcal positions.

The test procedure that was used for all other onboard signal-conditioning networks was as follows:

1. Set up per normal operating procedure.

2. List the output from each measurement circuit as measured at the output of the signal-conditioning jack on the patch panel.

Test 2

Ground power was supplied to the helicopter in the hangar to operate the instrumentation system. The filter-attenuator T-pads were turned to the position of no attenuation. The outputs from the -1 and -2 signal-conditioning modules, measured at the output of the filter-attenuator network, were measured and listed for both the balance and Rcal positions.

Test 3

With the helicopter provided with ground power, a test tape of the ambient noise levels on all channels was recorded.

Test 4

In this test the helicopter engines were started, the rotors were engaged, and the instrumentation system was powered from the aircraft alternators. A test tape of the ambient noise levels on all channels was recorded.

Test 5

The helicopter was flown in a hover and in forward flight. A third test tape of the ambient noise levels on all channels was recorded.

Test 6

Before beginning the data recording flights, a final system long-term drift and computer compatibility test was performed. The test was designed to document the following characteristics of the system:

1. The stability of the system over long periods of time with relatively small temperature changes.

2. The ability of the computer 6-step preflight calibration and 3-step in-flight calibration to compensate for changes in output caused by amplifier temperature drift.

3. The ability of the system to record and reproduce known input levels with the established degree of accuracy.

This test was conducted by performing a normal preflight calibration with the helicopter in the hangar. The covers were removed from the rotor head signal conditioners, and the conditioner temperatures stabilized at approximately 100°F. After the preflight calibration, the covers were installed and the conditioner temperatures were allowed to increase. After 3 hours, the temperatures stabilized at approximately 140°F. A short data burst was then recorded, followed by the 3-step in-flight calibration sequence. A second short data burst was recorded immediately, followed once more by the 3-step calibration sequence. The manual resistance-calibration switch was then energized, simulating a known input to all channels, and a third short data burst was recorded. This series constituted a first set of records. After 3 hours, a second

set of records was taken in the same sequence, followed by two more sets after similar time intervals. The resultant tape was then processed through the normal Stress Program path, and the printout was analyzed to verify design criteria.

EXPERIMENTAL RESULTS

COMPONENTS

The extensive component test programs for blade pressure transducers and accelerometers, described in Volume II of this report, verified the selection of these components for the Dynamic Airloads Program. The excellent amplitude-phase relationship of the Systron-Donner accelerometers considerably enhanced the value of the data obtained from this source. The characteristics of this unit were far superior to any similar instrument that had been used previously on a helicopter research program.

The evaluation of this Scientific Advances Incorporated pressure transducer confirmed the design analysis prediction that it was a versatile, stable, and accurate transducer for the measurement of dynamic airloads.

Amplifier Test Results

As shown in the Figure 51 histogram, of the 120 amplifiers tested, 104 amplifiers were accepted and 16 were rejected. The quantities and categories of rejection were as follows: 13 for temperature drift, 9 for gain stability, 3 for environmental, 1 for common mode rejection, 1 for noise, and 1 for balance. The total here exceeds 16, since most of the rejected amplifiers failed the tests in two or more categories.

SYSTEM TEST RESULTS

System tests for function and the in situ blade pressure calibrations were included; after some development, the tests indicated satisfactory performance of the applicable equipment. Results of these tests are discussed in the following section.

VCO Calibrator Circuit, MVCO, and VCO Test Results

The test to determine if the calibrator could supply voltages to a full load of VCO's revealed a 0.5-percent drop in voltage to the input of the VCO's when operated from no load to full load. This drop had no effect on the accuracy of the data, however, as the sensitivity of the system was based on changes in voltage from resistance-calibration techniques and not on absolute-voltage inputs.

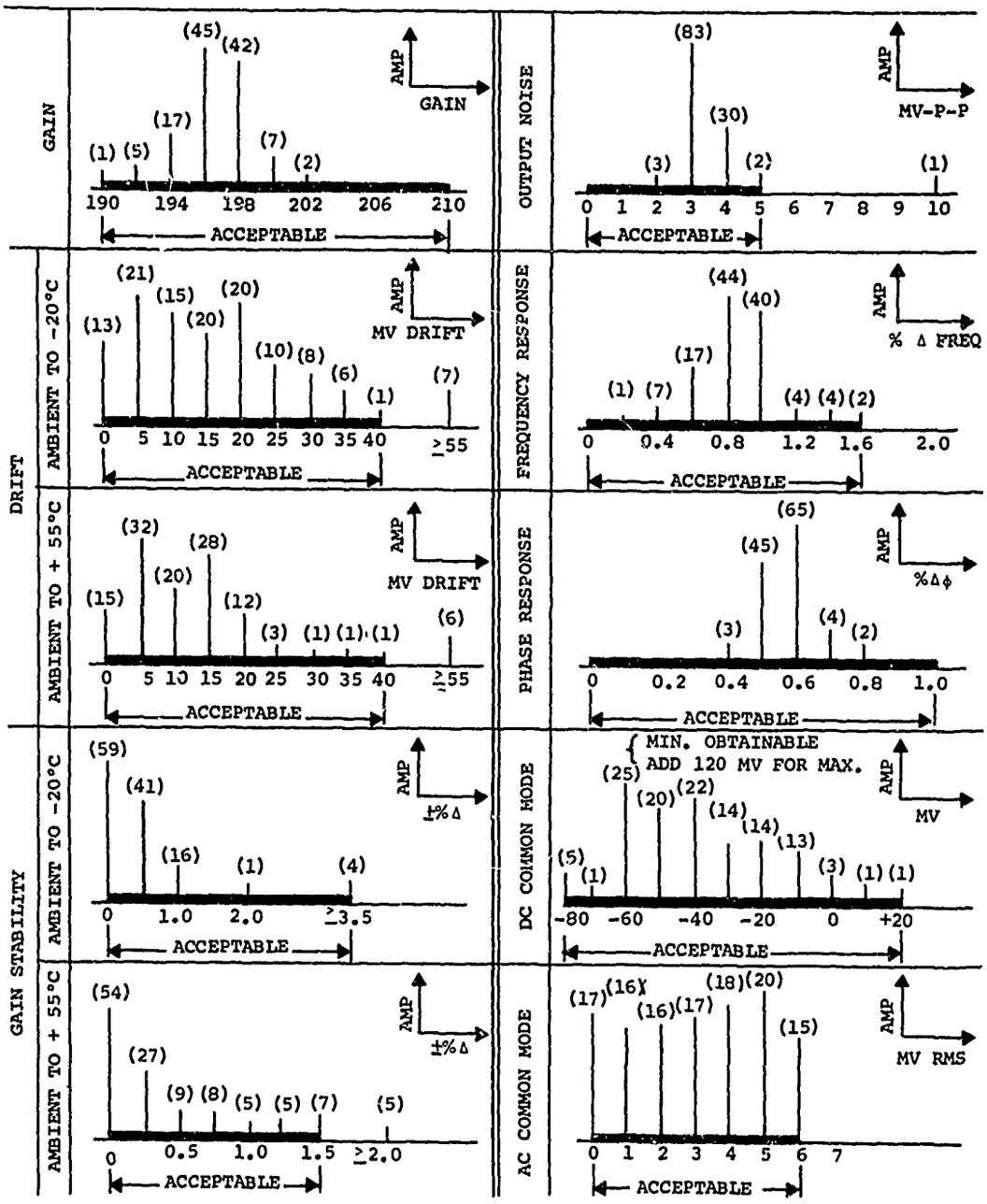

Figure 51. Histogram of Amplifier Operating Parameters.

The results of checking the VCO outputs by tape recordings indicated a 2- to 3-percent shift in band edges when band-edge information was recorded on the aircraft and played back in the ground station. Investigation revealed that the differences between the speeds of the recording and reproducing tape mechanisms were the cause of this band shift. The specification for tape speed, when related to the narrow-band (±7.5 percent) FM multiplex system being used, allowed for a ±3.5-percent tape speed difference between the mechanisms. It was determined that this speed difference would not affect data accuracy, since the preflight and in-flight calibration techniques compensated for sensitivity and band shift errors.

Rotating Signal-Conditioner Test Results

All circuits were set up and functionally checked by comparing the output voltages measured directly at the card output with the voltages measured at the corresponding point on the instrumentation table patch board. The initial set of measurements showed a 0.005-volt offset between the two points. Investigation showed that the offset resulted in a small amount of current being drawn through the amplifier power common line. This current resulted from a slight difference in the amount of current flowing in the + and - amplifier power supplies. The amplifier common line was also the data common bus; therefore, the 0.005 volt showed up as a data offset. This problem was eliminated by adding a small resistance in one side of the amplifier supply lines to balance the amplifier currents; this resulted in no current in the common line.

The filter-attenuator system performed to specification. The loss through the system was precisely 50 percent, as calculated. The output was continuously variable from 50 percent to infinity. With the attenuator turned to minimum attenuation and with an allowance for the 50-percent loss, the Δ Rcal voltage outputs as measured at the signal-conditioning card output test point were within ±1 percent of the values measured at the output of the filter-attenuator patch.

The output noise as measured at the card output test point correlated with the figures obtained during the breadboard mockup and the circuit board checkout. From 0.015 to 0.025 volt peak-to-peak, 400 cps appears on the output of the signal-conditioning cards. The signal-conditioning filter reduced the unwanted 400-cps component to less than 0.001 volt

peak-to-peak. This level was subsequently reduced to less than 1 percent of signal by the discriminator output filter.

The environmental shake test revealed several significant problems in the mechanical assembly of the rotating signal conditioner. In this test, the assembly was mounted on a shake table in the environmental test laboratory (see Figure 52). The complete electronic system was set up with dummy resistive bridges simulating the pressure transducers. The one exception to a full simulation of the flight test setup was that all channels were set to the same gain, minimum attenuation, or a gain of 100. In actual operation, the maximum gain would be 50, and only a small percentage of the measurements would operate at this gain. The nominal gain setting would be 20.

The object of the test was to subject the package to simulated flight loads for 8 hours without a failure due to mechanical problems. The simulated load was 2g at 12 cps, applied perpendicular to the vertical axis. A normal preflight check was accomplished before each test, and records were taken at 1-hour intervals. Provisions were included for sequentially scanning each channel.

During the first scan on the initial run, over 50 percent of the channels exhibited excessive response due to the shaker input (over 3 percent of bandwidth). The test was stopped and subsequent investigation, modification, and retesting proceeded for a period of over 30 days. The major problem areas and the resolutions were as follows:

1. The dummy bridge resistors caused an output unless they were properly secured. The dummy networks were securely taped to the circumference of the package.

2. The circuit board components were not securely mounted. The board design had not provided for a mechanical attachment for the filter capacitors. A silicone-rubber base was incorporated.

3. The circuit board printed-circuit plating was not formed properly. This presented the major problem. Due to improper plating, a large portion of the solder joints were of questionable quality. This

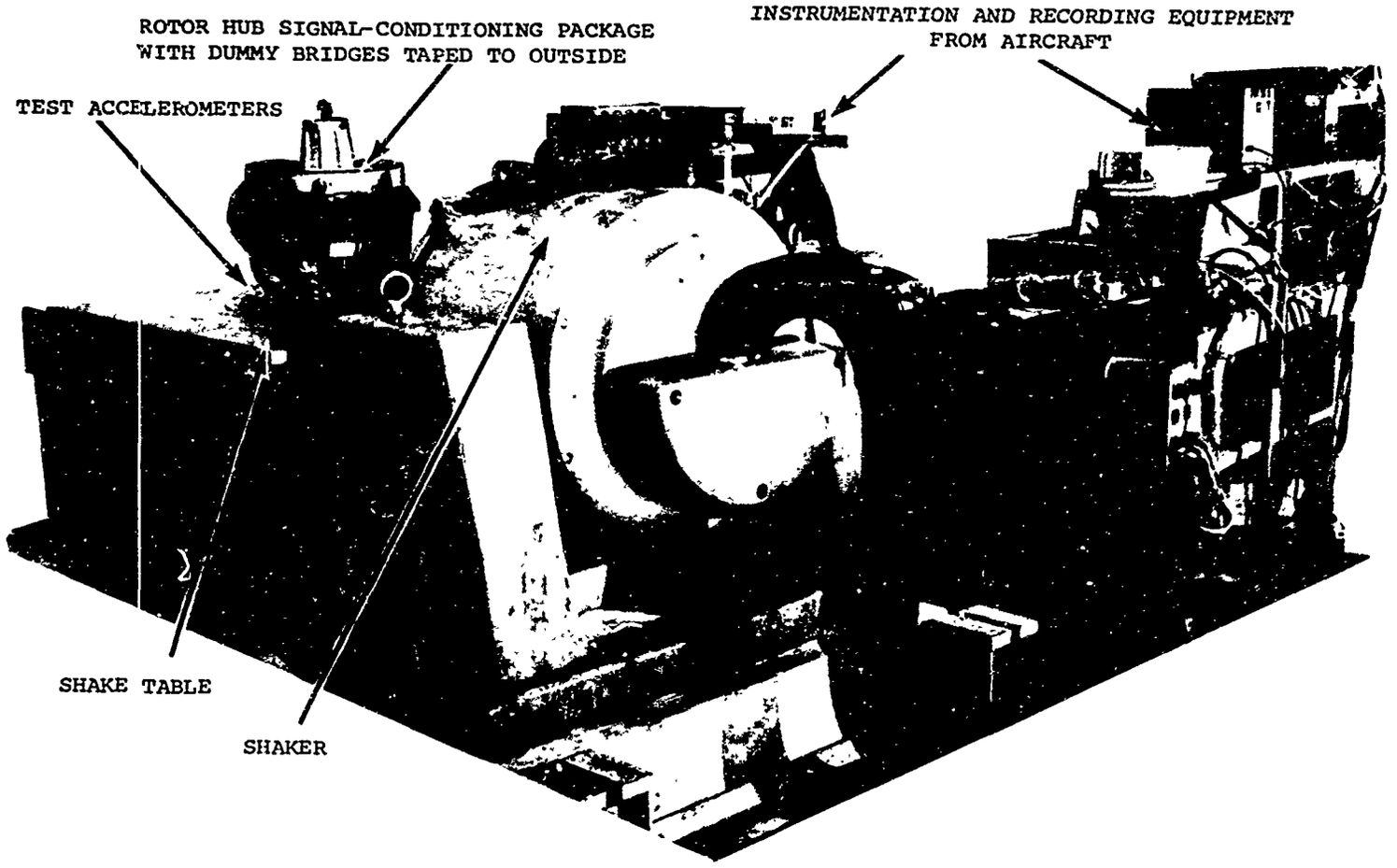

Figure 52. Shake Test of Rotor Hub Signal Conditioner.

was a continual problem, necessitating the cleaning and resoldering of all solder joints on all boards.

A sample of a typical oscillograph stripout obtained during the latter part of the testing is shown in Figures 53 and 54. This stripout shows the four strain-gage modules, three differential-pressure transducer modules, and four paired absolute-pressure transducer modules. Figure 53 shows the output with the shaker output parallel to the 0° axis of the package; Figure 54 shows the output with the shaker output parallel to the 90° axis. On these figures the full bandwidth sensitivity is 4 inches. All traces, with the exception of band 10, show a baseline of less than 3 percent of bandwidth. Band 10 illustrates a typical output from a bad solder joint. This channel was subsequently repaired. The sharp pips on band 12 were traced to pickup from the intervalometer switching contacts. This problem was eliminated by protecting the switch contacts. Following these modifications the objective of this test was achieved, with both the forward and aft rotating signal conditioners operating continuously for over 8 hours with no mechanical failures or outputs due to vibration.

In Situ Rotor Blade Pressure Transducer Test Results

The calibration of the blade pressure transducers, while mounted in the rotor blade (in situ), verified the integrity of the calibration procedures used by the manufacturer. All transducers checked out within specifications, and the laboratory calibration increased the overall accuracy by establishing the linearity and hysteresis of each transducer in the installed operating range of the measurement.

All calculated and theoretical data were within specified limits except for 6 differential transducers; the in situ calibrations established a more representative calibration point in relation to the operating range of the transducers.

The 6 transducers that did not operate within stated specification were subjected to a minimum of 2 complete pressure calibrations. The data from these calibrations were considered to be acceptable, and these units were used in the flight tests. No reason could be found for the apparent change in the characteristics of these 6 transducers; the only plausible explanation

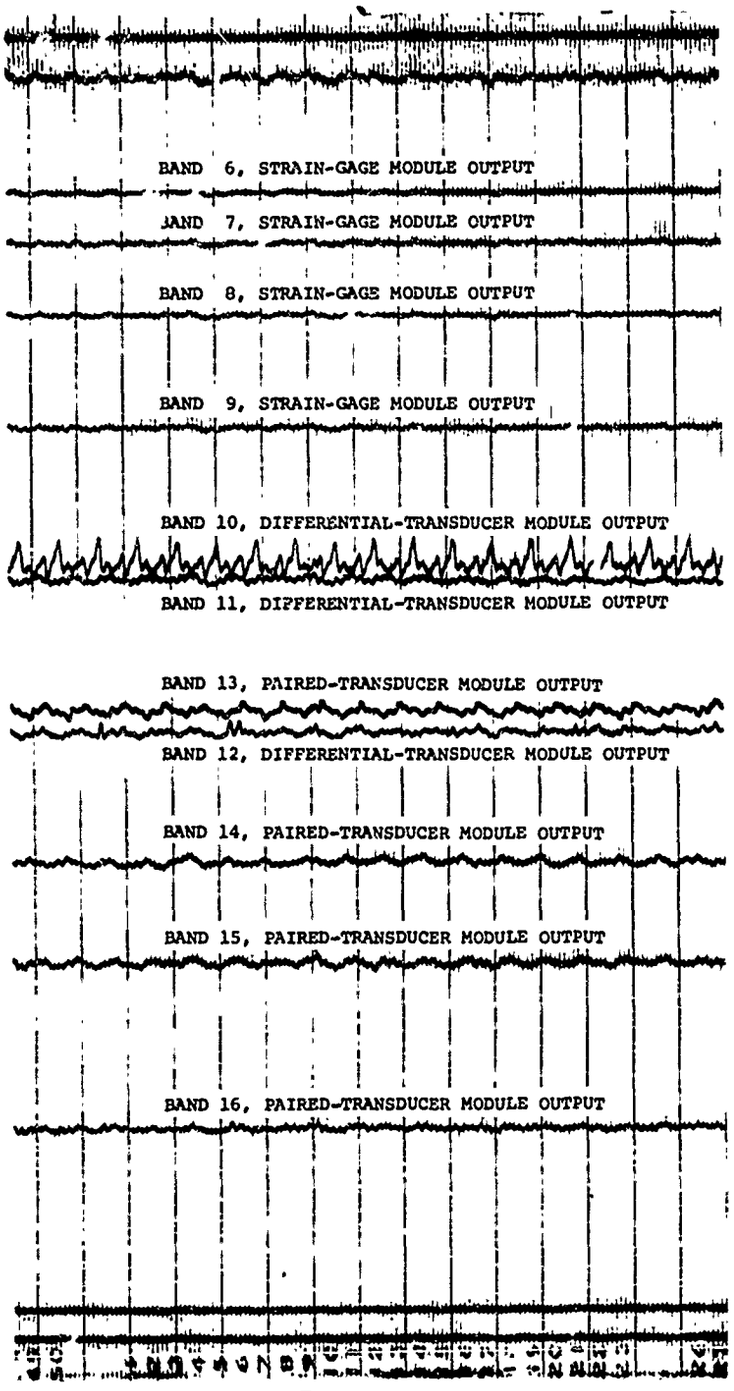

Figure 53. Oscillograph Stripout from Parallel Shake Test of Signal Conditioner.

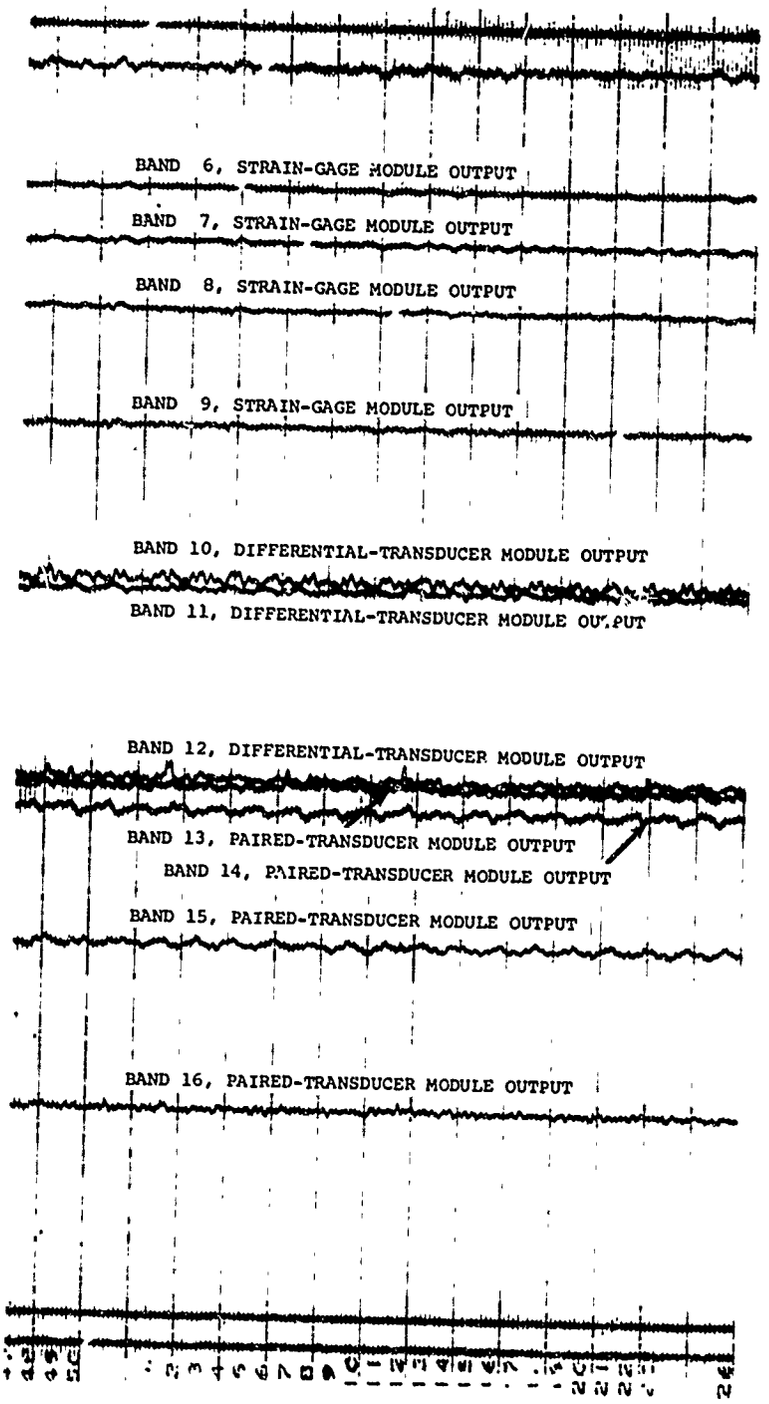

Figure 54. Oscillograph Stripout from Perpendicular Shake Test of Signal Conditioner.

was that the tags listing the performance characteristics of these transducers were somehow mixed in packing or unpacking.

System Test Results Obtained on Helicopter

The instrumentation system was installed on the aircraft without any undue delays. The voltage outputs at the signal-conditioning test points matched the output that were noted during the in situ blade calibration within normal measurement tolerances. Measurements taken at the patch panel output indicated, as in the preliminary laboratory checkout, a 0.005-volt baseline offset between the card output and the patch panel output. This was again eliminated by balancing the amplifier currents.

An instrumentation check ground run was made to monitor the noise level during the transition from ground power to aircraft power. No change in noise level was discerned during this transition.

For the first instrumentation check flight, all channels were set up with a nominal sensitivity (Rcal deflection 40 percent of bandwidth). The flight included a 30-minute hover and 40-knot forward flight. The analysis of the flight data revealed several minor problems and one major problem. The minor problems consisted of intermittent connections which were subsequently repaired. The major problem consisted of a considerable amount of noise, from 5 percent to 50 percent of bandwidth, on the baseline data. The baseline was recorded after each datum point, with bridge power being removed. A sample of this baseline noise is shown in the oscillograph stripout in Figure 55.

The investigation into this problem continued for several weeks. Two more check flights were made, with the condition remaining the same. The data for these flights were analyzed for baseline noise, and data obtained from channels with a significant amount of noise (over 5 percent) were noted and eliminated. The amount of noise was directly related to the gain of the system; and only the higher gain channels, those measuring the lower output pressures, were affected.

The cause of the noise problem was found to be a combination of factors involving a malfunction in the slipring assembly; this caused a loss of rings carrying amplifier power and several gage circuits to go to ground intermittently, which resulted

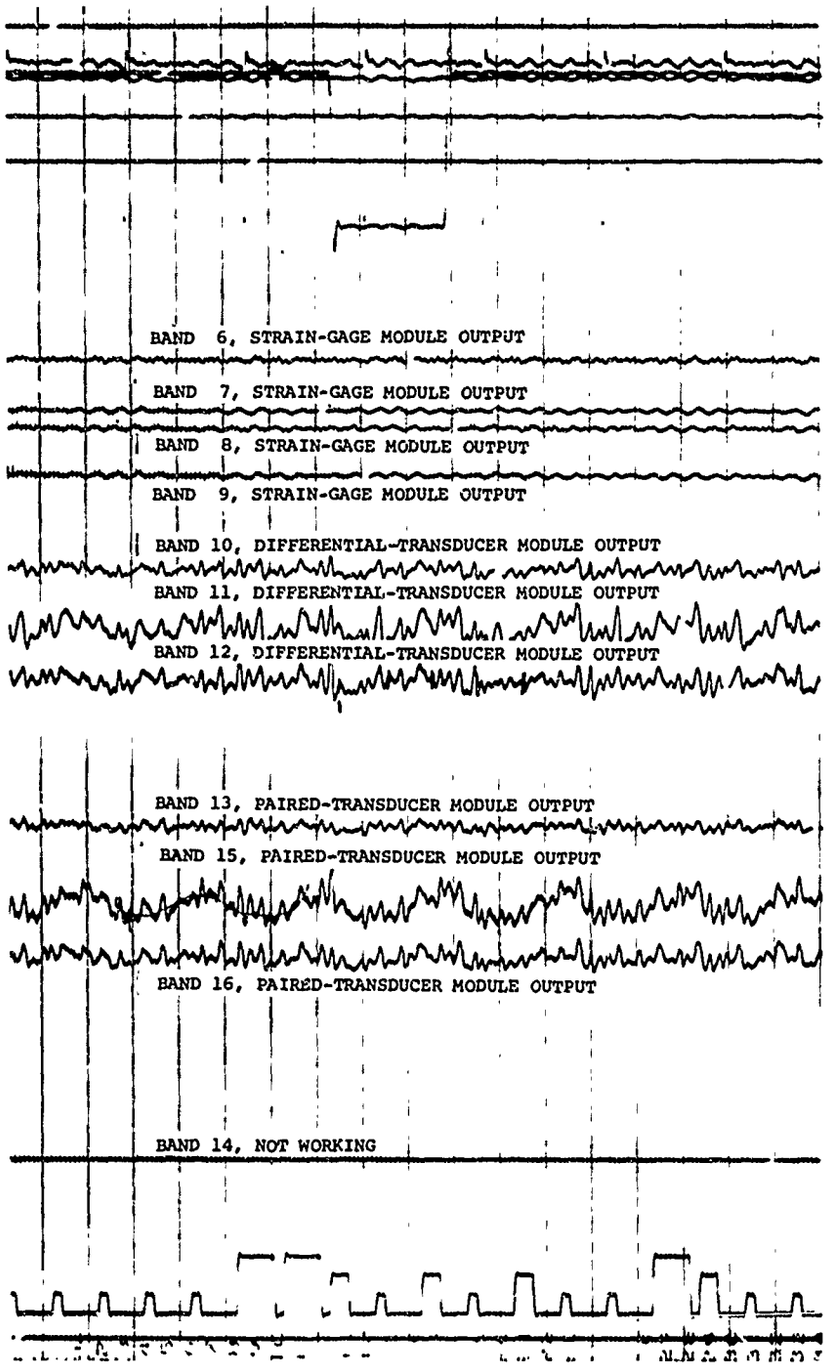

Figure 55. Oscillograph Stripout of Instrumentation System Output Showing Excessive Baseline Noise.

in an intermittent ground loop. The problem was resolved by maintaining the integrity of the gage circuits and by continuously monitoring the condition of the sliprings. Figure 56 shows an oscillograph stripout of the baseline noise level after the problem was corrected.

System Drift and Computer Compatibility Test Results

The long-term drift test gave considerable confidence in the capability and stability of the instrumentation system and the data system interface. The resulting data were as follows:

1. The amplifier drift, caused by the 40°F temperature rise when the covers were installed, was read out on the first data run of set number one. The computer, having been programmed to show a baseline of 0 psi on all pressure channels, printed out the equivalent pressure change caused by this amplifier drift. This pressure change was converted to equivalent input microvolts per 0°F temperature change, and in all cases was well within specification.

2. The second data run of the first set was analyzed to determine the correction made by the computer program for amplifier drift. The computer program compared the third step of the preflight calibration (baseline) with the third step of each succeeding in-flight calibration and performed the arithmetical subtractions necessary to correct for amplifier drift. The analysis of the data showed that the computer program corrected for more than 97 percent of the amplifier drift. This compared with the estimated 75-percent correction that was projected during the statistical accuracy analysis.

3. The third run of each data set was analyzed to determine the accuracy and repeatability of the known input simulation. The plot of all channels surveyed showed a typical Gaussian distribution about the mean, with the extreme error being ±6 percent and the 2σ error being less than ±3 percent. This distribution compares very favorably with the error distribution that was predicted by the statistical error analysis.

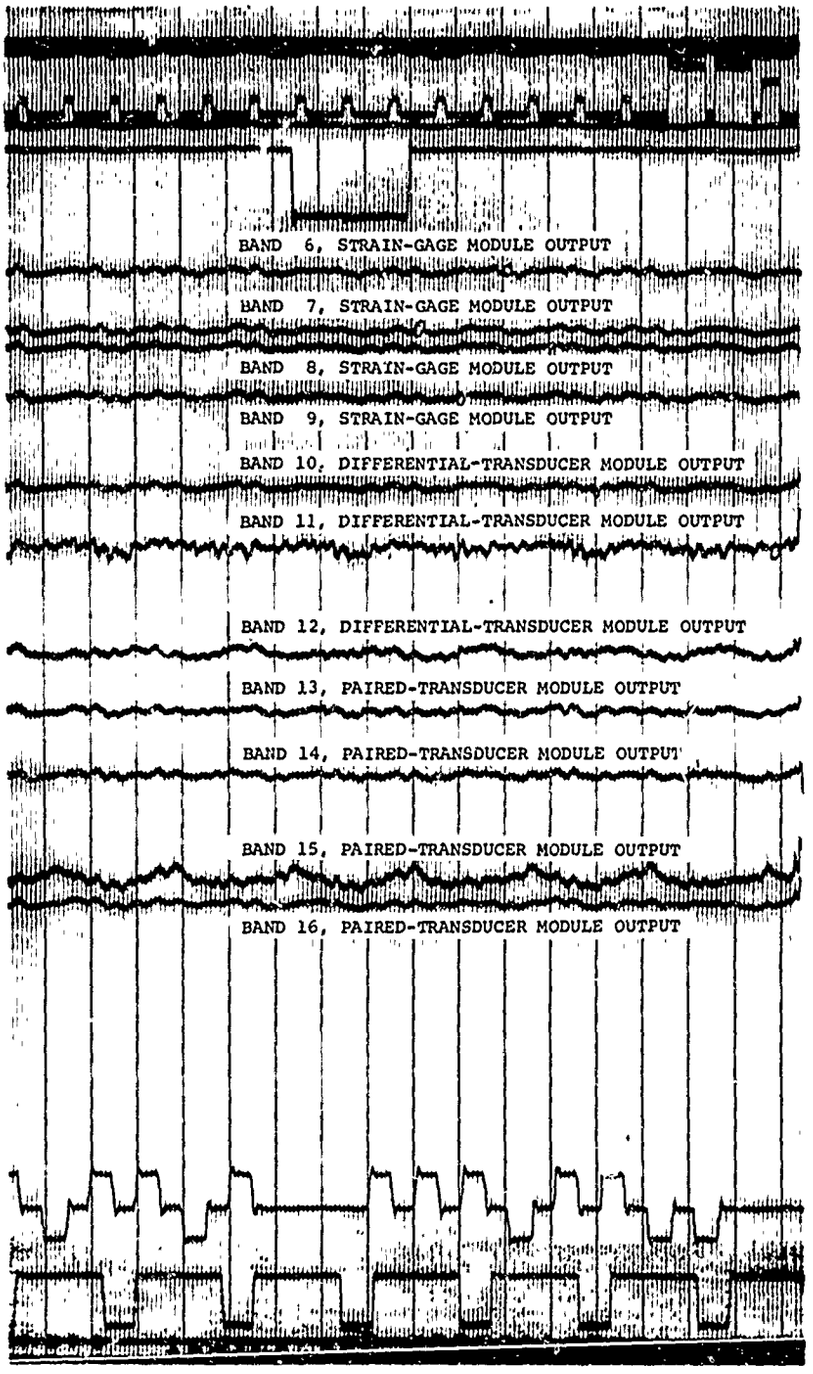

Figure 56. Oscillograph Stripout of Instrumentation System Output Showing Reduction in Baseline Noise.

This final test, in conjunction with all previous test procedures, established complete confidence in the system as designed. It was anticipated that the extensive test program outlined in this section would greatly enhance the operational phase of the Dynamic Airloads Program.

EVALUATION OF DESIGN BASED ON EXPERIMENTAL RESULTS

An evaluation of the measurement system, based on the experimental results, is presented in Table XVI. This table summarizes the attainable accuracies for the various measurement paths of the program. The details of the method used to determine the individual component statistics are presented in Appendix III. Table XVI indicates typical worst-case statistics for the various measurement paths and combines the individual accuracies to present them as system accuracy. The summary indicates that, for the pressure measurements, the transducer contributed the most significant part of the error, while for position and other strain-gage measurements, the tape-discriminator combination was the most significant contributor.

With the interpretation of these statistics in relation to specific measurement parameters, it should be realized that substantially better accuracies, on the order of two to three magnitudes, can be predicted for specific channels. One of the main reasons for the extensive evaluation of the pressure transducers, as documented in Volume II, was to have the necessary data to select the transducers with the best characteristics for the parameters that contributed the most significant information to the program.

TABLE XVI
SYSTEM ERROR ANALYSIS SUMMARY OF REPRESENTATIVE CONDITIONS
BASED ON EXPERIMENTAL RESULTS

Parameter	Full-Scale Range	Measurand	Worst-Case Environment	Individual Component Statistics in Percent of Measurand						RSS System Error in Percent of Measurand
				Transducer	Amplifier	VCO	Tape System	Discriminator	Analog to Digital	
Paired absolute-pressure	10 psid	5 psid	-40°F	7.6	2.2	1.1	2.5	1.0	0.1	± 8.6
Differential-pressure	10 psid	5 psid	-40°F	4.8	3.5	1.1	2.5	1.0	0.1	± 6.C
Differential-pressure	5 psid	2.5 psid	-40°F	4.8	3.0	1.0	2.5	1.0	0.1	± 6.3
Differential-pressure	2 psid	1 psid	-40°F	5.5	5.1	1.4	2.5	1.0	0.1	± 8.4
Attitude (vane)	60°	30°	n/a	2.0	n/a	1.0	2.5	1.0	0.1	± 3.5
Attitude (gyro)	90°	45°	n/a	0.7	n/a	1.0	2.5	1.0	0.1	± 2.9
Airspeed differential-pressure	140 kt	100 kt	-40°F	1.9	n/a	0.7	2.0	1.0	0.1	± 3.0
Pressure altitude	10,000 ft	5,000 ft	-40°F	2.8	n/a	1.0	2.5	1.0	0.1	± 4.0
Blade loads	50,000 in.-lb.	25,000 in.-lb.	-40°F	3.0	n/a	1.0	2.5	1.0	0.1	± 4.0
Shaft load, bending	50,000 in.-lb.	25,000 in.-lb.	n/a	3.0	n/a	1.0	2.5	1.0	0.1	± 4.0
Shaft load, torque	100,000 in.-lb.	100,000 in.-lb.	n/a	1.0	n/a	1.0	2.5	1.0	0.1	± 3.0

APPENDIX I

ADDITIONAL TEST DATA ON DIFFERENTIAL AMPLIFIERS

The amplifiers that did not meet the requirements of the specification failed for the following reasons:

Amplifier No. 3 - This amplifier was tested three times. The first test was conducted with the first test board* with the amplifier in position No. 2. The second and third runs were conducted on the second board* with the amplifier in position No. 5. This amplifier did not provide consistent results and was very sensitive to a tap on its case. Data from the three runs indicated a possible internal joint failure, probably on one of the pins.

Amplifier No. 12 - This amplifier was tested twice. Both tests were conducted with the amplifier mounted on the first test board in positions No. 4 and No. 5. The data indicated an 878-millivolt drift at -20°C and a change in gain stability of 16 percent.

Amplifier No. 32 - This amplifier was tested twice. Both tests were conducted on the second test board with the amplifier in position No. 7. Between tests the amplifier was removed from the board and then resoldered back in place. The data indicated a 780-millivolt drift at -20°C, a change in gain stability of 15 percent, and an unacceptable level of noise near 10g at 200 cps. These results indicated a possible internal joint failure.

Amplifier No. 35 - This amplifier was tested twice. Both tests were conducted with the first test board with the amplifier mounted in positions No. 1 and No. 7. The data indicated a 53-millivolt drift at +55°C and a 3.75-percent change in gain stability.

Amplifier No. 37 - This amplifier was tested twice. Both tests were conducted with the first test board with the amplifier in

---

*Note: The reason for assembling two test boards was that when testing began with the first test board, some amplifiers were found to be sensitive to a tap or temperature. The second board was constructed to determine if the sensitivity was caused by some fault in the assembly of the first test board. Since the second test board exhibited the same characteristics, the sensitivity was attributed to the amplifiers themselves.

positions No. 2 and No. 8. The data from both runs indicated an unacceptable noise level when subjected to environmental disturbances. When a force of 10g at 200 cps was applied to the amplifier, 20-millivolt spikes appeared in the output. This occurrence was intermittent. It was also noted that a tap on its case would produce similar results.

Amplifier No. 42 - This amplifier was tested twice and checked for internal connection problems. Both tests were conducted with the amplifier on the first test board in positions No. 1 and No. 5. The data obtained indicated a 646-millivolt drift at 55°C and a 4.6-percent change in gain stability. The amplifier was also checked for internal connection problems with the second board where the soldered pin connections provided unquestionable external continuity. The amplifier, however, was still very sensitive to a tap on its case.

Amplifier No. 52 - This amplifier was tested three times. One test was conducted on the first board in position No. 3, and the other two tests were conducted on the second board in position No. 4. Between the two runs on the second board, the amplifier was removed and then soldered back in place. The data indicated a 64-millivolt drift at -20°C, a 350-millivolt drift at +55°C, and a 5.9-percent change in gain stability at 55°C.

Amplifier No. 57 - This amplifier was tested four times. Three tests were conducted on the first board in positions No. 3, No. 6, and No. 7. The fourth test was conducted with the second board. The data indicated a 54-millivolt drift at -20°C.

Amplifier No. 72 - This amplifier was tested once on the second board in position No. 1 and was found to have a 38-millivolt drift at -20°C.

Amplifier No. 79 - This amplifier was tested twice on the first test board in positions No. 2 and No. 4. The data indicated a 6.85-volt and a 200-millivolt drift at -20°C and at +55°C respectively. There was also a change in gain stability of 274 percent and 3.3 percent at -20°C and +55°C respectively.

Amplifier No. 84 - This amplifier was placed in five different positions on the first test board and could not be balanced at any time.

Amplifier No. 85 - This amplifier was tested once on the first board and rechecked for output noise level. The output noise level was an acceptable value of 5 millivolts peak-to-peak before the amplifier was subjected to a temperature of +55°C. After a short stabilization period at this temperature, the output noise level was observed instantaneously to change to a value twice as large as it initially was (10 millivolts peak-to-peak). The output noise level remained at this high value after the amplifier was returned to ambient temperature. The data indicated a 5.45-volt drift at +55°C and a change in gain stability of 40 percent at +55°C.

Amplifier No. 87 - This amplifier was tested once on the second board and received two additional common mode checks on the same board but in different positions. The data indicated unacceptable common mode rejection. The best common mode rejection was obtained with the trim pots adjusted for minimum signal output (100Ω in one input and 3Ω in the other input). The best dc common mode rejection for this amplifier fell barely within specifications. The best ac common mode rejection, however, was 16 millivolts and was not within specifications.

Amplifier No. 103 - This amplifier was tested once on the second board and was rechecked for sensitivity to pressure on its case and sensitivity to a tap. It was found to be very sensitive to environmental disturbances independent of its position on the test board. The data indicated a 1021-millivolt and a 62-millivolt drift at -20°C and +55°C respectively. The gain stability changed 17.5 percent at -20°C. The noise level became very bad beginning near an acceleration of 9g at 200 cps. All test indications pointed toward a possible internal joint failure.

Amplifier No. 104 - This amplifier was tested once on the second board and was rechecked for sensitivity to a tap. It was found to be very sensitive to environmental disturbances independent of its position on the test board. The data indicated a change in gain stability of 2 percent at +55°C and bad noise levels at 3g at 50 cps and at 10g at 200 cps.

Amplifier No. 107 - This amplifier was tested four times, three of which were on the first board and the other on the second board. The amplifier did not provide consistent readings; it gave indications of a possible internal joint failure. The data indicated a 33-millivolt and a 61-millivolt drift at -20°C and +55°C respectively.

APPENDIX II

IN SITU PRESSURE TRANSDUCER CALIBRATION DATA

This appendix provides, in tabular form, fully detailed calibration statistics for the pressure transducers as installed on the forward and aft rotor blades. The initial listings of transducers, with serial numbers prefixed by the letter D, are for the matched pairs of absolute-pressure transducers. The listings for transducers with serial numbers prefixed by the letters E, F, or G are for the differential-pressure transducers which gave individual output signals. Table XVII provides the data for the transducers on the forward rotor blade; Table XVIII provides information for those on the aft rotor blade.

TABLE XVII

FORWARD ROTOR BLADE IN SITU PRESSURE TRAN

Data Code	Top Bot.	Serial Number	Signal Cond.Card	Sens.	Eb	F.S. Out x 200	Rcal Pres.	Rcal Out $R_L = 0$	
4226	T	D110	13A	0.0528	3.050	483	6	193	
	B	D79		0.0532	2.980	468	6	187	
4219	T	D84	11B	0.0544	3.053	498	6	199	
	B	D118		0.0553	2.934	487	6	195	
4212	T	D153	10A	0.0543	3.094	504	6	202	
	B	D120		0.0548	3.067	504	6	202	
4201	T	D39	7A	0.0545	3.022	494	6	198	
	B	D19		0.0580	2.813	490	6	196	
4194	T	D68	5B	0.0563	3.050	515	5	172	
	B	D61		0.0598	2.872	515	5	172	
4187	T	D22	4A	0.0580	3.107	541	3	108	
	B	D47		0.0608	2.843	518	3	104	
4182	T	D125	2B	0.0676	3.010	610	2	81.3	
	B	D38		0.0688	3.041	627	2	83.6	
4177	T	D57	1A	0.0678	3.191	649	2	86.5	
	B	D51		0.0739	2.926	659	2	86.5	
4202	T	D83	7B	0.0556	3.070	512	5	171	
	B	D112		0.0630	2.718	514	5	171	
4227	T	D154	13B	0.0629	2.997	566	6	236	
	B	D162		0.0672	2.858	576	6	230	
4220	T	D103	12A	0.0652	3.108	608	6	243	
	B	D127		0.0700	2.916	612	6	245	
4213	T	D82	10B	0.0488	3.089	452	5	151	
	B	D145		0.0542	2.783	542	5	151	
4203	T	D98	8A	0.0722	3.022	655	4	175	
	B	D56		0.0764	2.838	650	4	173	
4195	T	D37	6A	0.0644	3.010	582	3	116	
	B	D150		0.0684	2.875	589	3	118	
4188	T	D73	4B	0.0548	3.091	508	2	135	
	B	D25		0.0588	3.015	532	2	142	
4183	T	D64	3A	0.0526	3.043	480	2	64	
	B	D78		0.0534	2.865	489	2	65.2	
4178	T	D20	1B	0.0594	3.016	537	2	71.6	
	B	D76		0.0643	2.768	534	2	71.2	
4204	T	D137	8B	0.0645	3.058	592	3	118	
	B	D42		0.0662	2.900	576	3	115	
4205	T	D147	9A	0.0668	3.081	617	3	123	
	B	D50		0.0694	2.936	611	3	122	

A

TABLE XVII

IN SITU PRESSURE TRANSDUCER CALIBRATION DATA

Rcal Pres.	Rcal Out $R_L = 0$	R_L	Rcal Out Inc R_L	±1.5% F.S.	Meas. Output, mv	Calculated Rcal	Actual Rcal
6	193	1.7	186	7	184	100,880	99,850
6	187	1.7	181	7	-184	102,660	100,200
6	199	1.6	193	7	186	93,950	95,800
6	195	1.7	188	7	-186	93,620	92,700
6	202	1.6	195	7	195	96,100	92,850
6	202	1.6	195	7	-195	94,070	94,700
6	198	1.4	192	7	188	94,770	94,500
6	196	1.5	190	7	-188	91,450	84,200
5	172	1.3	168	8	169	98,390	107,600
5	172	1.3	168	8	-169	95,630	103,100
3	108	0.9	106	7	105	181,580	180,500
3	104	0.9	102	7	-105	166,140	160,050
2	81.3	0.62	80.3	8	78	221,920	220,800
2	83.6	0.7	82.4	8	- 78	224,780	243,200
2	86.5	0.25	86	9	86	211,180	224,100
2	86.5	0.30	86	9	- 86	200,090	197,100
5	171	1.4	166	8	166	104,410	113,850
5	171	1.5	166	8	-166	93,760	101,100
6	236	1.7	218	8	217	83,530	81,750
6	230	1.7	222	8	-217	80,140	79,900
6	243	1.7	235	8	236	81,640	78,725
6	245	1.7	237	8	-236	77,570	75,525
5	151	1.6	146	7	146	121,830	130,700
5	151	1.6	146	7	-146	108,460	113,400
4	175	1.4	170	9	166	104,760	103,100
4	173	1.5	168	9	-166	105,280	105,750
3	116	1.3	113	8	109	157,640	157,500
3	118	1.3	115	8	-109	154,100	158,200
2	135	0.9	66	7	67	289,620	282,250
2	142	0.9	69	7	- 67	271,270	269,100
2	64	0.6	63.2	7	62	289,180	286,400
2	65.2	0.65	64.3	7	- 62	291,970	280,000
2	71.6	0.25	71.2	7	70	246,410	247,800
2	71.2	0.3	70.7	7	- 70	228,010	226,600
3	118	1.4	115	8	116	160,450	155,800
3	115	1.5	112	8	-116	155,260	150,400
3	123	1.4	120	8	116	160,600	157,200
3	122	1.4	119	8	-116	163,090	150,200

B

TABLE XVII.- Continued

Data Code	Top Bot.	Serial Number	Signal Cond.Card	Sens.	Eb	F.S. Out x 200	Rcal Pres.	Rcal Out $R_L = 0$	R_L	Rcal Ou Inc R_L
4228	T	D91	14A	0.0715	3.135	672	4	179	1.7	173
	B	D121		0.0738	3.054	676	4	180	1.7	174
4221	T	D66	12B	0.0782	3.088	724	4	193	1.7	186
	B	D105		0.0809	2.865	695	4	185	1.7	179
4214	T	D149	11A	0.0645	2.995	579	3	116	1.7	112
	B	D136		0.0693	2.813	585	3	117	1.6	113
4206	T	D46	9B	0.0645	3.080	596	2	79.5	1.4	77.3
	B	D133		0.0664	3.020	602	2	80.3	1.5	77.9
4196	T	D67	6B	0.0662	3.126	621	2	82.8	1.3	80.6
	B	D152		0.0670	3.057	614	2	81.9	1.3	79.8
4189	T	D123	5A	0.0842	3.000	758	2	101	0.9	99
	B	D111		0.0848	2.970	756	2	101	0.9	99
4184	T	D139	3B	0.0735	2.992	649	2	86.5	0.6	85.5
	B	D97		0.0766	2.793	624	2	83.2	0.6	82.2
4179	T	D35	2A	0.0723	3.009	653	1	43.5	0.25	43.3
	B	D72		0.0745	2.916	652	1	43.5	0.25	43.3
						F.S. Output				
4222		G8	25B	0.0763	3.045	465	3	140	1.6	135
4215		G2	23B	0.0667	3.120	416	2	83.2	1.5	80.7
4207		G9	21A	0.0664	3.103	412	2	82.4	1.5	80
4197		F8	19A	0.0796	3.139	250	2	100	1.2	98
4190		F11	17A	0.1041	3.042	317	1	63.3	1.2	61.8
4229		G1	27B	0.0777	3.008	467	3	140	1.7	135
4223		G3	26A	0.0835	2.987	499	3	150	1.6	145
4216		G10	24A	0.0708	3.054	432	2	86.4	1.5	84
4208		F7	21B	0.0973	3.042	296	2	118	1.5	115
4198		F14	19B	0.1210	3.064	368	1	74	1.2	72
4191		E36	17B	0.0787	2.989	94	1	47	0.7	46
4185		E13	16A	0.0817	2.985	97.5	0.5	24.4	0.6	24.1
4180		E8	15A	0.1132	3.120	141	0.5	35.2	0.4	35
4224		F5	26B	0.1110	3.130	347	2	139	1.7	134
4217		F12	24B	0.1130	3.033	343	2	137	1.5	133
4209		E9	22A	0.0726	3.024	87.8	1	43.9	1.5	43
4199		E34	20A	0.0980	2.970	117	1	58.5	1.2	57.2
4192		E28	18A	0.1089	2.944	128	0.5	32	0..	31.5
4230		F1	28A	0.1269	3.107	394	2	158	1.7	153
4210		E22	22B	0.0955	3.075	117	1	58.7	1.5	56.9
4186		E24	16B	0.0860	3.046	105	0.5	26.2	0.6	25.9
4181		E44	15B	0.1000	2.940	118	0.5	29.5	0.4	29.3
4225		E27	27A	0.0997	3.030	120.8	1	60.4	1.7	58.3
4218		E45	25A	0.1039	3.027	125.8	1	62.9	1.5	61
4211		E32	23A	0.1210	3.066	148	1	74	1.5	72
4200		E16	20B	0.1083	3.067	132.9	1	66.5	1.2	65
4193		E40	18B	0.2209	3.152	278.5	0.5	69.6	0.9	68.3

A

E XVII.- Continued

Rcal res.	Rcal Out $R_L = 0$	R_L	Rcal Out Inc R_L	±1.5% F.S.	Meas. Output, mv	Calculated Rcal	Actual Rcal
4	179	1.7	173	9	171	117,070	113,800
4	180	1.7	174	9	-171	106,630	104,750
4	193	1.7	186	9	189	99,840	96,300
4	185	1.7	179	9	-189	95,470	88,400
3	116	1.7	112	8	113	163,050	159,675
3	117	1.6	113	8	-113	149,580	147,900
2	79.5	1.4	77.3	8	78	241,960	235,900
2	80.3	1.5	77.9	8	- 78	234,840	230,650
2	82.8	1.3	80.6	8	79	217,010	234,800
2	81.9	1.3	79.8	8	- 79	237,750	225,900
2	101	0.9	99	10	98	180,160	178,900
2	101	0.9	99	10	- 98	182,330	182,400
2	86.5	0.6	85.5	8	87	202,870	197,550
2	83.2	0.6	82.2	8	- 87	193,040	185,500
1	43.5	0.25	43.3	9	43	411,740	415,550
1	43.5	0.25	43.3	9	- 43	388,320	386,100
				±2% F.S.			
3	140	1.6	135	9	135	135,470	133,400
2	83.2	1.5	80.7	8	79	234,400	247,150
2	82.4	1.5	80	10	80	208,950	235,900
2	100	1.2	98	5	98	193,390	194,600
1	63.3	1.2	61.8	6	61	301,050	310,000
3	140	1.7	135	10	130	142,350	135,500
3	150	1.6	145	10	140	123,410	125,750
2	86.4	1.5	84	10	84	195,050	212,250
2	118	1.5	115	6	115	160,370	158,100
1	74	1.2	72	8	75	247,380	241,000
1	47	0.7	46	4	44	392,160	397,000
0.5	24.4	0.6	24.1	2	24.5	632,070	708,700
0.5	35.2	0.4	35	3	37	529,540	512,600
2	139	1.7	134	6	133	149,470	149,350
2	137	1.5	133	8	133	124,670	137,560
1	43.9	1.5	43	2	44	409,710	414,400
1	58.5	1.2	57.2	3	57	305,530	307,250
0.5	32	0.7	31.5	4	32	532,460	558,600
2	158	1.7	153	8	153	128,980	128,400
1	58.7	1.5	56.9	2	54	340,090	346,450
0.5	26.2	0.6	25.9	2	26	701,265	742,300
0.5	29.5	0.4	29.3	4	30	598,630	568,200
1	60.4	1.7	58.3	2.4	57	312,990	312,200
1	62.9	1.5	61	2.7	61	279,900	299,000
1	74	1.5	72	3.2	72	236,320	246,400
1	66.5	1.2	65	2.6	62	303,290	310,000
0.5	69.6	0.9	68.3	5.6	66	278,890	296,600

B

TABLE XVIII

AFT ROTOR BLADE IN SITU PRESSURE TRANSDUCER CALIBR

Data Code	Top Bot.	Serial Number	Signal Cond.Card	Sens.	Eb	F.S. Out x 200	Rcal Pres.	Rcal Out R_L - 0	R_L
4280	T	D49	13A	0.0554	3.102	516	6	206	1.7
	B	D58	13A	0.0601	2.84	512	6	205	1.7
4273	T	D144	11B	0.0543	3.09	503	6	201	1.7
	B	D30	11B	0.0607	2.79	508	6	203	1.7
4266	T	D99	10A	0.0579	3.124	543	6	217	1.5
	B	D122	10A	0.0595	3.005	536	6	214	1.6
4255	T	D135	7A	0.0713	3.058	653	6	261	1.4
	B	D81	7A	0.0729	2.983	653	6	261	1.5
4248	T	D148	5B	0.0647	3.017	576	5	185	1.3
	B	D104	5B	0.0670	2.968	586	5	189	1.3
4241	T	D109	4A	0.0595	3.114	556	3	111	0.9
	B	D95	4A	0.0642	2.768	533	3	107	0.9
4236	T	D24	2B	0.0655	3.053	600	2	80	0.6
	B	D132	2B	0.0737	2.713	600	2	80	0.6
4231	T	D74	1A	0.0740	3.07	682	2	91	0.35
	B	D102	1A	0.0786	2.97	700	2	93	0.32
4256	T	D70	7B	0.0538	3.022	488	5	163	1.4
	B	D140	7B	0.0587	2.776	489	5	163	1.5
4281	T	D160	13B	0.0589	3.135	554	6	222	1.7
	B	D60	13B	0.0650	2.840	554	6	222	1.7
4274	T	D100	12A	0.0617	3.147	639	6	256	1.6
	B	D108	12A	0.0700	3.047	640	6	256	1.7
4267	T	D71	10B	0.0538	3.120	503	5	168	1.5
	B	D53	10B	0.0561	2.983	502	5	167	1.6
4257	T	D117	8A	0.0691	3.307	686	4	183	1.4
	B	D88	8A	0.0733	2.824	621	4	166	1.5
4249	T	D48	6A	0.0629	3.071	579	3	116	1.3
	B	D93	6A	0.0657	3.035	598	3	120	1.3
4242	T	D75	4B	0.0589	3.082	545	2	73	0.9
	B	D85	4B	0.0630	2.880	544	2	73	0.9
4237	T	D141	3A	0.0585	2.995	526	2	70	0.6
	B	D156	3A	0.0613	2.853	525	2	70	0.6
4232	T	D63	1B	0.0593	3.020	537	2	72	0.3
	B	D41	1B	0.0614	2.80	516	2	69	0.3
4258	T	D26	8B	0.0647	2.983	579	3	116	1.4
	B	D65	8B	0.0685	2.771	569	3	114	1.5
4259	T	D80	9A	0.0628	3.156	595	3	119	1.4
	B	D131	9A	0.0660	3.024	599	3	120	1.4
4282	T	D87	14A	0.0769	3.032	699	4	186	1.6
	B	D45	14A	0.0846	2.763	701	4	187	1.7
4275	T	D106	12B	0.0773	3.010	698	4	186	1.6
	B	D89	12B	0.0873	2.662	697	4	185	1.6

A

TABLE XVIII

E IN SITU PRESSURE TRANSDUCER CALIBRATION DATA

F.S. Out x 200	Rcal Pres.	Rcal Out R_L - 0	R_L	Rcal Out Inc R_L	±1.5% F.S.	Meas. Output, mv	Calculated Rcal	Actual Rcal
516	6	206	1.7	199	7	19	94,600	93,330
512	6	205	1.7	198	7	-1[illegible]	87,750	87,600
503	6	201	1.7	195	7	193	96,150	92,800
508	6	203	1.7	196	7	-193	81,000	84,500
543	6	217	1.5	210	8	207	91,280	90,900
536	6	214	1.6	207	8	-207	87,510	86,200
653	6	261	1.4	254	10	247	68,940	71,700
653	6	261	1.5	253	10	-274	70,760	69,800
576	5	185	1.3	180	9	180	96,760	98,700
586	5	189	1.3	184	9	-180	90,950	93,750
556	3	111	0.9	109	7	110	182,690	173,300
533	3	107	0.9	105	7	-110	157,070	150,600
600	2	80	0.6	79	9	79	241,685	235,000
600	2	80	0.6	79	9	- 79	201,050	196,500
682	2	91	0.35	90	9	95	201,250	183,200
700	2	93	0.32	92	9	- 95	192,510	182,600
488	5	163	1.4	158	7	158	115,959	112,000
489	5	163	1.5	158	7	-158	109,122	104,500
554	6	222	1.7	214	7	214	90,960	87,600
554	6	222	1.7	214	7	-214	83,081	81,900
639	6	256	1.6	248	7	247	79,500	77,470
640	6	256	1.7	247	7	-247	73,370	72,580
503	5	168	1.5	163	7	163	117,404	114,600
502	5	167	1.6	162	7	-163	118,6[illegible]8	113,900
686	4	183	1.4	178	9	174	111,780	112,300
621	4	166	1.5	161	9	-174	106,410	96,000
579	3	116	1.3	113	7	113	161,170	160,150
598	3	120	1.3	116	7	-113	154,790	152,650
545	2	73	0.9	72	8	72	268,260	254,800
544	2	73	0.9	72	8	- 72	242,890	229,600
526	2	70	0.6	69	7	69	255,520	246,400
525	2	70	0.6	69	7	- 69	246,280	241,750
537	2	72	0.3	72	7	70	245,740	244,200
516	2	69	0.3	69	7	- 70	245,740	233,150
5[illegible]	3	116	1.4	113	8	110	159,490	160,600
569	3	114	1.5	111	8	-110	159,510	157,700
595	3	119	1.4	116	8	116	170,500	162,300
599	3	120	1.4	116	8	-116	154,080	150,200
699	4	186	1.6	180	9	177	100,560	100,100
701	4	187	1.7	181	9	-177	91,860	88,000
698	4	186	1.6	181	10	180	99,453	99,650
697	4	185	1.6	180	10	-180	95,770	96,000

B

TABLE XVIII - Continued

Data Code	Top Bot.	Serial Number	Signal Cond.Card	Sens.	Eb	F.S. Out x 200	Rcal Pres.	Rcal Out R_L - 0	R_L	Rca In
4268	T	D159	11A	0.0647	3.051	592	3	118	1.5	
	B	D40	11A	0.0667	3.101	621	3	124	1.5	
4260	T	D59	9B	0.0641	3.021	581	2	77	1.4	
	B	D116	9B	0.0645	3.005	581	2	77	1.4	
4250	T	D90	6B	0.0568	3.086	526	2	70	1.0	
	B	D55	6B	0.0598	2.891	519	2	69	1.2	
4243	T	D44	5A	0.0801	3.139	754	2	101	0.85	
	B	D28	5A	0.0850	2.961	755	2	101	0.85	
4238	T	D69	3B	0.0820	3.086	767	2	102	0.57	
	B	D192	3B	0.0870	3.044	795	2	106	0.58	
4233	T	D119	2A	0.0903	2.993	811	1	54.1	0.28	
	B	D107	2A	0.1073	2.495	803	1	53.5	0.30	
						F.S. Output				
4276		G14	25B	0.0566	3.011	340	3	102	1.6	
4269		G6	23B	0.0719	3.069	441	2	88	1.5	
4261		G13	21A	0.0666	3.029	440	2	88	1.4	
4251		F23	19A	0.0650	2.935	191	2	76	1.2	
4244		F15	17A	0.0998	3.062	306	1	61	0.9	
4283		G5	27B	0.0722	3.011	434	3	130	1.7	
4277		G11	26A	0.0732	3.016	442	3	132	1.7	
4270		G4	24A	0.0803	3.069	493	2	99	1.5	
4262		F13	21B	0.1018	3.021	307	2	122	1.45	
4252		F21	19B	0.0965	3.026	292	1	58.4	1.2	
4245		E19	17B	0.0914	2.988	109	1	54.5	0.9	
4239		E15	16A	0.08917	3.046	109	0.5	27.3	0.6	
4234		E14	15A	0.1122	3.102	139	0.5	35	0.35	
4278		F9	26B	0.1103	2.986	329	2	132	1.6	
4271		F18	24B	0.1047	2.996	314	2	125	1.5	
4263		E11	22A	0.0747	3.104	93	1	46.4	1.45	
4253		E29	20A	0.09	3.007	108.3	1	54.2	1.3	
4246		E12	18A	0.1075	3.167	136	0.5	34	0.9	
4284		F17	28A	0.1104	3.051	337	2	135	1.7	
4264		E41	22B	0.1092	3.088	135	1	67.5	1.5	
4240		E5	16B	0.1210	2.992	145	0.5	36.3	0.65	
4235		E6	15B	0.1209	2.987	144	0.5	36.1	0.38	
4279		E21	27A	0.1019	3.028	123	1	62	1.6	
4272		E42	25A	0.0910	3.034	110.4	1	55.2	1.6	
4265		E23	23A	0.1190	2.965	141	1	71	1.5	
4254		E7	20B	0.1055	3.016	127	1	63.5	1.4	
4247		E39	18B	0.2340	3.081	288	0.5	72	0.9	

TABLE XVIII - Continued

F.S. Out x 200	Rcal Pres.	Rcal Out R_L - 0	R_L	Rcal Out Inc R_L	±1.5% F.S.	Meas. Output, mv	Calculated Rcal	Actual Rcal
592	3	118	1.5	114	9	111	158,900	159,900
621	3	124	1.5	120	9	-111	168,370	171,500
581	2	77	1.4	75	7	75	249,970	240,500
581	2	77	1.4	75	7	- 75	244,430	236,400
526	2	70	1.0	69	7	69	257,000	258,900
519	2	69	1.2	68	7	- 69	256,230	250,600
754	2	101	0.85	99	10	99	196,510	188,300
755	2	101	0.85	99	10	- 99	175,351	170,700
767	2	102	0.57	101	10	101	174,790	172,300
795	2	106	0.58	105	10	-101	174,000	178,250
811	1	54.1	0.28	54	11	52	324,770	328,750
803	1	53.5	0.30	53	11	- 52	274,290	276,600
F.S. Output					±2% F.S.			
340	3	102	1.6	99	8	99	185,812	183,900
441	2	88	1.5	85	9	80	217,350	230,000
440	2	88	1.4	86	9	79	208,010	226,100
191	2	76	1.2	74.2	4	76	230,000	229,500
306	1	61	0.9	60	6	55	302,350	313,500
434	3	130	1.7	126	15	121	149,082	149,300
442	3	132	1.7	128	11	128	142,284	138,100
493	2	99	1.5	96	10	85	188,730	210,000
307	2	122	1.45	120	6	125	153,570	144,300
292	1	58.4	1.2	57	6	57	308,536	317,900
109	1	54.5	0.9	53.5	2	51	311,471	337,700
109	0.5	27.3	0.6	27	2	26.5	654,000	637,350
139	0.5	35	0.35	34.5	3	36	525,860	516,200
329	2	132	1.6	128	7	122	138,370	147,100
314	2	125	1.5	122	6	120	144,172	146,400
93	1	46.4	1.45	45	2	43	456,690	441,000
108.3	1	54.2	1.3	53	2	55	323,990	311,700
136	0.5	34	0.9	33.4	3	32	571,250	595,650
337	2	135	1.7	132	7	136	138,480	130,000
135	1	67.5	1.5	65.5	3	68	285,250	271,400
145	0.5	36.3	0.65	35.8	3	35.5	505,870	510,900
144	0.5	36.1	0.38	35.8	3	35.5	474,500	463,200
123	1	62	1.6	60	2	57	322,560	337,000
110.4	1	55.2	1.6	54	3	54	344,128	358,500
141	1	71	1.5	68	3	66	255,500	272,700
127	1	63.5	1.4	61.7	3	66	287,780	279,650
288	0.5	72	0.9	70.7	6	73	254,230	257,200

B

APPENDIX III

DETAILED STATISTICAL ANALYSIS OF INSTRUMENTATION SYSTEM ACCURACY

This section presents a statistical analysis of all factors determining the accuracy of individual system components. The individual component statistics are combined to present a system accuracy analysis for representative systems of the Dynamic Airloads Program.

DEFINITIONS

A list of simplified definitions of special terms involved in error analysis, as used in this document, is presented here. There is considerable variation in the definitions between the various approaches to error analysis, and it is important to define the terminology used in each case.

1. Measurand is the quantity to be measured and is often called the input.

2. System errors are the errors of a system including errors of zero shift, sensitivity shift, changes in linearity, etc. System errors are composed of individual errors which may be further separated into random errors and systematic errors.

3. Individual errors refer to the errors introduced by each potential source of error. Individual errors may be of known sign and are then called systematic errors, or of unknown sign and are called random errors.

4. Random errors are individual errors of uncertain algebraic sign. Not only is the sign unpredictable but the magnitude is usually unpredictable within limits. These limits, however, usually vary in a generally predictable way with the environment.

5. Systematic errors are individual errors having known sign. These errors are combined by algebraic addition; if significant, they may be corrected in the data so as to eliminate their effect. With each systematic error, there is an uncertainty of its magnitude; therefore, the expected or mean value is taken as the

systematic error and the uncertainty about this mean is added among the random errors, if significant.

6. RSS error is the combination of errors by square root of the sum of the squares of the random individual errors. It must be remembered that a change in the operating environment may increase or decrease some of the individual errors with the result that a different value will be calculated for the RSS error.

PROCEDURE

A sensor may be considered as a system for the purpose of error analysis. The output should be considered not as a single curve relating input and output but rather as a complex relation in which the output depends on the value of the measurand* and on the value of each of the error inputs. The input errors considered in this analysis were:

1. Temperature zero shift
2. Temperature sensitivity shift
3. Linearity
4. Hysteresis
5. Frequency response

The analytical procedure began by determining the independent errors resulting from each error input of a group of components. This information was obtained from the individual calibration data sheets. Each group of error figures was analyzed by methods subsequently defined to arrive at a standard deviation. All error inputs were computed to the same standard deviation, which for this document was 2σ. This means that the probability of the system error exceeding the mean by ± 2 times the standard deviation is 4.6 percent.

To compute the standard deviation, the following procedure was used:

1. The average value (arithmetic mean) of the individual error input was computed.

---

*A. M. Mood, Introduction to the Theory of Statistics, Sections 7.5 and 7.6, McGraw-Hill Book Co., Inc., New York, 1950.

2. The variance was then calculated. The variance is the average value of the square of the difference between the error value and the mean.

3. The standard deviation is the square root of the variance and is expressed in the same units as the individual sample values and the mean.

EVALUATION OF COMPONENTS

The following evaluation includes consideration of each component of the instrumentation system in various environmental situations. This analysis includes the ground station playback and discriminator errors, and therefore the resultant accumulated error should be applicable to the digitized data. Errors caused by the data analysis are not included.

Transducers

The transducers considered include the two types of blade pressure transducers; the position transducers (aircraft attitude, blade position, etc.); and the airspeed, altitude, and acceleration transducers. In each case the installation is briefly reviewed, the applicable data are presented, and a specific transducer error analysis is presented.

Pressure Transducers

Two types of transducers (absolute and differential) and four ranges of these transducers (5 - 20 psia, ±2 psid, ±5 psid, and ±10 psid) were evaluated in this analysis. The analysis of the differential-pressure transducers was straightforward, with a single transducer being used as part of a measurement system. The analysis of the absolute-pressure transducers was complicated by the fact that a pair of transducers was used as the input to the measurement system. The purpose in pairing the absolute-pressure transducers was to obtain a differential measurement between the top and bottom surfaces of the blade without having pressure ports which could impair the structural integrity of the blade spar.

The figures used for this analysis were obtained from calibrations performed at Vertol and from test data sheets supplied with each transducer by the manufacturer.

Paired Absolute-Pressure Configuration

The paired absolute-pressure transducers were connected so that their outputs canceled each other; that is, with the same pressure on both sides of the blade, the net output from the pair would be zero. Provisions were made within the signal-conditioning network to adjust the sensitivities of the paired transducers so that they had equivalent outputs for the same input. In this configuration, the systematic errors due to temperature canceled each other to the extent that the temperature error coefficients were matched. To provide a basis for statistical analysis of this type of configuration, the transducer data were tabulated listing the calibrated error figures for temperature drift in order of magnitude. The transducers were then paired, the selection being dependent on providing a pair whose sensitivity was matched within 10 percent (the adjustment span of the signal conditioner), and at the same time, matching temperature zero-drift coefficients as closely as possible.

An error figure for each pair of transducers was then calculated. The temperature zero-drift coefficient was taken as the difference between the individual coefficients, for in this configuration signals of the same sign act to cancel each other. The zero-drift error coefficient was determined by the extent of the mismatch. It was assumed that the temperature error input was equal for top and bottom transducers. Obtaining a combined temperature-sensitivity error presented a special problem, as this error was a slope change and was dependent on the pressure sensed by each transducer and not on the full-scale output. Since it was not possible to determine the individual pressures at any given moment, a statistical average for all the individual transducers was used. A combined linearity and hysteresis figure for a pair was obtained by adding the individual errors from the calibration data by the root sum squared method. Based on these assumptions, the statistical error coefficient for the group of 54 paired transducers was obtained as follows:

1. The arithmetic mean of each error input was determined.

2. The variance of the square of the difference between the arithmetic mean and the error input was calculated.

3. The average variance was then calculated.

4. The square root of the average variance was the standard deviation.

5. Twice the standard deviation was added to the arithmetic mean to provide the statistical error coefficient.

If the error coefficient was of known sign and the magnitude of the error input could be determined, the data were to be corrected in data reduction; therefore, these terms do not appear in this analysis.

Paired Absolute-Pressure Transducer Error Analysis

The mathematical procedures that were used for the error analysis of the absolute-pressure transducers are shown in Table XIX; the statistical data are shown in Table XX.

The values utilized to compile the absolute-pressure transducer statistics were as follows:

Assumed mean value of error input
Temperature = 70°F
Pressure = 15 psia

Summary of error specifications

Temperature zero shift	= 0.27 percent full scale/°F
Temperature sensitivity shift	= 0.074 percent indicated output/°F
Combined linearity	= ±1.5 percent full scale
Combined hysteresis	= ±1.0 percent full scale

TABLE XIX
STATISTICAL CALCULATIONS FOR ABSOLUTE-PRESSURE TRANSDUCERS

Parameter	Temperature Zero Shift	Temperature Sensitivity Shift	Linearity	Hysteresis
Arithmetic mean	0.010	0.050	1.00	0.54
Sum of variances	0.004026	0.015552	3.9475	2.8920
Average variance	$\frac{0.004026}{54}$	$\frac{0.015552}{108}$	$\frac{3.9475}{54}$	$\frac{2.8920}{54}$
	=0.000074	=0.000144	=0.073	=0.054
Deviation	0.0086	0.012	0.27	0.23
2σ error	=2(0.0086)	=2(0.012)	=2(0.27)	=2(0.23)
	+0.010	+0.050	+1.00	+0.54
	=0.027	=0.074	=1.54	=1.00

A component error analysis, representing 4 typical error inputs and using the 2σ error values, is shown in Table XXI.

TABLE XX

STATISTICAL ERROR ANALYSIS OF ABSOLUTE-PI

Transducer Location T = Top B = Bottom		Transducer Serial Number	Transducer Sensitivity mv/v/psi	Temperature Zero Shift %F.S./°F	Temperature Zero Shift of Pair	Temperatu Sensitivi Shift % Indicat Output/°F
1.	T	D154	0.061	-0.088	-0.011	0.027
	B	D162	0.066	-0.077		0.035
2.	T	D57	0.071	-0.055	-0.030	0.067
	B	D51	0.074	-0.085		0.039
3.	T	D144	0.052	-0.033	-0.022	0.037
	B	D118	0.055	-0.055		0.033
4.	T	D82	0.052	-0.033	-0.015	0.058
	B	D145	0.054	-0.048		0.037
5.	T	D68	0.062	-0.037	-0.031	0.051
	B	D108	0.067	-0.068		0.048
6.	T	D148	0.061	-0.032	-0.031	0.058
	B	D104	0.063	-0.063		0.049
7.	T	D103	0.063	-0.041	-0.017	0.044
	B	D127	0.068	-0.024		0.046
8.	T	D160	0.061	-0.034	-0.010	0.049
	B	D60	0.063	-0.044		0.043
9.	T	D100	0.063	-0.017	-0.011	0.048
	B	D61	0.065	-0.028		0.043
10.	T	D74	0.070	-0.020	-0.005	0.049
	B	D102	0.075	-0.015		0.052
11.	T	D87	0.075	-0.028	-0.012	0.049
	B	D45	0.078	-0.016		0.040
12.	T	D91	0.071	-0.004	-0.021	0.047
	B	D121	0.074	-0.025		0.053
13.	T	D84	0.054	-0.011	-0.001	0.113
	B	D62	0.060	-0.012		0.042
14.	T	D117	0.069	+0.003	+0.012	0.041
	B	D88	0.071	+0.015		0.051
15.	T	D123	0.081	+0.007	+0.012	0.045
	B	D111	0.084	+0.019		0.047
16.	T	D153	0.052	+0.011	+0.003	0.047
	B	D120	0.053	+0.014		0.050
17.	T	D112	0.065	+0.012	+0.007	0.049
	B	D93	0.066	+0.019		0.046
18.	T	D110	0.052	+0.016	+0.000	0.060
	B	D79	0.053	+0.016		0.046

TABLE XX

RROR ANALYSIS OF ABSOLUTE-PRESSURE TRANSDUCERS

Temperature Zero Shift of Pair	Temperature Sensitivity Shift % Indicated Output/°F	Linearity %F.S.	Linearity of Pair (RSS Method)	Hysteresis %F.S.	Hysteresis of Pair (RSS Method)
-0.011	0.027	0.62	0.71	0.34	0.52
	0.035	0.36		0.42	
-0.030	0.067	0.99	1.22	0.31	0.37
	0.039	0.70		0.21	
-0.022	0.037	0.70	0.76	0.12	0.23
	0.033	0.28		0.20	
-0.015	0.058	0.59	1.28	0.21	0.41
	0.037	1.14		0.35	
-0.031	0.051	0.47	0.82	0.43	0.50
	0.048	0.73		0.25	
-0.031	0.058	1.22	1.42	0.37	0.45
	0.049	0.75		0.30	
-0.017	0.044	0.60	1.28	0.31	0.45
	0.046	1.12		0.33	
-0.010	0.049	0.44	1.04	0.35	0.49
	0.043	0.94		0.35	
-0.011	0.048	1.13	1.54	0.59	0.66
	0.043	0.72		0.28	
-0.005	0.049	0.86	1.16	0.27	0.52
	0.052	0.78		0.45	
-0.012	0.049	0.56	1.70	0.41	0.55
	0.040	1.60		0.37	
-0.021	0.047	1.53	1.50	1.57	1.58
	0.053	0.37		0.27	
-0.001	0.113	0.25	0.73	0.29	0.41
	0.042	0.69		0.26	
+0.012	0.041	0.70	0.87	0.75	0.80
	0.051	0.59		0.27	
+0.012	0.045	0.79	0.93	0.32	0.49
	0.047	0.48		0.31	
+0.003	0.047	0.79	0.93	0.66	0.70
	0.050	0.48		0.25	
+0.007	0.049	0.83	0.93	0.36	0.52
	0.046	0.46		0.43	
+0.000	0.060	0.52	0.66	0.70	0.73
	0.046	0.40		0.21	

TABLE XX - Continued

Transducer Location T = Top B = Bottom		Transducer Serial Number	Transducer Sensitivity mv/v/psi	Temperature Zero Shift %F.S./°F	Temperature Zero Shift of Pair	Tempe Sensi Shift % Ind Outpu
19.	T	D37	0.064	+0.021	+0.005	0.048
	B	D77	0.068	+0.016		0.038
20.	T	D109	0.057	+0.019	+0.000	0.041
	B	D95	0.060	+0.019		0.052
21.	T	D78	0.052	0.029	+0.014	0.045
	B	D99	0.055	0.015		0.055
22.	T	D44	0.080	0.016	+0.006	0.049
	B	D28	0.085	0.022		0.033
23.	T	D47	0.060	0.027	+0.009	0.027
	B	D140	0.061	0.018		0.047
24.	T	D98	0.072	0.021	+0.008	0.053
	B	D56	0.076	0.013		0.044
25.	T	D83	0.060	0.025	+0.002	0.058
	B	D48	0.061	0.023		0.049
26.	T	D125	0.067	0.025	+0.006	0.053
	B	D38	0.069	0.031		0.050
27.	T	D22	0.055	0.033	0.003	0.056
	B	D54	0.058	0.030		0.045
28.	T	D71	0.058	0.033	0.003	0.087
	B	D53	0.060	0.030		0.062
29.	T	D20	0.060	0.032	0.008	0.040
	B	D96	0.061	0.040		0.056
30.	T	D39	0.055	0.031	0.007	0.060
	B	D70	0.057	0.038		0.056
31.	T	D49	0.055	0.049	0.007	0.040
	B	D58	0.060	0.032		0.049
32.	T	D24	0.065	0.036	0.002	0.060
	B	D42	0.066	0.034		0.037
33.	T	D89	0.075	0.031	0.007	0.062
	B	D97	0.078	0.038		0.066
34.	T	D26	0.065	0.047	0.007	0.042
	B	D65	0.065	0.040		0.053
35.	T	D66	0.078	0.041	0.029	0.050
	B	D105	0.080	0.070		0.048
36.	T	D137	0.062	0.041	0.001	0.037
	B	D80	0.063	0.040		0.074
37.	T	D159	0.062	0.043	0.013	0.040
	B	D40	0.065	0.056		0.035
38.	T	D19	0.058	0.059	0.001	0.058
	B	D55	0.060	0.058		0.046

TABLE XX - Continued

Temperature Zero Shift of Pair	Temperature Sensitivity Shift % Indicated Output/°F	Linearity %F.S.	Linearity of Pair (RSS Method)	Hysteresis %F.S.	Hysteresis of Pair (RSS Method)
+0.005	0.048	0.42	1.26	0.27	0.38
	0.038	1.21		0.25	
+0.000	0.041	1.36	0.61	0.30	0.38
	0.052		1.22	0.24	
+0.014	0.045	0.57	0.96	0.25	0.39
	0.055	0.78		0.30	
+0.006	0.049	0.27	0.66	0.42	0.90
	0.033	0.61		0.82	
+0.009	0.027	0.59	1.26	0.22	0.45
	0.047	1.19		0.41	
+0.008	0.053	0.43	1.00	0.77	0.81
	0.044	0.90		0.24	
+0.002	0.058	0.41	0.94	0.43	0.48
	0.049	0.86		0.17	
+0.006	0.053	0.26	0.93	0.38	0.43
	0.050	0.88		0.23	
0.003	0.056	0.98	1.40	0.31	0.52
	0.045	1.02		0.42	
0.003	0.087	0.76	1.16	0.67	0.73
	0.062	0.87		0.29	
0.008	0.040	0.49	1.10	0.30	0.49
	0.056	1.02		0.38	
0.007	0.060	0.38	1.10	0.37	0.50
	0.056	1.04		0.33	
0.007	0.040	0.37	0.61	0.16	0.27
	0.049	0.47		0.22	
0.002	0.060	0.81	0.85	0.72	0.77
	0.037	0.29		0.28	
0.007	0.062	1.38	1.45	0.41	0.76
	0.066	0.47		0.64	
0.007	0.042	0.66	1.12	1.14	1.18
	0.053	0.91		0.29	
0.029	0.050	0.97	1.03	0.22	0.33
	0.048	0.34		0.25	
0.001	0.037	0.84	1.00	0.50	0.71
	0.074	0.59		0.49	
0.013	0.040	0.74	0.82	0.20	0.28
	0.035	0.36		0.21	
0.001	0.058	0.51	0.99	0.27	0.29
	0.046	0.85		0.18	

TABLE XX - Continued

Transducer Location T = Top B = Bottom		Transducer Serial Number	Transducer Sensitivity mv/v/psi	Temperature Zero Shift %F.S./°F	Temperature Zero Shift of Pair	Temperature Sensitivity Shift % Indicated Output/°F
39.	T	D63	0.060	0.050	0.015	0.073
	B	D41	0.061	0.065		0.038
40.	T	D139	0.071	0.058	0.007	0.050
	B	D81	0.073	0.051		0.043
41.	T	D150	0.064	0.055	0.016	0.049
	B	D131	0.065	0.071		0.049
42.	T	D147	0.066	0.074	0.010	0.043
	B	D50	0.069	0.064		0.069
43.	T	D73	0.054	0.078	0.002	0.067
	B	D25	0.059	0.076		0.054
44.	T					
	B	D43	0.062	0.081		
45.	T	D64	0.052	0.089	0.006	0.070
	B	D122	0.057	0.095		0.041
46.	T	D59	0.064	0.099	0.015	0.057
	B	D116	0.066	0.084		0.170
47.	T	D136	0.068	0.114	0.018	0.058
	B	D72	0.073	0.097		0.052
48.	T	D75	0.058	0.093	0.002	0.024
	B	D85	0.063	0.095		0.033
49.	T	D149	0.063	0.092	0.008	0.052
	B	D135	0.067	0.106		0.051
50.	T	D46	0.063	0.117	0.001	0.040
	B	D133	0.064	0.116		0.052
51.	T	D69	0.080	0.186	0.029	0.099
	B	D115	0.086	0.157		0.059
52.	T	D141	0.058	0.169	0.011	0.059
	B	D156	0.059	0.158		0.068
53.	T	D35	0.073	0.168	0.032	0.037
	B	D106	0.076	0.205		0.055
54.	T	D119	0.097	0.190	0.003	0.050
	B	D107	0.104	0.193		0.060

A

TABLE XX - Continued

Temperature Zero Shift of Pair	Temperature Sensitivity Shift % Indicated Output/°F	Linearity %F.S.	Linearity of Pair (RSS Method)	Hysteresis %F.S.	Hysteresis of Pair (RSS Method)
0.015	0.073	0.53	1.33	0.34	1.40
	0.038	1.20		1.35	
0.007	0.050	0.69	0.84	0.33	0.49
	0.043	0.45		0.37	
0.016	0.049	1.24	1.30	0.35	0.50
	0.049	0.40		0.34	
0.010	0.043	0.28	0.85	0.23	0.38
	0.069	0.80		0.32	
0.002	0.067	0.45	1.00	0.37	0.80
	0.054	0.91		0.71	
0.006	0.070	0.80	1.00	0.32	0.39
	0.041	0.64		0.23	
0.015	0.057	1.06	1.15	0.28	0.43
	0.170	0.49		0.34	
0.018	0.058	0.55	0.70	0.42	0.56
	0.052	0.45		0.38	
0.002	0.024	0.72	0.79	0.11	0.36
	0.033	0.32		0.35	
0.008	0.052	0.50	1.22	0.48	0.83
	0.051	1.13		0.66	
0.001	0.040	0.45	0.81	0.41	0.53
	0.053	0.67		0.34	
0.029	0.099	1.09	1.25	1.63	1.65
	0.059	0.49		0.31	
0.011	0.059	0.47	1.10	0.80	0.91
	0.068	0.98		0.44	
0.032	0.037	0.42	0.60	0.12	0.37
	0.055	0.43		0.35	
0.003	0.050	1.46	1.54	0.37	0.50
	0.060	0.62		0.35	

B

TABLE XXI

COMPONENT ERROR ANALYSIS FOR ABSOLUTE-PRESSURE

Value of Measurand	Absolute Pressure Top & Bottom	Parameter of Error Input	Assumed Mean Value of Error Input	Assumed Deviation from Mean	Statistic Value of Error Specif
5 psid	T = 8 psia B = 13 psia	Temp.zero shift	70°F	-20°F	0.027% F.S
		Temp.sens.shift	70°F	-20°F	0.074%/°F
		Linearity	-	-	±1.54%/F.S.
		Hysteresis	-	-	±1.00%/F.S.
					Summar
10 psid	T = 5 psia B = 15 psia	Temp.zero shift	70°F	-20°F	0.027% F.S
		Temp.sens.shift	70°F	-20°F	0.074%/°F
		Linearity	-	-	±1.5%/F.S.
		Hysteresis	-	-	±1.0%/F.S.
					Summar
5 psid	T = 8 psia B = 13 psia	Temp.zero shift	70°F	-40°F	0.027%F.S.
		Temp.sens.shift	70°F	-40°F	0.074%/°F
		Linearity	-	-	±1.5% F.S.
		Hysteresis	-	-	±1.00% F.S.
					Summar
10 psid	T = 5 psia B = 15 psia	Temp.zero shift	70°F	-40°F	0.027%F.S.
		Temp.sens.shift	70°F	-40°F	0.074%/°F
		Linearity	-	-	±1.5% F.S.
		Hysteresis	-	-	±1.0% F.S.
					Summar

1 Temperature zero shift was compensated for in the analysis program; therefore, the error was co exact temperature of the transducers contributed to a random temperature zero shift error. In

A

TABLE XXI

ERROR ANALYSIS FOR ABSOLUTE-PRESSURE TRANSDUCERS

Mean Error Input	Assumed Deviation from Mean	Statistical Value of Error Specification	Total Error Pressure Equivalent	Systematic Error (Correctable)	Random Error of Pairs	Square of Random Errors
°F	-20°F	0.027% F.S./°F	0.08 psi	0.08 psi [1]	±0.02 psi	0.000730
°F	-20°F	0.074%/°F	0.11 psi 0.02 psi	-	±0.13 psi	0.017000
	-	±1.54%/F.S.	0.23 psi	-	±0.23 psi	0.053000
	-	±1.00%/F.S.	0.15 psi	-	±0.15 psi	0.022500
		Summary	Sum of squares = 0.09250 RSS error = 0.3 psi or ±6% of measurand			
°F	-20°F	0.027% F.S./°F	0.08 psi	0.08 psi	±0.02 psi	Negligible
°F	-20°F	0.074%/°F	0.15 psi 0.0 psi	-	±0.15 psi	0.0225
	-	±1.5%/F.S.	-	-	±0.23 psi	0.0530
	-	±1.0%/F.S.	-	-	±0.15 psi	0.0225
		Summary	Sum of squares = 0.0975 RSS error = 0.31 psi or ±3.1% of measurand			
°F	-40°F	0.027%F.S./°F	0.16 psi	0.16 psi	±0.02 psi	Negligible
°F	-40°F	0.074%/°F	0.2 psi 0.06 psi	- -	±0.26 psi	0.0670
	-	±1.5% F.S.	0.23 psi	-	±0.23 psi	0.053
	-	±1.00% F.S.	0.15 psi	-	±0.15 psi	0.022
		Summary	Sum of squares = 0.142 RSS error = 0.38 psi or 7.6% of measurand			
°F	-40°F	0.027%F.S./°F	0.16 psi	0.16 psi	±0.02 psi	Negligible
°F	-40°F	0.074%/°F	0.3 psi 0.0 psi	- -	0.3 psi	0.0900
	-	±1.5% F.S.	0.23 psi	-	0.23 psi	0.0530
	-	±1.0% F.S.	0.15 psi	-	0.15 psi	0.0220
		Summary	Sum of squares = 0.1550 RSS error = 0.4 psi or ±4.0% of measurand			

[1] lysis program; therefore, the error was considered systematic. The inability to monitor the random temperature zero shift error. In this system the uncertainty was ±5°F.

B

TABLE XXII
STATISTICAL ERROR ANALYSIS OF DIFFERENTIAL-PRESSURE TRANSDUCERS

Serial Number	Sens. mv/v/psi	Temp. Zero Shift % F.S./°F	Temp. Sens. Shift % Ind. Output/°F	Linear. % F.S.	Hyster. % F.S.
			± 2 PSID		
E29	0.09	-0.112	0.037	0.75	0.55
E34	0.10	-0.068	0.034	0.38	0.67
E24	0.09	-0.057	0.021	0.20	0.20
E28	0.11	-0.052	0.011	0.60	0.38
E37	0.08	-0.049	-0.003	0.33	0.42
E12	0.11	-0.044	0.036	0.65	0.63
E22	0.10	-0.043	0.027	1.04	0.60
E41	0.11	-0.033	0.014	0.31	0.46
E44	0.10	-0.031	0.042	0.40	0.34
E40	0.23	-0.030	0.048	1.56	0.71
E43	0.11	-0.019	0.023	0.49	0.55
E39	0.24	+0.016	0.047	0.55	0.99
E5	0.12	+0.019	0.041	0.59	0.41
E4	0.07	+0.022	0.017	0.93	0.33
E13	0.09	+0.023	0.027	0.72	0.45
E27	0.10	+0.020	0.017	0.29	0.34
E3	0.18	+0.027	0.051	1.23	1.15
E36	0.08	+0.031	0.024	0.23	0.32
E32	0.13	+0.029	0.037	0.41	0.58
E6	0.12	+0.034	0.019	0.67	0.80
E11	0.07	+0.047	0.021	0.20	0.33
E9	0.07	+0.049	0.015	1.42	0.12
E15	0.09	+0.055	0.033	0.56	0.57
E14	0.11	+0.067	0.022	0.23	0.38
E8	0.11	+0.073	0.028	0.47	0.29
E42	0.11	+0.066	0.015	0.36	0.51
E45	0.11	+0.084	0.046	0.87	0.68
E21	0.10	+0.075	0.029	0.35	0.41
E23	0.12	+0.093	0.017	0.74	0.27
E16	0.11	+0.104	0.049	0.60	0.31
E7	0.11	+0.104	0.036	0.69	0.40
E19	0.09	+0.104	0.025	0.30	0.18
E26	0.07	+0.109	0.030	0.22	0.23

TABLE XXII - Continued

Serial Number	Sens. mv/v/psi	Temp. Zero Shift % F.S./°F	Temp. Sens. Shift % Ind. Output/°F	Linear. % F.S.	Hyster. % F.S.
			± 5 PSID		
F8	0.08	-0.088	+0.023	1.15	0.23
F1	0.13	-0.065	+0.052	1.11	0.60
F18	-	-0.057	+0.012	-	-
F12	0.12	-0.050	+0.039	0.50	0.66
F21	-	-0.048	+0.026	-	-
F11	0.10	-0.038	+0.026	0.26	0.39
F2	0.12	-0.030	+0.036	1.27	1.25
F14	0.12	+0.007	+0.029	0.50	0.66
F15	0.10	+0.017	+0.031	1.06	0.27
F19	0.08	+0.027	+0.028	0.31	0.61
F17	0.11	+0.041	+0.014	1.15	0.43
F13	0.10	+0.063	+0.020	1.30	0.43
F7	0.10	+0.066	+0.030	0.55	0.38
F9	0.11	+0.077	+0.049	0.40	0.36
F5	0.11	+0.086	+0.034	0.47	0.75
			± 10 PSID		
G13	0.08	-0.086	0.029	0.45	1.15
G10	0.08	-0.032	0.026	0.60	0.80
G14	0.06	-0.016	0.022	0.18	0.35
G12	0.07	+0.010	0.026	0.23	0.46
G8	0.09	+0.011	0.019	0.33	0.51
G6	0.07	+0.018	0.019	0.53	0.26
G2	0.07	+0.022	0.044	0.54	0.66
G4	0.08	+0.039	0.025	0.74	0.63
G3	0.08	+0.050	0.024	0.47	0.48
G7	0.08	+0.050	0.025	0.58	0.44
G11	0.09	+0.056	0.025	0.82	0.64
G1	0.08	+0.064	0.055	0.74	0.94
G5	0.08	+0.065	0.021	0.54	0.57
G9	0.08	+0.082	0.022	0.58	0.43
G15	0.07	+0.083	0.026	0.39	0.68

The values utilized to compile the statistics for the ±2 psid differential-pressure transducers were as follows:

Summary of error specifications

Temperature zero shift	=0.086 percent full scale/°F
Temperature sensitivity shift	=0.048 percent indicated output/°F
Linearity	=±0.9 percent full scale
Hysteresis	=±0.8 percent full scale

The mathematical procedures that were used to calculate the statistics for the ±2 psid transducers are shown in Table XXIII.

TABLE XXIII

STATISTICAL CALCULATIONS FOR ±2 PSID DIFFERENTIAL-PRESSURE TRANSDUCERS

Parameter	Temperature Zero Shift	Temperature Sensitivity Shift	Linearity	Hysteresis
Arithmetic mean	0.042	0.024	0.50	0.46
Sum of variance	0.0142	0.0042	1.2122	0.8720
Average variance	$=\frac{0.0142}{28}$	$=\frac{0.0042}{28}$	$=\frac{1.2122}{28}$	$=\frac{0.8720}{28}$
	=0.0005	=0.000015	=0.0430	=0.031
Deviation	0.022	0.012	0.2	0.17
2σ error	=2(0.022)	=2(0.012)	=2(0.2)	=2(0.17)
	+0.042	+0.024	+0.5	+0.46
	=0.086	=0.048	=0.9	=0.8

The values utilized to compile the statistics for the ±5 psid differential-pressure transducers were as follows:

Summary of error specifications

Temperature zero shift	=0.08 percent full scale/°F
Temperature sensitivity shift	= 0.04 percent indicated output/°F
Linearity	=±0.8 percent full scale
Hysteresis	=±0.7 percent full scale

The 2σ error values that were obtained for the ±5 psid transducers are shown in Table XXIV.

TABLE XXIV
STATISTICAL CALCULATIONS FOR ±5 PSID DIFFERENTIAL-PRESSURE TRANSDUCERS

Parameter	Temperature Zero Shift	Temperature Sensitivity Shift	Linearity	Hysteresis
2σ error	0.80	0.04	0.8	0.7

The values utilized to compile the statistics for the ±10 psid differential-pressure transducers were as follows:

Summary of error specifications

Temperature zero shift	=0.08 percent full scale/°F
Temperature sensitivity shift	=0.04 percent indicated output/°F
Linearity	=±0.8 percent full scale
Hysteresis	=±0.7 percent full scale

The 2σ error values that were obtained for the ±10 psid transducers are shown in Table XXV.

TABLE XXV
STATISTICAL CALCULATIONS FOR ±10 PSID
DIFFERENTIAL-PRESSURE TRANSDUCERS

Parameter	Temperature Zero Shift	Temperature Sensitivity Shift	Line-arity	Hyster-esis
2σ error	0.08	0.04	0.8	0.7

A component error analysis, using the 2σ error values and showing 4 typical error inputs for each transducer range, is shown in Table XXVI.

Position Transducer Error Analysis

Measurements of angle of attack, angle of sideslip, aircraft attitude, blade positions, and control positions were accomplished by transforming the motion into a resistance change by means of rotary or linear potentiometers. The resistance change was measured by a voltage-divider circuit or by shunting the resistance across a 4-arm bridge and monitoring the output of the bridge. With either method, the output voltage was directly proportional to the change in resistance.

In the Dynamic Airloads Program instrumentation system, the accuracy of the position transducers was directly dependent on the accuracy of the calibration method and the tolerance of the mechanical linkage between the actuating device and the potentiometer. The linearity of the potentiometers was better than 0.1 percent of full scale.

The following paragraphs describe the method of calibration that was used for each type of measurement and assign a statistical accuracy figure for this procedure. Details are presented on the mechanical system that was used to convert the motion to a resistance change and its effect on system accuracy. When these uncertainties were added by the root sum square approximation to the figures established for the subsequent associated components of the measurement system, a statistical accuracy figure was derived for that group of measurements.

Angle of Attack and Angle of Sideslip (Boom Instrumentation Error Analysis)

The calibration fixture for angle of attack and angle of sideslip consisted of a precisely drilled quadrant that could be clamped to the boom with a pin-locking device to locate the vane at 2-degree intervals. The locating holes were accurate to ±15 minutes.

The zero-reference position was established by alining the vane with the centerline or the waterline of the aircraft with a string. The accuracy of this reference was estimated to be ±30 minutes.

The mechanical coupling between the vane and the potentiometer was direct and did not enter into this analysis.

The full-scale range of the angle-of-attack instrumentation was ±30 degrees. The full-scale range of the angle-of-sideslip instrumentation was ±45 degrees.

The RSS summation of the two random calibration errors was as follows:

Calibration jig	= ±15 minutes	= 0.0225
Reference	= ±30 minutes	= 0.0900
		0.1125
RSS error	$=\sqrt{0.1125}$	= ±34 minutes
For angle of attack	= ±34 minutes was ±1 percent of full scale.	
For angle of sideslip	= ±34 minutes was ±0.63 percent of full scale.	

Pitch, Roll, and Yaw Attitude Instrumentation Error Analysis

The transducers used for measuring the pitch, roll, and yaw attitudes were gyros with potentiometer outputs. One two-axis gyro measured pitch and roll; a second modified gyro measured yaw.

TABLE XXV

COMPONENT ERROR ANALYSIS FOR DIFFE

Value of Measurand	Full-Scale Range	Parameter of Error Input	Assumed Mean Value of Error Input	Assumed Deviation from Mean	Statist Value Error Spec
2 psid	±2 psid	Temp.zero shift	70°F	-20°F	0.086%F
		Temp.sens.shift	70°F	-20°F	0.048%/
		Linearity			0.9% F.
		Hysteresis			0.8% F.
2 psid	±2 psid	Temp.zero shift	70°F	-40°F	0.086%/
		Temp.sens.shift	70°F	-40°F	0.048%/
		Linearity			0.9% F.
		Hysteresis			0.8% F.
1 psid	±2 psid	Temp.zero shift	70°F	-20°F	0.086%F
		Temp.sens.shift	70°F	-20°F	0.048%/
		Linearity			0.9% F.
		Hysteresis			0.8% F.
1 psid	±2 psid	Temp.zero shift	70°F	-40°F	0.086%F
		Temp.sens.shift	70°F	-40°F	0.048%/
		Linearity			0.9% F
		Hysteresis			0.8% F
5 psid	±5 psid	Temp.zero shift	70°F	-20°F	0.080%/
		Temp.sens.shift	70°F	-20°F	0.04%/
		Linearity			0.8% F
		Hysteresis			0.7% F

A

TABLE XXVI

S FOR DIFFERENTIAL-PRESSURE TRANSDUCERS

Statistical Value of Error Specification	Total Error Pressure Equivalent	Systematic Error (Correctable)	Random Error of Pairs	Square of Random Errors
0.086%F.S./°F	±0.07 psi	+0.07 psi	±0.017 psi	.000290
0.048%/°F	0.02 psi		±0.02 psi	.000400
0.9% F.S.	0.036 psi		±0.036 psi	.001300
0.8% F.S.	0.032 psi		±0.032 psi	.001000
	Summary	Sum of squares = 0.002990		
		RSS error = 0.054 psi or 2.7% of measurand		
0.086%/F.S./°F	+0.14 psi	+0.14 psi	±0.02 psi	.000400
0.048%/°F	+0.038 psi		±0.038 psi	.001400
0.9% F.S.	0.036 psi		0.036 psi	.001300
0.8% F.S.	0.032 psi		0.032 psi	.001000
	Summary	Sum of squares = 0.004100		
		RSS error = 0.064 psi or 3.2% of measurand		
0.086%F.S./°F	+0.07 psi	+0.07 psi	±0.017 psi	.000290
0.048%/°F	+0.01 psi		±0.01 psi	.000100
0.9% F.S.	0.036 psi		0.036 psi	.001300
0.8% F.S.	0.032 psi		0.032 psi	.001000
	Summary	Sum of squares = 0.002690		
		RSS error = 0.052 psi or 5.2% of measurand		
0.086%F.S./°F	+0.14 psi	+0.14 psi	±0.02 psi	.000400
0.048%/°F	+0.02 psi		±0.02 psi	.000400
0.9% F.S.	0.036 psi		±0.036 psi	.001300
0.8% F.S.	0.032 psi		±0.032 psi	.001000
	Summary	Sum of squares = 0.003100		
		RSS error = 0.055 psi or 5.5% of measurand		
0.080%F.S./°F	0.16 psi	0.16 psi	±0.04 psi	.0016
0.04%/°F	0.04 psi		±0.04 psi	.0016
0.8% F.S.	0.08 psi		±0.08 psi	.0064
0.7% F.S.	0.07 psi		±0.07 psi	.0049
	Summary	Sum of squares = 0.0145		
		RSS error = ±0.12 psi or 2.4% of measurand		

3

TABLE XXVI - Continu

Value of Measurand	Full Scale Range	Parameter of Error Input	Assumed Mean Value of Error Input	Assumed Deviation from Mean	Stati Valu Error Sp
5 psid	±5 psid	Temp.zero shift	70°F	-40°F	0.080%F
		Temp.sens.shift	70°F	-40°F	0.04%/°
		Linearity			0.8% F.
		Hysteresis			0.7% F.
2.5 psid	±5 psid	Temp.zero shift	70°F	-20°F	0.08% F
		Temp.sens.shift	70°F	-20°F	0.04%/°
		Linearity			0.8% F.
		Hysteresis			0.7% F.
2.5 psid	±5 psid	Temp.zero shift	70°F	-40°F	0.08% F
		Temp. sens.shift			0.04%/°
		Linearity			0.8% F.
		Hysteresis			0.7% F.
10 psid	±10 psid	Temp.zero shift	70°F	-20°F	0.08% F
		Temp.sens.shift	70°F	-20°F	0.04%/°
		Linearity			0.8% F.
		Hysteresis			0.7% F.
10 psid	±10 psid	Temp.zero shift	70°F	-40°F	0.08% F
		Temp.sens.shift	70°F	-40°F	0.04/°F
		Linearity			0.8% F.
		Hysteresis			0.7% F.

A

LE XXVI - Continued

med Lon from n	Statistical Value of Error Specification	Total Error Pressure Equivalent	Systematic Error (Correctable)	Random Error of Pairs	Square of Random Errors
0°F	0.080%F.S./°F	0.32 psi	0.32 psi	±0.04 psi	0.0016
0°F	0.04%/°F	0.08 psi		±0.08 psi	0.0064
	0.8% F.S.	0.08 psi		±0.08 psi	0.0064
	0.7% F.S.	0.07 psi		±0.07 psi	0.0049
	Summary	Sum of squares = 0.0193			
		RSS error = +0.14 psi or 2.8% of measurand			
0°F	0.08% F.S./°F	0.16 psi	0.16 psi	±0.04 psi	0.0016
0°F	0.04%/°F	0.02 psi		±0.02 psi	0.0004
	0.8% F.S.	0.08 psi		±0.08 psi	0.0064
	0.7% F.S.	0.07 psi		±0.07 psi	0.0049
	Summary	Sum of squares = 0.0133			
		RSS error = 0.11 psi of 4.4% of measurand			
0°F	0.08% F.S./°F	0.32 psi	0.32 psi	±0.04 psi	0.0016
	0.04%/°F	0.04 psi		±0.04 psi	0.0016
	0.8% F.S.	0.08 psi		±0.08 psi	0.0064
	0.7% F.S.	0.07 psi		±0.07 psi	0.0049
	Summary	Sum of squares = 0.0145			
		RSS error = ±0.12 psi or 4.8% of measurand			
0°F	0.08% F.S./°F	0.32 psi	0.32 psi	±0.08 psi	0.0064
0°F	0.04%/°F	0.08 psi		±0.16 psi	0.0064
	0.8% F.S.	0.16 psi		±0.16 psi	0.0255
	0.7% F.S.	0.14 psi		±0.14 psi	0.0195
	Summary	Sum of squares = 0.0578			
		RSS error = 0.24 psi or ± 2.4% of measurand			
0°F	0.08% F.S./°F	0.64 psi	0.64 psi	±0.08 psi	0.0064
0°F	0.04/°F	0.16 psi		±0.16 psi	0.0255
	0.8% F.S.	0.16 psi		±0.16 psi	0.0255
	0.7% F.S.	0.14 psi		±0.14 psi	0.0195
	Summary	Sum of squares = 0.0769			
		RSS error = 0.27 psi or ± 2.7% of measurand			

B

TABLE XXVI - Conti

Value of Measurand	Full Scale Range	Parameter of Error Input	Assumed Mean Value of Error Input	Assumed Deviation from Mean	Stat Val Error S
5 psid	±10 psid	Temp.zero shift	70°F	-20°F	0.08%F
		Temp.sens.shift	70°F	-20°F	0.04%/
		Linearity			0.8% F
		Hysteresis			0.7% F
5 psid	±10 psid	Temp.zero shift	70°F	-40°F	0.08%F
		Temp.sens.shift	70°F	-40°F	0.04%/
		Linearity			0.8% F
		Hysteresis			0.7% F

TABLE XXVI - Continued

sumed tion from ean	Statistical Value of Error Specification	Total Error Pressure Equivalent	Systematic Error (Correctable)	Random Error of Pairs	Square of Random Errors
20°F	0.08%F.S./°F	0.32 psi	0.32 psi	±0.08 psi	0.0064
20°F	0.04%/°F	0.04 psi		±0.04 psi	0.0016
	0.8% F.S.	0.16 psi		±0.16 psi	0.0255
	0.7% F.S.	0.14 psi		±0.14 psi	0.0195
		Summary	Sum of squares = 0.0530		
			RSS error = ±0.22 psi or 4.4% of measurand		
40°F	0.08%F.S./°F	0.64 psi	0.64 psi	±0.08 psi	0.0064
40°F	0.04%/°F	0.08 psi		±0.08 psi	0.0064
	0.8% F.S.	0.16 psi		±0.16 psi	0.0255
	0.7% F.S.	0.14 psi		±0.14 psi	0.0195
		Summary	Sum of squares = 0.0578		
			RSS error = 0.24 psi or ± 4.8% of measurand		

The specifications for the gyro itself had little effect on the accuracy of the data channel when a complete system calibration was performed. The accuracy of the calibration procedure and the specifications of subsequent components of the measurement system were the determining factors. The one specification of the gyro that had a significant relationship to the system accuracy was the relationship to true vertical. The specification stated that the erection system would hold the gyro relationship to true vertical within ±0.15 degree or approximately ±10 minutes. This specification related only to the pitch and roll measurements. In order to use this type of gyro for yaw, the erection circuit was disabled and the gyro was caged until a record was taken. The specification then relevant to the yaw circuit was the drift rate, which was 0.4 degree per minute. If it is assumed that the time between the uncaging of the gyro and the end of the data recording was 30 seconds, drift could cause a random error of ±10 minutes of yaw yaw.

The calibration jig used in the aircraft was a Vernier-controlled tilt table, monitored by a Hilger-Watts Vernier angle gage. The resolution of the Vernier gage was 1 minute. In the aircraft environment, without precision surfaces, the accuracy of the measurement was estimated to be 15 minutes.

Calculation of the RSS random error due to specifications and calibration procedure was as follows:

True vertical or drift	= ±10 minutes
Calibration	= ±15 minutes
Sum of squares	= 325 minutes
$\sqrt{325}$	= ±18 minutes
Full-scale pitch attitude	= ±45 degrees
Random error in percent of full scale	= ±0.35 percent
Full-scale roll attitude	= ±45 degrees
Random error in percent of full scale	= ±0.35 percent

Full-scale yaw attitude	= ±30 degrees
Random error in percent of full scale	= ±0.5 percent

Airspeed Instrumentation Error Analysis

A pitot-static pressure port, mounted on the swiveling pitot-static head, transmitted the airspeed pressure signal to a differential-pressure transducer mounted in the nose compartment of the aircraft.

The transducer used for this application was a Statham Model PL283 TC-.5-350, a strain-gage differential-pressure transducer. The following pertinent specifications, extracted from the manufacturer's data sheets, were found to be statistically representative of the transducers used in this program:

Combined linearity and hysteresis	= ±1 percent of full scale
Temperature zero shift	= 0.02 percent full scale per°F
Temperature sensitivity shift	= 0.01 percent of indicated output per °F

The analysis was conducted for a measurand of 100 knots and an error input of -40°F, assuming that no corrections were made. The full-scale range of the transducer was 140 knots.. Calculations gave the following results:

Linearity and hysteresis	= ±1 percent of full scale = ±1.4 knots
Temperature zero shift	= 0.02 percent of full scale/°F = 1.2 knots
Sensitivity shift	= 0.01 percent = 0.4 knot

Emphasis was placed on the fact that linearity, zero shift, and sensitivity shift errors could be corrected to a certain degree in the analysis program. If corrections were made, a part of the error was considered systematic. If no corrections were made, the entire specification had to be considered random and could be combined by root sum square methods to yield a statistical accuracy figure.

Summary of Airspeed Calculations

Linearity and hysteresis - $(\pm 1.0$ percent of 140 knots$)^2$	$= 2.0$
Temperature zero shift - $(0.02$ percent of 140 knots x 40°F$)^2$	$= 1.4$
Temperature sensitivity shift - $(0.01$ percent of 100 knots x 40°F$)^2$	$= \underline{0.16}$
Sum of squares	$= 3.56$
Root sum square	$= \pm 1.9$ knots

The solution (± 1.9 knots) is ± 1.9 percent of the measurand.

Altitude Instrumentation Error Analysis

The static port on the nose boom swiveling pitot-static head was ported to a 0 - 15 psia absolute-pressure transducer, mounted in the nose compartment of the aircraft.

The transducer used for this application was a CEC Model 4-312, 0 - 15 psia unit. The following specifications, extracted from the manufacturer's data sheets, were found to be statistically representative of the transducers used in this program:

Linearity and hysteresis	$= \pm 0.5$ percent of full scale
Temperature zero shift	= 0.012 percent full scale per °F

Temperature sensitivity shift = 0.010 percent per °F

The use of a 0 - 15 psia transducer to measure altitudes in the 0-to-10,000-foot range dictated the use of calibration data to relate transducer performance to statistical accuracy. The calibration data for the transducer used in this application indicated linearity and hysteresis to be ±1 percent of 10,000 feet. Temperature zero shift was 0.025 percent of 10,000 feet per °F. The analysis was conducted for a measurand of 5,000 feet and an error input of -40°F; the full-scale range of the system was 10,000 feet. This analysis presumed that no corrections were made and that the errors were considered to be random.

Summary of Altitude Calculations

		Error
Linearity and hysteresis - ±1 percent of 10,000 feet	= ±100 feet	= 10,000
Temperature zero shift - 0.025 percent of 10,000 feet x 40°F	= 100 feet	= 10,000
Temperature sensitivity shift - 0.010 percent of 5,000 feet x 40°F	= 20 feet	= 400
	Sum of squares	= 20,400
	Root sum square	= ±143 feet

The solution ±143 feet is 2.8 percent of the measurand.

Accelerometer Error Analysis

The accelerometers used for the Dynamic Airloads Program were Model 4310A types manufactured by Systron-Donner. The following criteria were used in determining the acceptance or rejection of an accelerometer:

1. Amplitude response

7 cps	-	100 percent
20 cps	-	101.5 percent ±3 percent
40 cps	-	104.5 percent ±7 percent

These nominal values were derived from the midpoint of the range of the measured values of the acceptable units. The tolerances combine the allowance to the manufacturer, plus a Vertol measurement error allowance, by the root sum square method, as shown in the following table.

TABLE XXVII
ACCELEROMETER AMPLITUDE RESPONSE TOLERANCES

Frequency - cps	Vendor Tolerance	Vertol Measurement Tolerance
20	± 2%	± 1.6%
40	± 5%	± 5%

2. Phase response

7 cps - 19 degrees ±7 degrees
20 cps - 44 degrees ±7 degrees
40 cps - 99 degrees ±7 degrees

These nominal values were derived from the midpoint of the range of the measured values of the acceptable units. The tolerances include a 5-degree allowance to the manufacturer plus a 5-degree Vertol measurement error allowance, combined by the root sum square method.

3. Maximum total static error - ±0.0045g

This value includes case misalinement, cross-axis sensitivity, hysteresis, nonlinearity, and non-repeatability. The limit of ±0.0045g is derived from the root sum square of the specified limits of each factor plus 0.001g measurement error. This error is the maximum deviation from the best straight line derived from a least square solution of 40 data points taken in 360 degrees of accelerometer rotation in the gravitational field of the earth.

Differential Amplifier Error Analysis

The output of the transducer systems was connected directly

into the inputs of the signal-conditioning differential amplifiers. The amplifiers were mounted on the signal-conditioning circuit boards in the rotating signal-conditioning package. The purpose of the amplifiers was to raise the level of the transducer output to the 20 millivolt full-scale signal necessary to drive the voltage-controlled oscillators. A statistical presentation of the amplifier test data is not presented in this analysis, for it will be demonstrated that the only specification contributing a significant input to the error analysis is the temperature zero-drift specification; a statistical presentation would show that a 2σ figure would closely approximate the specification. For the purpose of this analysis, the specification figures for temperature zero drift, temperature sensitivity shift, and linearity are used; the latter two specifications are included to demonstrate the relationships of the different magnitudes of errors when combined to present a statistical analysis.

Four conditions are analyzed. These represent the worst-case figures from the tranducer analysis; that is, the transducers were at their lowest anticipated outputs and the error input deviation at its highest. In order to present a clearer picture of the relationships of the error inputs, these error inputs were converted into equivalent pressures and the final figure was referred to as percent of measurand. The statistical values of the specifications and their verification were as follows:

1. Temperature zero drift = 1.5 microvolts per °F, referred to the input.

   The specification listed two sets of figures for this parameter; e.g., 2.5 microvolts per °C from -5°C to +20°C, and 5 microvolts per °C from +20°C to +55°C. Because the program was flown during the cooler months, it was anticipated that the temperature coefficients would be in the negative direction, and that portion of the specification would be used. Also, since the transducer specification was presented in °F, it was convenient to convert these specifications to the same units.

2. Temperature sensitivity shift = ±0.025 percent of indicated output per °F.

This requirement described a slope change, and its effect on the signal was directly dependent on the level of the signal being measured and not on the full scale output.

3. Linearity = ±0.1 percent from best straight line.

   This parameter indicated that any point on the measuring curve could be displaced by ±0.1 percent of full-scale output from the true value.

The computations of the statistical error data for the differential amplifiers utilized the amplifier specifications and the transducer data shown in Table XXI. The following procedure is illustrated by use of the calculations shown under Case 1 of the 4 sample worst-case sets of calculations which immediately follow this section. The step-by-step procedure, using the data from Case 1, was as follows:

Sample data

Full-scale range	= 10 psid, with the paired absolute-pressure transducer configuration
Measurand	= 5 psid
Error input	= -40°F

Step 1. Calculate the full-scale millivolt output of the transducer for expected signal and expected drift.

The output sensitivity for the 5 - 20 psia absolute transducers is 0.05-millivolt-per-volt excitation per psi input. As the transducer excitation is nominally 3 volts, the output is 0.150 millivolt per psi, and for the assumed full-scale 10 psi pressure, the output is 1.500 millivolts. The output due to transducer shift is calculated from the equivalent pressure due to temperature zero shift, which in this case is 0.16 psi (see Table XXI). Multiplying by 0.150 mv/psi yields an equivalent voltage input to the amplifier of 0.024 millivolt.

Step 2. Calculate the equivalent input voltage due to temperature change of the amplifier. The amplifier specification of 1.5 microvolts per °F is multiplied by the expected error input of -40°F to yield an equivalent input voltage of 0.060 millivolt.

Step 3. Total the input voltages to determine maximum expected input range. Divide maximum expected input

into 20 millivolts (maximum amplifier output) to determine the gain setting of the amplifier.

	Amplifier Input	x	Gain	=	Amplifier Output
Transducer press.	1.500 mv	x	12	=	18.00 mv
Transducer shift	0.024 mv	x	12	=	0.28 mv
Amplifier shift	0.060 mv	x	12	=	0.72 mv
Total	1.584 mv	x	12	=	19.00 mv

Step 4. Determine the temperature zero shift equivalent pressure error by calculating the voltage relationship between the signal and drift output voltages.

$$\text{Equivalent pressure due to amplifier drift} = \frac{0.060}{0.150}$$

$$= 0.4 \text{ psi} \quad (3)$$

Step 5. Multiply temperature sensitivity shift coefficient by temperature error input and pressure measurand.

$$0.025 \times 40 \times 5 = 0.05 \text{ psi}$$

Step 6. The linearity specification of the amplifier is ±0.1 percent of full scale. Full-scale output of the amplifier is nominally 20 millivolts. ±0.1 percent of full scale is ±0.20 millivolt. Calculate the equivalent pressure for 20 millivolts.

$$\text{Amplifier output due to transducer pressure} = 18 \text{ mv}$$

$$\text{Pressure error} = \frac{0.020 \quad (10)}{18.0}$$

$$= 0.011 \text{ psi}$$

Step 7. The systematic error is that part of the total error that is predictable and can be corrected. Although most errors can be corrected to a certain extent, it is evident from the figures placed in the total error column that the temperature zero shift is the greatest contributing factor in this case; and since it can be directly attributed to the temperature change, it could be

correctable to a certain extent. Again, the degree of correction is directly related to how closely the temperature change can be determined or how closely the output directly associated with the temperature zero shift error input can be measured.

In this case, during the in-flight calibration procedure, bridge power was turned off during one of the steps. The output of the amplifier was recorded and compared for each record by the computer with the output of the amplifier at the initial balance point, or baseline. The difference in output between the baseline and the in-flight bridge-power-off step was a direct measurement of amplifier shift.

The next problem was to determine how accurately the error output could be measured. This was directly related to the relationship of the error output to the full-scale range of the measuring system and the accuracy of the subsequent components of the system. The analysis of the subsequent components predicted a statistical error of ±0.2 percent of full scale for measuring amplifier shift. Relating this figure to the full-scale output for each measurement condition yielded a random error figure. Therefore, the systematic or correctable error was that amount of the error signal that was greater than the random error.

Differential Amplifier Error Analysis Worst-Case Calculation Summary

The following 4 examples represent the worst-case figures from the transducer analysis as they apply to the amplifier analysis. In each case the transducer is shown at its lowest anticipated output and the error input deviation is at its highest. Case 1 is a condensation of the detailed step-by-step procedure that was given in the preceding paragraphs.

Case 1

System range = 10 psid full scale, with paired absolute-pressure transducer configuration
Measurand = 5 psid, output = 0.05 mv/v/psi
Error input deviation = 30°F or ΔT of -40°F

	Amplifier Input	x	Gain	=	Amplifier Output
Transducer pressure	= 1.500 mv	x	12	=	18.00 mv
Transducer shift	= 0.024 mv	x	12	=	0.55 mv
Amplifier shift	= 0.060 mv	x	12	=	1.40 mv
	1.584 mv	x	12	=	19.00 mv

Error Input	Total Error in PSI	Systematic Error in PSI	Random Error in PSI	Square of Random Error
Temperature zero shift	0.4	0.4	0.1	0.01
Temperature sensitivity shift	0.05	n/a	0.05	0.0025
Linearity	0.011	n/a	0.011	0.000121

Statistical value of combined random errors = 0.11 psi
Random error in percent of measurand = 2.2 percent of 5 psi

Case 2

Full scale = 10 psid, with ±10 psid transducer
Measurand = 5 psid, output = 0.066 mv/v/psi
Error input deviation = 30°F or ΔT of -40°F

	Amplifier Input	x	Gain	=	Amplifier Output
Transducer pressure	= 2.000 mv	x	9	=	18.00 mv
Transducer shift	= 0.134 mv	x	9	=	1.20 mv
Amplifier shift	= 0.060 mv	x	9	=	0.54 mv
	2.2 mv	x	9	=	19.74 mv

Error Input	Total Error in PSI	Systematic Error in PSI	Random Error in PSI	Square of Random Error
Temperature zero shift	0.67	0.67	0.17	0.0285
Temperature sensitivity shift	0.05	n/a	0.05	0.0025

Error Input	Total Error in PSI	Systematic Error in PSI	Random Error in PSI	Square of Random Error
Linearity	0.01	n/a	0.01	0.0001

Statistical value of combined random errors = 0.175 psi
Random error in percent of measurand = 3.5 percent of 5 psi

Case 3

Full scale = 5 psid with ±5 psid transducer
Measurand = 2.5 psid, output = 0.08 mv/v/psi
Error input deviation = 30°F or ΔT of -40°F

	Amplifier Input	x	Gain	= Amplifier Output
Transducer pressure	= 1.200 mv	x	15	= 18.00 mv
Transducer shift	= 0.076 mv	x	15	= 1.15 mv
Amplifier shift	= 0.060 mv	x	15	= 0.90 mv
	1.336 mv	x	15	= 20.05 mv

Error Input	Total Error in PSI	Systematic Error in PSI	Random Error in PSI	Square of Random Errors
Temperature zero shift	0.25	0.25	0.07	0.0049
Temperature sensitivity shift	0.025	n/a	0.025	0.000610
Linearity	0.006	n/a	0.006	0.000036

Statistical value of combined random errors = 0.074 psi
Random error in percent of measurand = 3 percent of 2.5 psi

Case 4

Full scale = 2 psid with ±2 psid transducer
Measurand = 1 psid, output = 10 mv/v/psi
Error input deviation = 30°F or ΔT of -40°F

	Amplifier Input	x	Gain	=	Amplifier Output
Transducer pressure	= 0.600 mv	x	28	=	16.80
Transducer shift	= 0.042 mv	x	28	=	1.18
Amplifier shift	= 0.060 mv	x	28	=	1.68
	0.702 mv	x	28	=	19.66

Error Input	Total Error in PSI	Systematic Error in PSI	Random Error in PSI	Square of Random Errors
Temperature zero shift	0.2	0.15	0.05	0.0025
Temperature sensitivity shift	0.01	n/a	0.01	0.0001
Linearity	0.002	n/a	0.001	0.000004

Statistical value of combined random error = 0.051 psi
Random error in percent of measurand = 5.1 percent of 1 psi

Differential Amplifier Error Analysis Summary

The results of the amplifier error analysis, after the completion and refinement of all calculations, were reduced to the following data.

Temperature zero shift = 1.5 microvolts per °F, referred to the input

Temperature sensitivity shift = ±0.025 percent of indicated output per °F

Linearity = ±0.1 percent of full scale

Voltage-Controlled Oscillator Error Analysis

The output of the signal-conditioning amplifiers was used to modulate the voltage-controlled oscillators (VCO's). The VCO's accepted a full-scale signal of 0 to 20 millivolts and converted the voltage signal to a frequency signal. All MVCO's, VCO's, and mixer amplifiers were tested by the manufacturer under the supervision of a Vertol engineering representative. The documentation furnished by these tests can be analyzed by the same procedure as previously outlined to arrive

at a statistical summary of the specifications. The specifications for the MVCO's used in this program were as follows:

1. Linearity = ±0.5 percent from best straight line
2. Temperature frequency shift = ±1.5 percent design bandwidth from -5°C to +55°C
3. Temperature sensitivity change = ±1.0 percent of nominal from -5°C to +55°C
4. Source impedance = A change in source impedance from 0 to 1000 ohms shall not cause center frequency to change by more than ±1 percent of design bandwidth.

The preflight and in-flight calibration sequences, in conjunction with the computer data correction program, eliminated any discernible effects of temperature frequency shift, temperature sensitivity change, and source impedance change.

The preflight sequence provided two precision voltage steps to establish the band-edge and sensitivity characteristics of the MVCO. The in-flight sequence applied these same two points after each data record, and the computer program compared each in-flight calibration with the preflight calibration to detect any MVCO drift (compared lower band edges) or sensitivity changes (compared delta frequency from lower band edge to 40 percent of bandwidth).

The source impedance specification was not relative to the accuracy of the MVCO in the operational mode of the measurement system for this program. The third step of the preflight calibration sequence, denoted as baseline, established the reference point for all data measurements. This baseline reference was established with the MVCO receiving its nominal data input impedance which did not change during data acquisition.

Voltage-Controlled Oscillator Error Analysis Worst-Case Calculation Summary

The following situations represent the worst-case figures from the transducer analysis as they apply to the oscillator analysis. In each case the transducer is shown at its lowest anticipated output, and the error source is due to nonlinearity.

Case 1

System range = 10 psid full scale, double absolute-pressure transducer configuration
Measurand = 5 psid

Full-scale transducer pressure = 1.500 mv x gain of 12
= 18.0 mv

MVCO full scale = 20.0 mv

0.5 percent of 20 mv = 0.1 mv

Equivalent pressure for 0.1 mv = $\frac{0.1}{18}$ x 10 = 0.055 psi (4)

Statistical value of random error = ±0.055 psi
Random error in percent of measurand = ±1.1 percent of 5 psi

Case 2

System range = 10 psid full scale, ±10 psid transducer
Measurand = 5 psid

Full-scale transducer pressure = 2.0 mv x gain of 9
= 18.0 mv

MVCO full scale = 20.0 mv

0.5 percent of 20 mv = 0.1 mv

Equivalent pressure for 0.1 mv = $\frac{0.1}{18}$ x 10 = 0.055 psi (5)

Statistical value of random error = ±0.055 psi
Random error in percent of measurand = ±1.1 percent of 5 psi

Case 3

System range = 5 psid full scale, ±5 psid transducer
Measurand = 2.5 psid

Full-scale transducer pressure = 1.2 mv x gain of 15
= 18.0 mv

MVCO full scale = 20.0 mv

0.5 percent of 20.0 mv = 0.1 mv

Equivalent pressure for 0.1 mv = $\frac{0.1}{18} \times 5 = 0.028$ psi (6)

Statistical value of random error = 0.028 psi
Random error in percent of measurand = ±1 percent of 2.5 psi

Case 4

System range = 2 psid full scale, ±2 psid transducer
Measurand = 1 psid

Full-scale transducer pressure = 0.6 mv x gain of 28
= 16.8 mv

MVCO full scale = 20.0 mv

0.5 percent of 20.0 mv = 0.1 mv

Equivalent pressure for 0.1 mv = $\frac{0.1}{16.8} \times 2 = 0.014$ psi (7)

Statistical value of random error = ±0.041 psi
Random error in percent of measurand = ±1.4 percent of 1 psi

Tape Recording System Error Analysis

Up to 12 MVCO or VCO frequency outputs were combined within the mixer amplifier circuitry and transmitted via coaxial cable to the input of the tape system direct-recording amplifier. The direct-recording amplifier conditioned the signal, and the composite signal of the 12 VCO outputs was recorded on one track of the magnetic tape. On playback, the composite signal was retrieved from the tape track through the ground station direct-reproducing amplifier, and the composite signal was presented to the input of the FM discriminator system.

This analysis established the statistical accuracy of this recording/reproducing system, analyzing the factors affecting data accuracy as related to the Dynamic Airloads Program.

The manufacturer's specifications for the tape recording system, with a tape speed of 30 inches per second, were as follows:

1. Tape speed variation (long-term) = ±0.25 percent maximum from nominal
   This is equivalent to a ±1.8-percent FM deviation for the ±7.5-percent bandwidth system being used.

2. Wow and flutter (short-term) = ±0.8-percent maximum equivalent bandwidth noise

3. Harmonic distortion = signal-to-noise ratio of 44 db at 30 ips, equivalent to ±1 percent of bandwidth

The sensitivities of the measurement systems were based on a resistance-calibration technique that provided a delta level change corresponding to a known input stimulus. If the initial baseline and sensitivity of the recording system were established, and if these factors were applied to the system to establish data sensitivity, the effect of long-term tape speed variations was eliminated.

The preflight and in-flight calibration sequence provided the system sensitivity measurement, and the preflight Rcal established data sensitivity relative to system sensitivity. This relationship remained fixed, independent of long-term tape speed error.

Wow, flutter, and harmonic distortion directly affected data accuracy and were treated as random error.

Tape Recording System Error Analysis Summary

The results of the recording system error analysis, after the completion and refinement of all calculations, were reduced to the following data:

Wow and flutter	= 0.8 percent	= $(0.8)^2$	= 0.64
Harmonic distortion	= 1 percent	= $(1)^2$	= 1.00
	Sum of squares		= 1.64
	RSS error = $\sqrt{1.64}$		= ±1.25 percent of full scale

(8)

Discriminator Error Analysis

The output of the tape system reproducing amplifier was channeled to the input of the EMR 189D discriminator system. The discriminator system separated the individual subcarrier channels and discriminated the signal to reproduce the original data signal.

The units available for this program were extremely stable and accurate, being installed in a fixed environment and not limited in size and weight, and contributed only a small percentage to the system error.

The manufacturer's specifications for the discriminator system were as follows:

Maximum rms output noise = 0.1 percent of full bandwidth
Harmonic distortion = up to 1 percent for all intelligence frequencies up to channel cutoff. As intelligence frequencies approach dc, harmonic distortion approaches 0.1 percent
Output stability = ±0.5 percent of full bandwidth in a 15-hour period
Sensitivity stability = ±0.25 percent of bandwidth in a 15-hour period

The preflight and in-flight calibration procedures eliminated the small effects of stability and sensitivity specifications.

Discriminator Error Analysis Summary

Because of the relationship of harmonic distortion to frequency, it was difficult to ascribe a single statistical value to this error. For the purposes of this analysis, a ±1 percent of measurand figure was used for the statistical value of this component.

Instrumentation System Error Analysis Summary

The combination of transducers, amplifiers, VCO's, tape channels, and discriminators comprised a complete measurement system for the Dynamic Airloads Program. This section, which is the final section of the statistical error analysis, integrates the results of the individual component analyses and produces representative statistical error figures for the combined system.

Eleven examples were analyzed for the system, with the summary shown in Table XVI in a previous section of this report. Each case represents a worst-case extreme of the parameters. The factors applicable to the first eight parameters that are summarized in Table XVI are as follows:

Case 1 - The double absolute-pressure transducer configuration, 10 psid full scale, measuring 5 psid with a -40°F Δ temperature

Case 2 - Differential-pressure transducer, 10 psid full scale, measuring 5 psid with a -40°F Δ temperature

Case 3 - Differential-pressure transducer, 5 psid full scale, measuring 2.5 psid with a -40°F Δ temperature

Case 4 - Differential-pressure transducer, 2 psid full scale, measuring 1 psid with a -40°F Δ temperature

Case 5 - Angle-of-attack potentiometer, ±30 degrees full scale, measuring 30 degrees, temperature effect not applicable

Case 6 - Pitch-attitude gyro, ±45 degrees full scale, measuring 45 degrees, temperature effect not applicable

Case 7 - Airspeed, 0 to 140 knots full scale, measuring 100 knots with a Δ temperature of -40°F

Case 8 - Altitude, 0 to 10,000 feet full scale, measuring 5,000 feet with a Δ temperature of -40°F

APPENDIX IV

INSTRUMENTATION SIGN CONVENTION

The following instrumentation sign convention was used throughout the program.

Parameter	Positive Direction
Acceleration (angular)	Nose up, nose right, right side down
Acceleration (linear)	Upward, forward, to right
Actuator travel	Extension
Airspeed	Forward and right sideward flight
Altitude	Above sea level
Angle of attack (referred to relative wind)	Nose up
Blade flap angle	Up from droop stop
Blade flap bending moment	Tension in lower fibers
Blade lag angle	Lead
Blade torsion	Leading edge up with root end fixed
Blade pitch angle	Leading edge up from rig position
Blade chord bending	Tension in forward fibers
Blade pressures	Lift pressure
Collective pitch stick force	Pull
Collective pitch stick position	Up
Displacement	Upward, forward, to right
Drag	Aft
Drag bending moment	Tension in forward fibers
Events, including 1/rev., 12/rev., and calibration sequence (A-D system)	OFF position
Lateral stick force	Right
Lateral stick position	Right
Loads (aircraft structure)	Upward, forward, right
Longitudinal stick force	Forward
Longitudinal stick position	Forward
Moments (aircraft structure)	Tension in lower and left-hand fibers
Pitch angle (referred to horizontal)	Nose up

Parameter	Positive Direction
Pitch rate	Nose up
Pitch moment	Nose up
Roll angle	Right side down
Roll moment	Right side down
Roll rate	Right side down
Rotor azimuth angle	Increasing angles in direction of rotation with missing spline forward as zero position for shafts
Rotor shaft bending moment	See Figure 57
Rotor shaft lift	See Figure 57
Rotor shaft shear	See Figure 57
Rotor shaft torque	See Figure 57
Rudder pedal force	Push right pedal
Rudder pedal position	Right pedal forward
Sideslip (referred to relative wind)	Nose left
Stress	Tension
Thrust	Forward
Velocity	Upward, forward, to right
Yaw angle (referred to fixed azimuth)	Nose right
Yaw moment	Nose right
Yaw rate	Nose right

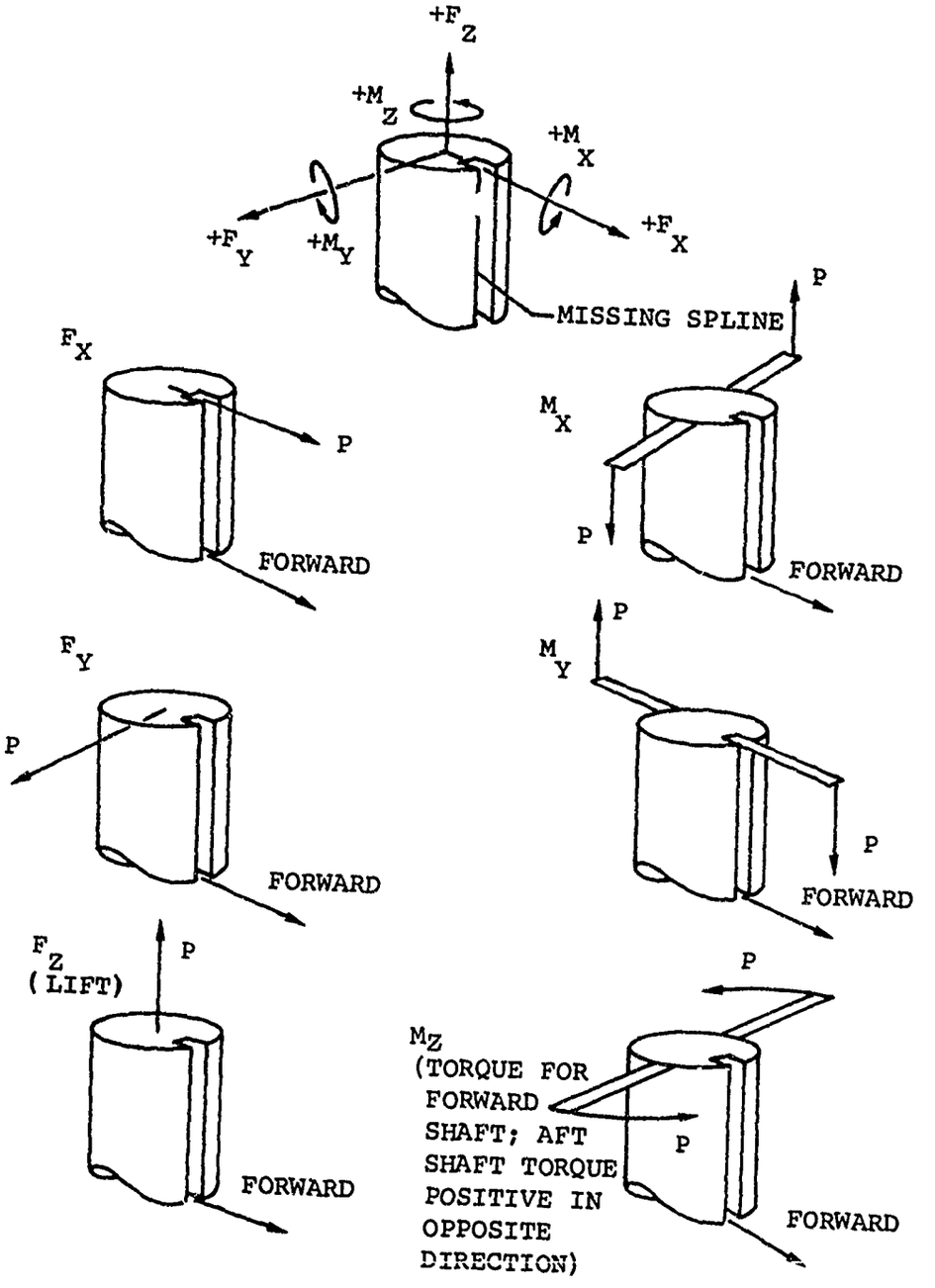

Figure 57. Forward and Aft Vertical Shafts Sign Conventions and Load Applications.

UNCLASSIFIED

Security Classification

DOCUMENT CONTROL DATA - R&D

(Security classification of title, body of abstract and indexing annotation must be entered when the overall report is classified)

1 ORIGINATING ACTIVITY (Corporate author) The Boeing Company Vertol Division Morton, Pa. 19070	2a. REPORT SECURITY CLASSIFICATION Unclassified 2b GROUP None

3. REPORT TITLE IN-FLIGHT MEASUREMENT OF ROTOR BLADE AIRLOADS, BENDING MOMENTS, AND MOTIONS, TOGETHER WITH ROTOR SHAFT LOADS AND FUSELAGE VIBRATION, ON A TANDEM ROTOR HELICOPTER

VOLUME I INSTRUMENTATION AND IN-FLIGHT RECORDING SYSTEM

4. DESCRIPTIVE NOTES (Type of report and inclusive dates)

Part 1 of a 5-part final report

5. AUTHOR(S) (Last name, first name, initial)

Golub, Roy, and
McLachlan, William

6. REPORT DATE	7a. TOTAL NO. OF PAGES	7b. NO. OF REFS
May 1967	169	1

8a. CONTRACT OR GRANT NO. Contract DA 44-177-AMC-124(T) b. PROJECT NO. c. Task 1P125901A14604 d.	9a. ORIGINATOR'S REPORT NUMBER(S) USAAVLABS Technical Report 67 9A 9b. OTHER REPORT NO(S) (Any other numbers that may be assigned this report) D8-0382-1

10. AVAILABILITY/LIMITATION NOTICES

Distribution of th s document is unlimited.

11. SUPPLEMENTARY NOTES	12. SPONSORING MILITARY ACTIVITY
None	U.S. Army Aviation Materiel Laboratories Fort Eustis, Virginia

13 ABSTRACT

An extensively instrumented tandem rotor helicopter was developed to measure the rotor blade airloads and the resulting rotor blade motions and bending moments, rotor shaft loads and moments, and fuselage vibration. This report details the design, assembly, and testing of the instrumentation system and documents the capability of the system for fulfilling the requirements of the program.

The selection and testing of the system components are described in detail, along with the integration of these components into the overall instrumentation and recording system. The exhaustive tests of the system, both on the ground and in flight, are described in step-by-step sequence. The capacities and capabilities of the system are delineated and illustrated.

Four technical appendixes, giving precise engineering data and statistical records, are included in the report.

DD FORM 1 JAN 64 1473

UNCLASSIFIED

Security Classification

UNCLASSIFIED

Security Classification

14. KEY WORDS	LINK A		LINK B		LINK C	
	ROLE	WT	ROLE	WT	ROLE	WT
IN-FLIGHT MEASUREMENT OF HELICOPTER AIRLOADS						
INSTRUMENTATION AND RECORDING SYSTEM						
PRESSURE TRANSDUCERS						
SIGNAL-CONDITIONING AND TRANSMITTING SYSTEM						
MINIATURE DATA AMPLIFIERS						
ELECTROMECHANICAL SWITCHING DEVICE						
COMPONENT AND SYSTEM ACCURACIES						
BLADE PRESSURE MEASUREMENTS						
VALIDATION OF PROPER SYSTEM OPERATION						

INSTRUCTIONS

1. ORIGINATING ACTIVITY: Enter the name and address of the contractor, subcontractor, grantee, Department of Defense activity or other organization *(corporate author)* issuing the report.

2a. REPORT SECURITY CLASSIFICATION: Enter the overall security classification of the report. Indicate whether "Restricted Data" is included. Marking is to be in accordance with appropriate security regulations.

2b. GROUP: Automatic downgrading is specified in DoD Directive 5200.10 and Armed Forces Industrial Manual. Enter the group number. Also, when applicable, show that optional markings have been used for Group 3 and Group 4 as authorized.

3. REPORT TITLE: Enter the complete report title in all capital letters. Titles in all cases should be unclassified. If a meaningful title cannot be selected without classification, show title classification in all capitals in parenthesis immediately following the title.

4. DESCRIPTIVE NOTES: If appropriate, enter the type of report, e.g., interim, progress, summary, annual, or final. Give the inclusive dates when a specific reporting period is covered.

5. AUTHOR(S): Enter the name(s) of author(s) as shown on or in the report. Enter last name, first name, middle initial. If military, show rank and branch of service. The name of the principal author is an absolute minimum requirement.

6. REPORT DATE: Enter the date of the report as day, month, year, or month, year. If more than one date appears on the report, use date of publication.

7a. TOTAL NUMBER OF PAGES: The total page count should follow normal pagination procedures, i.e., enter the number of pages containing information.

7b. NUMBER OF REFERENCES: Enter the total number of references cited in the report.

8a. CONTRACT OR GRANT NUMBER: If appropriate, enter the applicable number of the contract or grant under which the report was written.

8b, 8c, & 8d. PROJECT NUMBER: Enter the appropriate military department identification, such as project number, subproject number, system numbers, task number, etc.

9a. ORIGINATOR'S REPORT NUMBER(S): Enter the official report number by which the document will be identified and controlled by the originating activity. This number must be unique to this report.

9b. OTHER REPORT NUMBER(S): If the report has been assigned any other report numbers *(either by the originator or by the sponsor)*, also enter this number(s).

10. AVAILABILITY/LIMITATION NOTICES: Enter any limitations on further dissemination of the report, other than those imposed by security classification, using standard statements such as:

(1) "Qualified requesters may obtain copies of this report from DDC."

(2) "Foreign announcement and dissemination of this report by DDC is not authorized."

(3) "U. S. Government agencies may obtain copies of this report directly from DDC. Other qualified DDC users shall request through _____."

(4) "U. S. military agencies may obtain copies of this report directly from DDC. Other qualified users shall request through _____."

(5) "All distribution of this report is controlled. Qualified DDC users shall request through _____."

If the report has been furnished to the Office of Technical Services, Department of Commerce, for sale to the public, indicate this fact and enter the price, if known.

11. SUPPLEMENTARY NOTES: Use for additional explanatory notes.

12. SPONSORING MILITARY ACTIVITY: Enter the name of the departmental project office or laboratory sponsoring *(paying for)* the research and development. Include address.

13. ABSTRACT: Enter an abstract giving a brief and factual summary of the document indicative of the report, even though it may also appear elsewhere in the body of the technical report. If additional space is required, a continuation sheet shall be attached.

It is highly desirable that the abstract of classified reports be unclassified. Each paragraph of the abstract shall end with an indication of the military security classification of the information in the paragraph, represented as *(TS), (S) (C),* or *(U)*

There is no limitation on the length of the abstract. However, the suggested length is from 150 to 225 words.

14 KEY WORDS: Key words are technically meaningful terms or short phrases that characterize a report and may be used as index entries for cataloging the report Key words must be selected so that no security classification is required. Identifiers, such as equipment model designation, trade name, military project code name, geographic location, may be used as key words but will be followed by an indication of technical context. The assignment of links, rules, and weights is optional.

UNCLASSIFIED

Security Classification